Geotechnical
Engineering

USF
UNIVERSITY OF
SOUTH FLORIDA

EVALUATION OF THE PURDUE TDR METHOD FOR SOIL WATER CONTENT AND DENSITY MEASUREMENT

Amr M. Sallam
Newel K. White
Alaa K. Ashmawy

Report prepared for

Florida Department of Transportation
Contract Number BC-353-30
April 2004

Technical Report Documentation Page

1. Report No.	2. Government Accession No.	3. Recipient's Catalog No.

4. Title and Subtitle	5. Report Date
Evaluation of the Purdue TDR Method for Soil Water Content and Density Measurement	12 April 2004
	6. Performing Organization Code
7. Author(s)	8. Performing Organization Report No.
Amr M. Sallam, Newel K. White, and Alaa K. Ashmawy	GEO-0301
9. Performing Organization Name and Address	10. Work Unit No. (TRAIS)
University of South Florida – Civil & Environmental Engineering 4202 E. Fowler Avenue, ENB 118 Tampa, FL 33620-5350	11. Contract or Grant No. BC-353-30
12. Sponsoring Agency Name and Address	13. Type of Report and Period Covered
Florida Department of Transportation **605 Suwannee St. MS 30** **Tallahassee, Florida 32399** **(850)414-4615**	**Final Report**
	14. Sponsoring Agency Code

15. Supplementary Notes

Prepared in cooperation with the USDOT and FHWA

16. Abstract

The use of time domain reflectometry to measure soil density and water content in geotechnical engineering is relatively new. The Purdue Method, now accepted as the ASTM Standard Method (D6780-02), outlines the procedure for obtaining the water content and the dry density of a given soil. The method relies on the measurement of the dielectric constant of the soil and relating it to the water content by propagating an electromagnetic wave through the soil.

In this report, an extensive research program is carried out to obtain the TDR calibration constants for sandy soils commonly encountered in Florida. Two ASTM TDR probes have been acquired, and their use in the lab and in the field has provided useful feedback for evaluating and improving the software. A critical assessment of the TDR method's accuracy and precision was also conducted. A correlation between the energy required to drive the TDR spikes and the soil's LBR is developed.

17. Key Word	18. Distribution Statement
TDR. Moisture content. Field density. LBR	**No Restriction** **This report is available to the public through the NTIS, Springfield, VA 22161**

19. Security Classif. (of this report)	20. Security Classif. (of this page)	21. No. of Pages	22. Price
Unclassified	**Unclassified**	127	

EVALUATION OF THE PURDUE TDR METHOD FOR SOIL WATER CONTENT AND DENSITY MEASUREMENT

Amr M. Sallam
Newel K. White
Alaa K. Ashmawy

Report prepared by
University of South Florida
Department of Civil and Environmental Engineering

for
Florida Department of Transportation
Tallahassee, Florida
Contract Number BC-353-30

April 2004

Acknowledgements

The authors would like to express their sincere appreciation to the State Materials Office personnel in Gainseville for their continuous support throughout the course of the project. In specific, the help of Dr. David Horhota, Ms. Renée Murch, Mr. Ronnie Lewis, Mr. Rick Venick, Mr. David Drawdy is acknowledged. The assistance of Dr. Vincent P. Drnevich and his research team at Purdue University is greatly appreciated.

Disclaimer

This report reflects the views of the authors only, not the Florida Department of Transportation. The content of this report do not constitute a standard, regulation, or specification.

Table of Contents

1. Introduction

1.1. Background

Compaction quality control is essential to virtually all earthwork and highway construction projects. This is done to ensure that design conditions are actually met in the field. It is essential to measure the in-place moisture content and density when evaluating the quality compaction control of an earthwork project. Currently there are many methods used for determination of these important parameters. This project is primarily concerned with the evaluation of a new method for measuring soil water content and density involving time domain reflectometry (TDR). Although TDR technology has been used for some time in other fields it is relatively new to the field of geotechnical engineering and is an altogether different approach to measuring soil properties than traditional geotechnical methods. Current methods used to measure soil density and moisture content rely, in most cases, on separate and independent tests that are often run on different soil samples. The TDR method measures both density and water content at the same time using the same soil sample by evaluating an electromagnetic wave that is sent into the soil medium. The TDR method for measuring in-situ water content and density was recently standardized in the form of ASTM D6780. The formation of ASTM D6780 is credited largely to work done at Purdue University; hence the method is commonly referred to as the Purdue TDR Method. The evaluation of this method will be the primary focus of the following chapters.

1.2. Problem Statement

The Purdue TDR method for measuring soil water content and density (ASTM D6780) is a relatively new method. Preliminary research indicates the method to be accurate and viable in terms of use in geotechnical applications. Extensive analysis and testing has yet to be carried out to determine the accuracy and utility of the TDR method. A program of testing and analysis must be implemented to properly evaluate the prospects of widespread implementation of the TDR method in the state of Florida.

1.3. Project Objectives

The specific objectives of this project are:

1) Performing an extensive literature review – A review of previous research carried out in the field of time domain reflectometry was conducted to gain competency in the understanding of the TDR basics. Review of current methods of determining soil moisture content and density was executed in an effort to compare the TDR method to those currently used. Particular attention was given to reviewing of research done at Purdue University as this project is part of a nationwide beta testing program to evaluate the method.
2) Familiarization with proposed Purdue TDR equipment – In an effort to aid in the improvement of the TDR method extensive use of the TDR equipment allowed for educated recommendations for method and equipment improvement.
3) Recommendations for soil constants "a" and "b" for common Florida soils – A good portion of research efforts was concentrated on testing soils common to Florida to establish reliable soil calibration constants that can be used in practice in the State. Studies on the effects of changing these soil constants were performed to evaluate the sensitivity of these parameters as they pertain to the TDR measured soil properties.
4) Establishing accuracy of TDR method – The TDR measurements were evaluated for accuracy after obtaining the soil constants. This was done by comparing measurements to calibrated soils with know properties.
5) Formulating a correlation of the LBR test with the TDR spike driving procedure – As an extension of the TDR research it was proposed to develop a correlation relating the LBR test with the TDR spike driving process. This was accomplished with the implementation of a field testing program.
6) Compare the TDR method to other field testing methods – The TDR method was compared to a limited number of other methods used to determine soil moisture content and density. This was done to evaluate the TDR method as opposed to other methods in terms of accuracy.

7) Compilation of data – The data collected along with future data generated by FDOT is to be compiled in an easy to use format. As such, a database was created for this purpose using Microsoft Access 2000.

1.4. Report Organization

This report is divided into 9 chapters:

- Chapter 2 is a literature review of current methods used for determining soil moisture content and density. It also reviews research done previously in time domain reflectometry and discusses the evolution of technology as it arrives to the field of geotechnical engineering. The chapter also reviews work done at Purdue University in the development of ASTM D6780. The dielectric constant, and its use as it pertains to TDR technology, is explored.
- Chapter 3 is a detailed explanation of the equipment and procedure involved for proper use of TDR equipment.
- Chapter 4 involves the determination of soil constants "a" and "b." The testing procedure and scope is described. Studies involving the effects of compaction energy on the soil constants are discussed as well as a theoretical evaluation of the effects on measured results due to variability in the soil constants. All results from testing are analyzed and discussed.
- Chapter 5 entails several studies designed to investigate the normalized and absolute accuracy of the TDR method. Actual data collected was compiled and used to determine possible sources of error. Tests involving operator dependency, variability in compaction and inherent error were carried out to investigate their effect on the accuracy of the method.
- Chapter 6 is primarily concerned with establishing a correlation of the TDR spike driving process to the in place LBR test. Methods and procedures used are reviewed here, and a recommended correlation is developed.
- Chapter 7 deals with the accuracy of current methods compared to the accuracy of the TDR method. Discussion here is based largely on the comparison of the different methods and offers suggestions as to why certain methods perform better than others.

- Chapter 8 discusses the formation of a database that was designed to handle the experimental data acquired during the testing phase of the project.
- Chapter 9 gives a summary of the report and reviews the project recommendations.

2. Literature Review

Several methods are currently being used to measure both soil density and water content. It is important to understand both the theoretical and functional background of these methods to properly evaluate the TDR method. A working understanding of current methods and limitations in their application is crucial in assessing the viability and practicality of the TDR method. The theory behind the use of time domain reflectometry is also discussed in this chapter. An effort to map out its course to the field of geotechnical engineering was made. A review of recent work done by Purdue University is discussed here briefly, and more in depth in chapters 3 and 4.

2.1. Different Methods Used to Determine the Moisture Content

Several methods are used for determining the soil moisture content in both field and laboratory. The following is a summary of these tests with commentary on the limitations of each.

2.1.1. Laboratory Determination of Water Content of Soil and Rock (FM 1-T 265)

Equivalent Methods: AASHTO T 265 and ASTM D2216

This method is widely known in geotechnical practice as the "Oven Dry Method". The principle behind the test is to determine both the weight of solids and water contained in a particular soil sample using heating processes. A conventional oven is utilized and kept at 110°C for 24 hours. The wet and dry weights of the soil are determined before and after drying. The apparatus consists of: a drying oven, balances, specimen containers, desiccators, and a container-handling device.

The procedure can be summarized in the following steps:

1. Determine and record the weight of empty container.
2. Select representative wet soil sample.
3. Place the wet specimen into the container and determine the weight of the wet soil plus the container.
4. Place the container in the oven at 110°C up to the desired time length (usually 24 hrs).

5. After the material has dried to constant mass, allow the container to cool down and determine the weight of the dry soil plus the container.
6. Calculate the water content of the specimen.

The method is not suitable for materials containing extraneous matter, some organic material that may be decomposed by oven dried, and materials containing gypsum. Material containing water with an amount of soluble solids will give higher mass of solids than the true value. This method should not use with contaminated soils unless adequate health and safety precautions are taken.

2.1.2. Microwave Oven Method (FM 5-535)

Equivalent Method: ASTM D 4643

This method is similar to the oven dry procedure, except for the use of a microwave oven instead of normal oven in drying the soil specimen.

The procedure can be summarized as follows:

1. Determine and record the weight of the empty container.
2. Select representative wet soil sample.
3. Place the wet specimen into the container and determine the weight of the wet soil plus the container.
4. Place the soil and the container in a microwave oven for about 3 min.
5. Remove the container, let it cool down, and determine the weight of the container plus soil.
6. With a small spatula carefully mix the soil.
7. Place the soil and the container in a microwave oven again for about 1 min.
8. Repeat steps 5, 6, 7 until the change between two constitutive mass determinations is insignificant.
9. Use the final mass measurement to calculate the water content.

Highly organic soils or soil containing oil or other contaminates may ignite during microwave drying. This method is best suited to minus No. 4 sized materials. The use of this method is not preferred when highly accurate results are required.

2.1.3. Direct Heating Method (ASTM D4959)

The idea behind this method is the same as the previous two methods, but the difference is in the use of direct heat; such as a hotplate, stove, or blowtorch for drying the sample. The method yield results faster than the oven dry method, but is less accurate. A moist sample is placed in a container and the weight is determined. The soil is allowed to dry using a direct heating and is then weighed. This procedure is continued until the change in the dry weight becomes negligible. Using this weight, the water content can be determined.

2.1.4. Calcium Carbide Gas Pressure Tester Method (FM 5-507)

Equivalent Methods: AASHTO T 217 and ASTM D4944

Referred to as the "speedy moisture content" method, this method is used for determining the water content of soil from the results of chemical reaction using calcium carbide as a reagent to react with the soil pore water. Two steel balls are used to ensure that the reagent can contact all the available water in the soil, producing Acetylene gas. A measurement is made of the gas pressure produced when a specified mass of wet soil is placed in a testing device with an appropriate volume of reagent and mixed. The apparatus consists of a calcium carbide pressure tester set, a small scoop, two steel balls, No. 4 sieve, a supply of calcium carbide, and clothing/safety equipment (Figure 2-1).

The procedure is summarized in the following steps:

1. Remove the cap from the testing chamber and place the desired amount of calcium carbide reagent along with the two steel balls into the testing chamber.
2. Obtain a specimen of soil according to the amount recommended by the device manufacturer.
3. Place the soil specimen in the testing chamber cap.
4. Shake the apparatus vigorously with a rotating motion so that the steel balls roll around the inside circumference and cause a grinding effect on the soil and reagent.
5. When the pressure dial gage needle stops moving, read the dial while holding the apparatus into a horizontal position.

6. Use the appropriate calibration curve to determine the corrected water content in percent of dry mass of soil.

Figure 2-1 Speedy moisture content device

The method is not accurate for highly plastic clays and soils containing minerals that dehydrate with heat. The test method is limited to soils with particles less than No. 4 sieve size. Flammable and explosive acetylene gas is involved, appropriate guidelines and rules should be followed by the operator.

2.1.5. Nuclear Method (Shallow Depth) (FM 1-T 238)

Equivalent Methods: AASHTO T 310 and ASTM D3017

In this method, a fast neutron source is applied to the surface of the soil. Using a surface slow neutron detector, the slowing ratio of the fast neutron is measured. Using this ratio and the calibration data, the moisture content of the soil is calculated. The hydrogen present in water is the main factor in this test. The apparatus consists of fast neutron source and detector, readout device, housing, reference standard, and site preparation equipment.

The procedure can be summarized in the following steps:

1. Standardize the instrument.
2. Select a test location and remove all disturbed materials (total contact is required).
3. Seat the instrument firmly and place the source in its position and take a reading.
4. Determine the ratio of the reading to the standard count and determine the in-place water content from the calibration and adjustment data.

The apparatus is more sensitive to water contained in soil near the surface (2-3 in). Hydrogen in forms other than water will cause reading in excess of the true value. Some chemical elements such as boron, chlorine, and minute quantities of cadmium cause measurements lower than the true value.

2.2. Different Methods Used to Determine In-place Density

Several methods are used for determining the in-place density of soil. Following is a summary of the test procedures and limitations for each of these methods.

2.2.1. Nuclear Method (FM 1-T 238)

Equivalent Method: ASTM D5195

The basic idea behind the nuclear method is to insert radiation tube containing source and detector of gamma radiation into the soil to the desired depth in order to measure the attenuation of gamma radiation through soil. The soil density is then determined by comparing the detected rate of gamma radiation with previously established calibration data. The apparatus consists of sealed source of high-energy gamma radiation, gamma detector, timed scale and power supply, cylindrical probe, reference standard, access tubing, and hand auger or drilling equipment (Figure 2-2).

The test procedure can be summarized as follows:

1. Drill the access tube hole and install the access tube.
2. Record the ground water table and if saturated conditions are expected, seal the tube.
3. Lower a dummy probe down the access tube to verify proper clearance.
4. Standardize the apparatus.

5. Seat the apparatus firmly on the access tube and take readings at the selected time period then, using the calibration data, determine the in-place density.

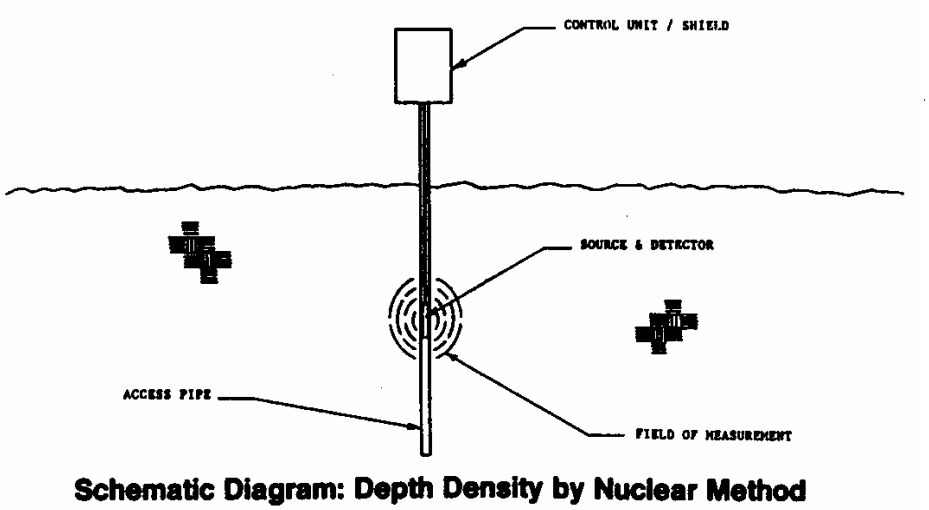

Figure 2-2. Nuclear method for determining in-field density

If the dry unit weight is required, the measurement of the in-place water content is needed. Measurements will be higher than the actual values if some elements with greater atomic numbers than 20 are encountered. Voids around the access tube can greatly affect the measurements. The equipment utilizes radioactive materials that may cause hazards, so proper precautions have to be taken by the users.

2.2.2. Nuclear Method (shallow depth) (FM 1-T 238)

Equivalent Methods: AASHTO T 310 and ASTM D3017

The shallow depth nuclear method is the same as the regular nuclear method, but either the source and detector remains on the surface (Backscatter Method) or one of them is at the surface while the other is at a known depth up to 300mm (Direct Transmission Method).

2.2.3. Sleeve Method (ASTM D4564)

The idea is to work a metal sleeve into the soil, removing the soil within the sleeve, and determining the dry mass of soil removed per linear inch of the depth of the excavation within

the sleeve. The mass per linear inch is related to the dry density of the in-place soil through a calibration equation. The sleeve method is used for soils that are predominantly fine gravel size, with a maximum of 5% fines, and a maximum grain size of ¾" (19 mm). For each particular soil type to be tested, calibration equation is predetermined. The test is applicable for cohesionless soils in a confined or limited space since the test method requires less working area compared to the other methods. The Sleeve apparatus consists of template, sleeve, measurement plate, and driver. Balances, driving equipment, and miscellaneous equipments are also required for the complete set up (Figure 2-3).

The procedure can be summarized in the following steps:

1. Prepare a smooth, level working area.
2. Put the template and place the beveled edge on the soil surface inside the hole of the template.
3. Place the driver on the sleeve and slowly rotate the sleeve in clockwise direction while pushing the sleeve into the soil.
4. Remove the driver, extract the soil from inside the sleeve, and place the extracted soil in a moisture-proof container.
5. Continue rotating and advancing the sleeve and extracting material in the sequence determining in the calibration procedure until the driver rests on the template.
6. Flatten the bottom of the hole as much as possible, place the measurement plate on the soil at the bottom of the hole, and rotate gently to seat it.
7. Measure and record the depth of the hole from the top of the measurement plate to the top of the template.
8. Determine the mass of the soil removed from the test hole and record.
9. Determine the water content of the removed material from the hole.
10. Calculate the dry mass per inch of the test hole.
11. Using the calibration equation, calculate the in-place dry density.

Consistency in the gradation and particle angularity of the soil being tested is critical to the test. The test is operator sensitive. The sleeve should be checked periodically for wear.

2.2.4. Drive-Cylinder Method (FM 1-T 204)

Equivalent Methods: AASHTO T 204 and ASTM D2937

The idea behind this method is to drive a thin-wall steel cylinder into a smoothed soil surface using a falling hammer. Following that, the soil has to be dug out around the cylinder to allow for removal. Using a straightedge, the ends of the cylinder have to be trimmed.

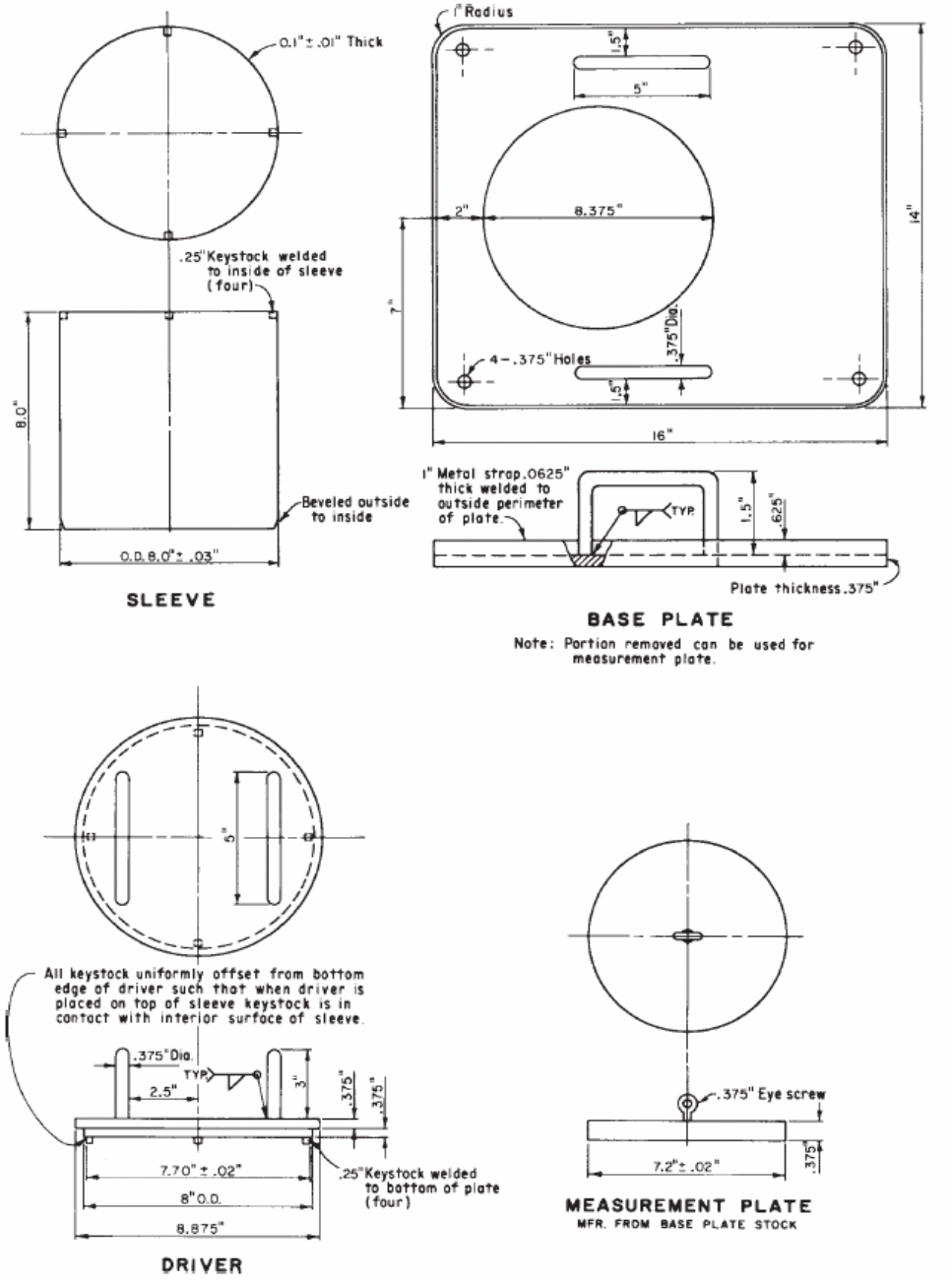

Figure 2-3. Sleeve method for determining in-field density

Knowing the weight and the volume of empty cylinder and the weight of the cylinder and removed soil, the unit weight of the soil can be determined. To get the dry unit weight of the soil, the moisture content has to be determined using a standard method. The apparatus consists of a drive cylinder that meets the clearance ratio requirements of Hvorslev, drive head, steel straightedge, shovel, balances, drying equipment, and miscellaneous equipment (Figure 2-4). The test is not applicable for organic soil, very hard natural soils, heavily compacted soils, and soils which contain appreciable amount of sand. The cutting edge of the cylinder should be checked after each test to ensure that it is still sharp. If any damage occurs to the cylinder edge or body, the test results should be discarded.

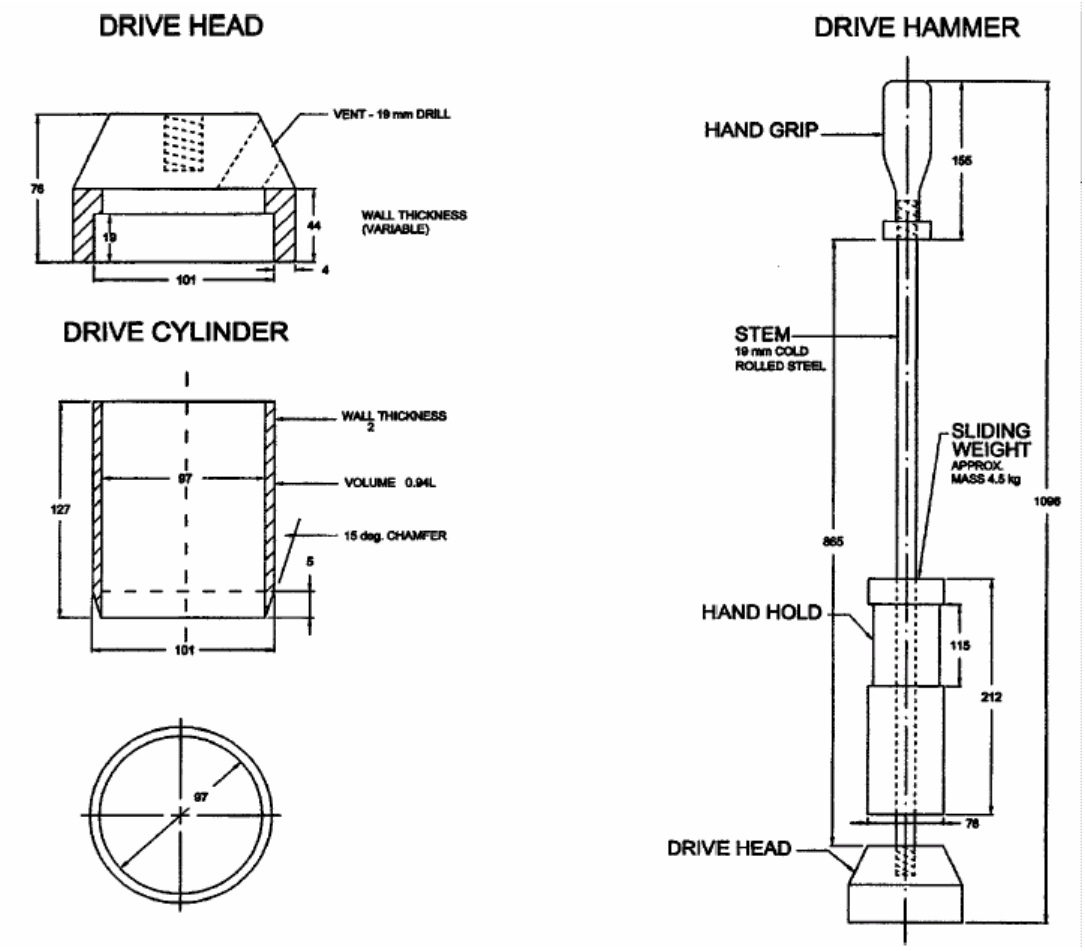

Figure 2-4. Drive cylinder for determining in-field density

2.2.5. Sand-Cone Method (AASHTO T 191)

Equivalent Method: ASTM D1556

In the Sand Cone Method a hole is excavated in the ground and the excavated soil is weighed. The volume of the hole is then determined using standard sand replacement. The used sand should be dry, clean, uniform, uncemented, durable, and free flowing. Knowing the weight of the standard sand filling the hole and the density of the sand, the volume of the hole can be calculated. The density of the excavated soil can be computed accordingly. To obtain the dry density of the soil, the water content of the extracted portion is determined using a standard method. Finally the dry density of soil can be determined using both wet density and water content. The apparatus consists of sand-cone density apparatus, standard sand, balances, drying equipment, and miscellaneous equipment (Figure 2-5).

The procedure can be summarized in the following steps:

1. Select a test location and prepare the surface.
2. Seat the template on the plane surface and dig a hole through the center hole of the template.
3. Invert the sand-cone apparatus and seat the sand-cone funnel into the flanged hole of the template. Allow the sand to flow into the hole and the cone by opening the valve.
4. Determine the weight of the apparatus with the remaining sand. Knowing the weight of the apparatus when it is full of sand and the standard sand weight required to fill the cone and the template, we can get weight of sand in the hole. The volume of the hole (soil) and the wet density of the soil can therefore be determined.
5. The dry density of soil can be determined knowing both wet density and water content.

The method is not suitable for saturated, soft, organic, deformable or highly compressible soils. It is also not suitable for soils that contain appreciable amount of rock or coarse materials (more than 38mm).

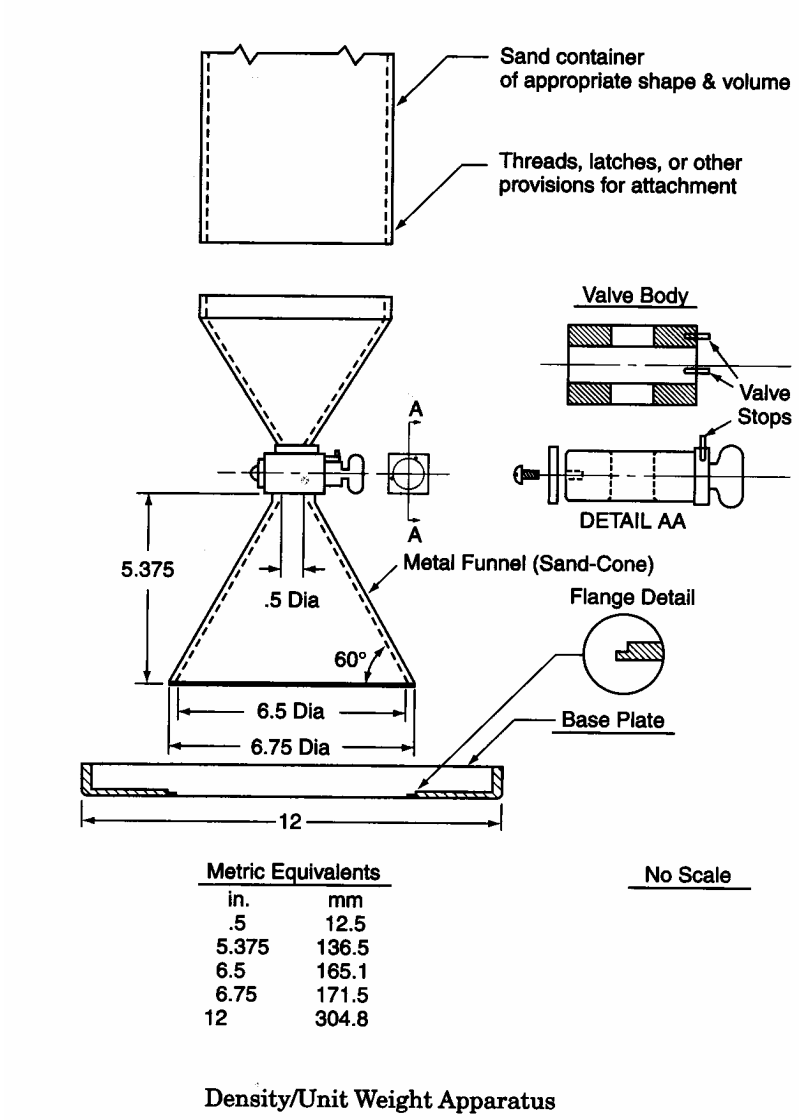

Figure 2-5. Sand cone method for determining in-field density

2.2.6. Rubber Balloon Method (ASTM D2167)

The concept behind the rubber balloon method is the same as the sand-cone method, but instead of replacing the soil with standard sand, water is used. A flexible membrane filled with water and connected to a water-filled calibrated vessel is used to measure the volume of the hole after extracting the soil. The equipment consists of rubber balloon apparatus, template, balances, drying equipment, and miscellaneous equipments (Figure 2-6).

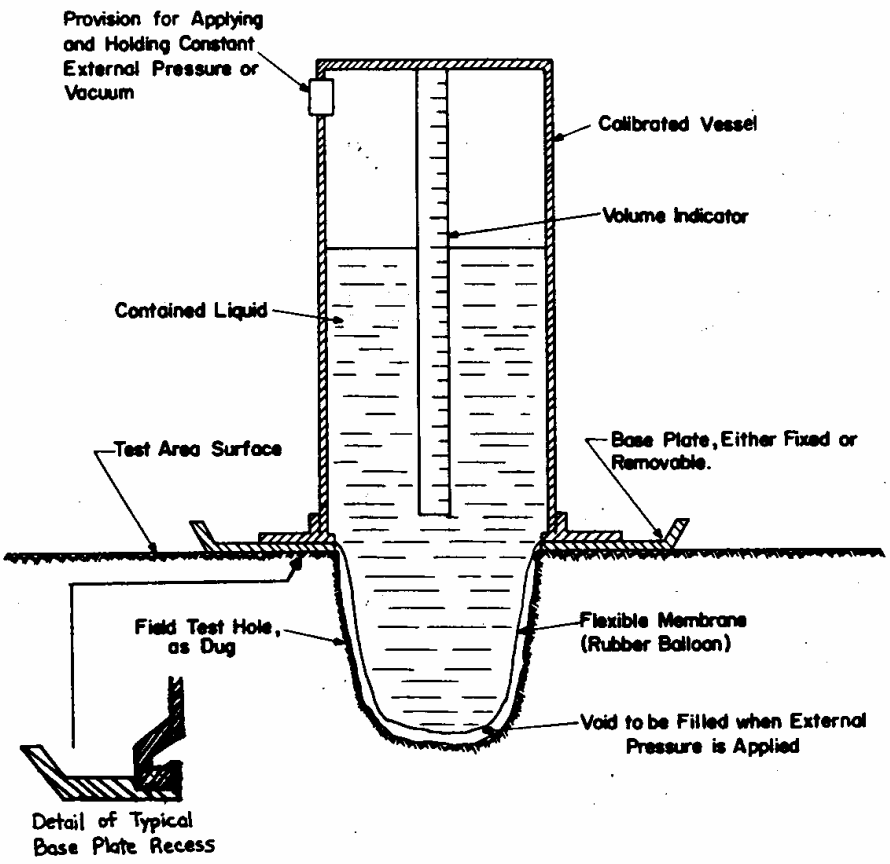

Figure 2-6. Rubber balloon method for determining in-field density

The procedure can be summarized as follows:

1. Prepare the surface at the test location.
2. Assemble the template and the rubber balloon apparatus (using the same pressure and surcharge load used during calibration) and take an initial reading on the volume indicator.
3. Dig a hole within the template.

4. Place the apparatus over the template and apply the same pressure and surcharge load used during calibration and take final reading.
5. Using the two readings, the volume of the hole (soil) can be determined. Knowing the weight of the extracted soil, the wet density can be calculated.
6. The dry density of soil can be determined knowing both wet density and water content.

Prior to first use, the apparatus should be calibrated. The suitability of this method is the same as the sand-cone method.

2.2.7. Other Methods

There are two more methods to measure the density of soil in-place. These methods are the sand replacement method in a test pit and the water replacement method in a test pit. These tests rely on the same concepts as the sand-cone and the balloon methods However, the sand-cone and the balloon methods are more advanced and widely used.

2.3. Summary of Existing Methods

A summary of key points of the more commonly run tests is displayed in Table 2-1. For the purposes of this report, the nuclear method is used most frequently. The nuclear method requires training and special licensing to operate and field measurements are only as good as the calibration of the device. On the other hand, the Sand Cone method relies heavily on the skill of the test operator. Further discussion on the comparison of these tests with the TDR method will be addressed in Chapter 7.

Table 2-1. Comparison of current methods.

Test	Application	Required Time	Major Source of Error
Oven Dry	Water Content	24 hours	Considered as baseline measurement
Speedy Moisture	Water Content	15-20 min + calibration	Operator's ability to perform test correctly
Nuclear Method	Wc and Density	30 min + calibration	Highly dependant on proficient calibration
Sand Cone	Density	30 min + calibration	Operator dependant

2.4. Time Domain Reflectometry Basics

O'Connor and Dowding (1999) define Time Domain Reflectometry (TDR) as "a broad range remote sensing electrical measurements to determine the location and nature of various reflectors." TDR is similar to radar in that a short electromagnetic pulse is first emitted, and a reflection is returned when an anomaly is encountered. Measuring the time between transmission and receipt and knowing the speed of light, the distance to the object could be calculated. To this end, TDR devices are sometimes called cable radar. The main two features of the TDR reflected waveform are the travel time through the probe, and the steady state voltage amplitude of the waveform at long times. Additional details of the reflecting object can be obtained from detailed analysis of the echo. TDR technology has been used to locate faults in transmission lines since the 1930's (Lin et al., 2000). Freller-Feldegg (1969) used them for measuring permittivity of liquids. Developments made by Topp et al. (1980) demonstrated a "unique relationship between the relative dielectric constant and the volumetric water content for a large range of soils" (Dasberg and Dalton, 1985). This research proved to be very promising for water content measurement in the field and for use of TDR technology in geotechnical applications.

2.4.1. Complex Dielectric Permittivity

Electrical permittivity can be measured by placing the material between two plates of a capacitor or into a coaxial line and measuring the complex impedance. For a complete characterization, a number of measurements over a wide frequency range are required. The same information could be obtained by making measurements in time domain instead of frequency domain using time domain reflectometer (TDR) (Fellner-Feldegg, 1969). Since this time, TDR has been used extensively to measure the complex dielectric permittivity of polar and non-polar liquids (Giese and Tiemann, 1975; Clarkson et al, 1977). Further developments by Topp et al. (1980) led to the development of a relationship between the complex dielectric constant and water content of soil. This relationship measured the real portion of the dielectric constant and assumed the imaginary losses to be negligible. The relationship developed was in fact between the apparent dielectric constant and soil water content. This relationship between the apparent dielectric constant and water content led to several other developments in TDR technology.

2.4.2. TDR waveform

Maxwell's equations are the source for and derived equation to solve electromagnetic fields. The propagation of an electromagnetic field through a transmission line is governed by the wave equation derived from Maxwell's equations. Drnevich et al. (2000) stated that: "There are two important components of the wave equation solution; the characteristics impedance, Z, and the propagation constant, (γ). The characteristics impedance is the ratio of voltage to current propagating along the line. It is a function of the geometry of the transmission line and the dielectric permittivity of the insulating material." It can be derived, for a coaxial line, as:

$$Z = \frac{\ln\left(\frac{b}{a}\right)}{2\pi}\sqrt{\frac{\mu_0}{\varepsilon_0}}\frac{1}{\sqrt{\varepsilon_r^*}} = \frac{Z_p}{\sqrt{\varepsilon_r^*}} \qquad (2\text{-}1)$$

Where "b" is the inner diameter of the outer conductor, "a" is the outer diameter of the inner conductor, ε_0 is the vacuum permittivity (8.854×10^{-12}), μ_0 is the vacuum permeability ($4\pi \times 10^{-7}$ H/m), ε_r^* is the equivalent dielectric permittivity, and Z_p is defined as the impedance of the same line filled with air as the medium (Krauss, 1984).

The propagation constant is the other intrinsic property of a transmission line. It is only a function of the dielectric permittivity of the insulating material. It can be derived, for a coaxial line, as:

$$\gamma = \frac{j2\pi f}{c}\sqrt{\varepsilon_r^*} = \alpha + j\beta \qquad (2\text{-}2)$$

In which c is the velocity of the electromagnetic waves in free space, and α and β are the real and imaginary parts of the propagation constant, respectively. The real part represents the attenuation of the wave, whereas the imaginary part is the spatial frequency, which gives the velocity of wave propagation when divided by temporary frequency ($2\pi f$). The TDR waveform recorded by sampling oscilloscope is a result of multiple reflections and dispersion. A typical TDR output waveform is shown in Figure 2-7.

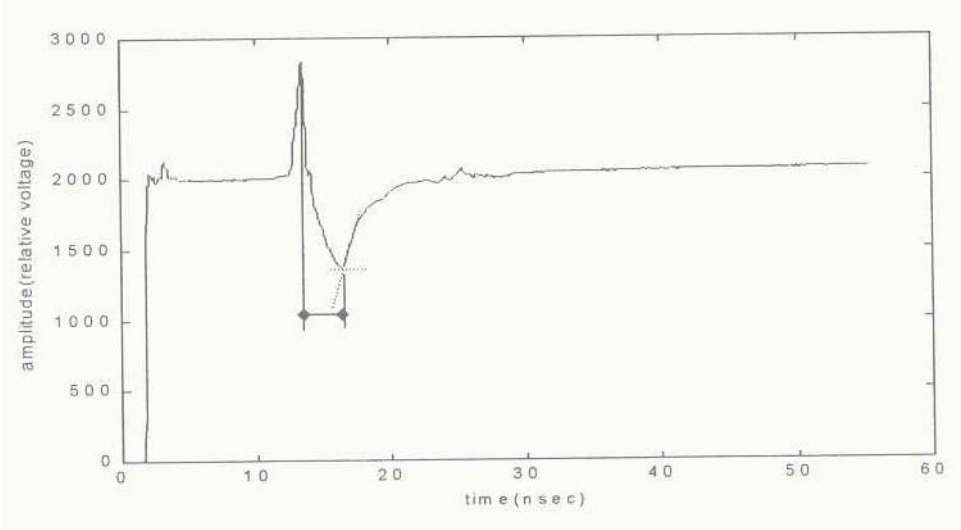

Figure 2-7. Typical TDR output voltage

2.4.3. Developments in TDR Technology

Topp et al. (1980) suggested that research be carried out to develop transmission line components that would be sufficiently accurate for water content measurement purposes. Several research projects were carried out to evaluate different transmission line configurations (Ledieu et al., 1986; Topp et al., 1982; and Dasberg and Dalton, 1985). Although results from these tests indicated a reliable relationship between the dielectric constant to water content, the need for a reliable and routine field technique was still evident. Zeglin et al. (1989) studied several coaxial probe configurations and found that three and four wire configurations were superior to a two wire system. Studies investigating cable length, quality and type of probe and cable dimensions were carried out by Heimovaara (1993) to determine their influence on the accuracy of TDR measurements. Improvements in calibration were made by Dirksen and Dasberg (1993), which accounted for certain differences in mineralogy. These and other improvements of the TDR method led to research done at Purdue University (Drnevich et al., 2000) in the development of the Purdue TDR method. There work recently warranted the acceptance of the method as ASTM standard D 6780 in 2002. A more in depth discussion of the developments made at Purdue University will be dealt with in Chapter 4.

2.4.4. Equipment

TDR instruments (sometimes referred to as cable radar) basically consists of a pulse generator and a sampling oscilloscope. An electrical pulse along a coaxial cable is sent by the generator and observed by the oscilloscope (Drnevich et al, 2000). The reflected pulse is measured and analyzed to compute the apparent dielectric constant. Figure 2-8 shows the configuration of typical TDR system, whereas Figure 2-9 shows an example of a TDR system used for measuring soils dielectric properties.

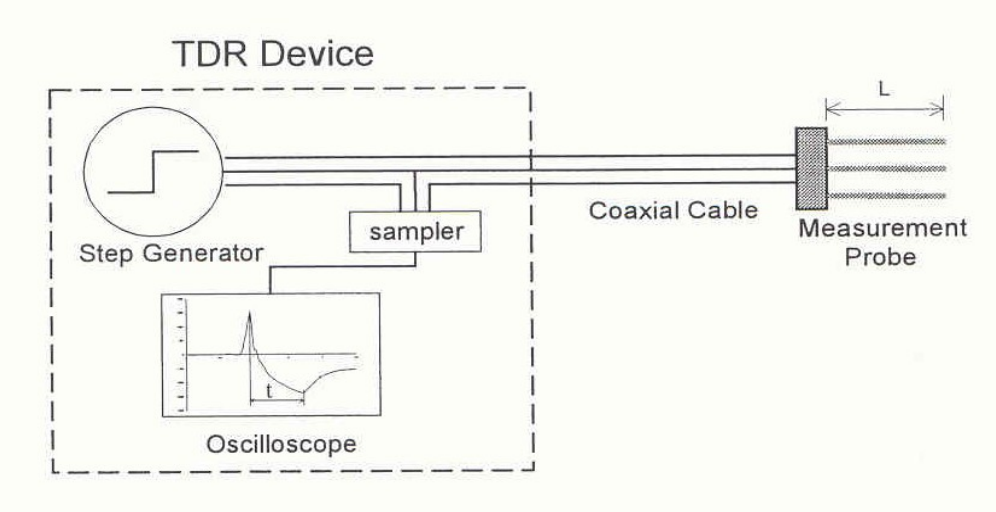

Figure 2-8. TDR system configuration

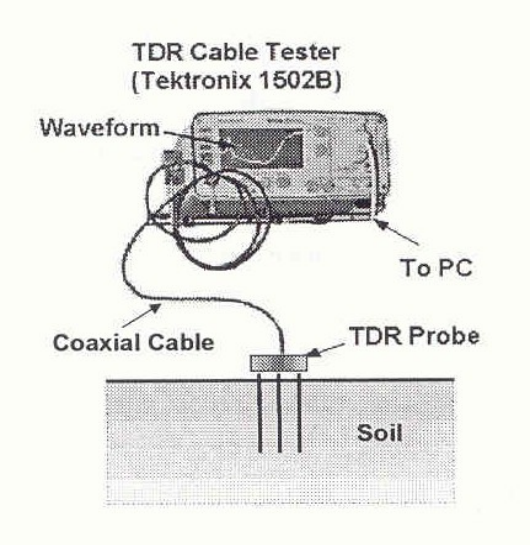

Figure 2-9. Example of TDR system used for soils

2.4.5. Concerns with TDR Measurement

Significant research has been carried out to determine possible sources of error in TDR measurements. Particularly problems with "lossy" materials and multiple reflections have received attention. Mojid et al. (2003) studied problems with geotechnical TDR measurement in lossy materials. The reflected TDR wave consists of a real and imaginary portion. Current TDR methods assume that the imaginary portion of the TDR wave can be neglected and the measured real portion is adequate for measurement. This is accomplished by operating in the frequency range of 1 MHz to 1 GHz. In this range the frequency does not strongly affect the measured real portion of the dielectric constant. This assumption is consistent with research carried out by Davis and Annan (1977). However, in highly conductive materials a dispersive or lossy phenomenon is observed. These lossy or dispersive materials are mostly fine-grained materials or conductive materials where large amounts of ions are present in the pore water (Mojid et al. 2003). Yanuka et al. (1988) also discuss the significant error that arises when taking TDR measurements in conductive materials. Developments at Purdue University have addressed the problem of testing lossy material. The addition of a protective sleeve over the TDR probes can be used to minimize the reflected wave loss into conductive material, thus minimizing wave reflection loss. The result is a more accurate representation of the actual dielectric constant from the apparent dielectric constant. Studies carried out for the purposes of this report did not include testing of dispersive materials, due to their scarceness in the State of Florida. Research was primarily concerned with typical Florida construction soils (sands). Recommendations in this report are made accordingly and do not apply to highly lossy fine grained soils.

3. Equipment and Procedure

3.1. Introduction

As discussed in the previous chapter, the use of TDR technology is relatively new to the field of geotechnical engineering. Several advancements and improvements to the method led Purdue University researchers to develop a TDR measurement system for widespread use. Siddiqui and Drnevich (1995) studied the factors which influence the wave transmission. Based on the results obtained from their study, transmission line components were designed and built to be robust, easy to use, and provide superior wave transmission for field measurements of moisture content and dry density.

The system configuration of the TDR device is shown in Figure 3-1. The TDR device used in this study is ASTM Standard compliant, and was acquired from Purdue University (Figure 3-2).

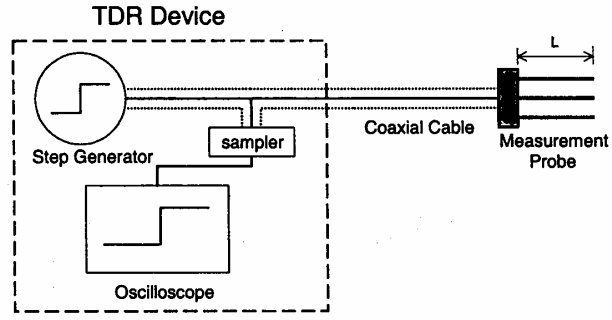

Figure 3-1. TDR system configuration. [Source: Lin et al. (2000)]

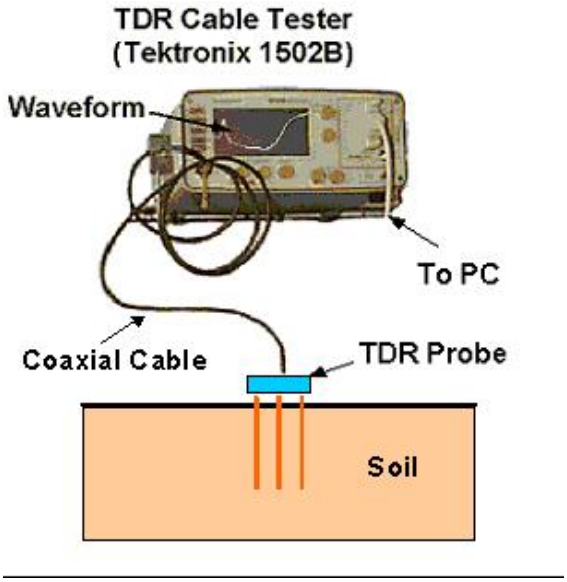

Figure 3-2. Example of TDR system [Source: TDR User's Manual]

3.2. TDR Prototype Equipment

TDR device consists generally of three main parts:

1 - A coaxial cable.

2 - A coaxial head (CH).

3 - Either a coaxial cylinder (CC) or multiple rod probe (MRP).

The coaxial cable consists of a center conducting wire surrounded by a cylinder casing, which acts as the outer conductor (Lin et al., 2000). The coaxial head (CH) consists of three parts; a coaxial line similar to the actual coaxial cable, a solid cylindrical head with an insolating material, and multiple rod section that contains three perimeter rods and one center rod without any insolating material. Figure 3-3 shows the main components of the coaxial head. The coaxial head (CH) serves as a transition between the actual coaxial cable and coaxial cylinder (CC)/multiple rod probe (MRP). It could be used for both field probe and compaction mold. The coaxial head (CH) has one center stud and three perimeter studs. The center stud and two of the perimeter studs are of the same length (21mm), whereas the third perimeter stud length can

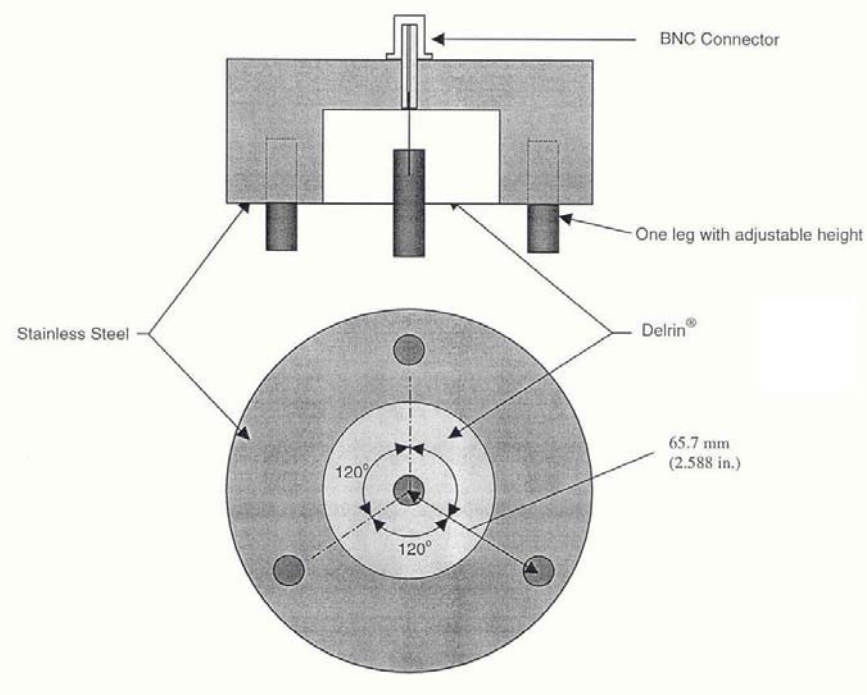

Figure 3-3. Configuration of coaxial head [Source: TDR User's Manual]

be adjusted to ensure full contact with the four probes in field or the ring and center probe in mold.

The coaxial cylinder (CC) transmission line consists generally of a CC mold, a CC ring, and a central rod. The CC mold looks like the compaction mold with an inner diameter of 101.6 mm and a length of 232.87 mm. The CC ring has to fit on top of the CC mold. It works as an extension during the compaction stage and as a part of the coaxial cylinder (CC) during the measuring stage. The central rod is made of stainless steel and has a length of 234 mm and a diameter of 8 mm. A guide template is used to guide the central rod during driving stage. Figure 3-4 shows the coaxial cylinder configuration.

The multiple rod probe (MRP) consists of one central rod and three perimeter rods, which have to be inserted into the soil so that the soil acts as an insolating material. The configuration of the MRP rods has to be the same as the coaxial head (CH). This is achieved with the help of a

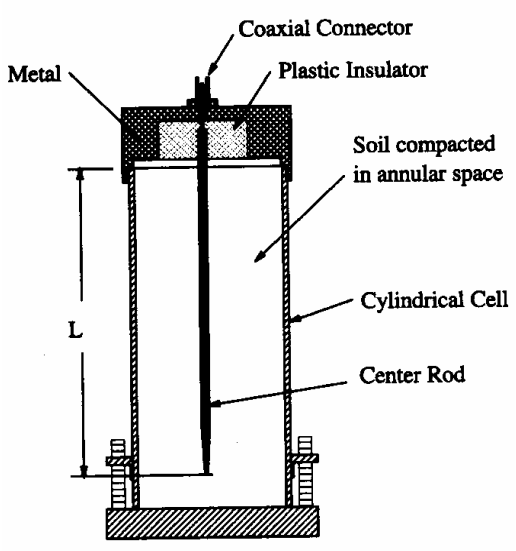

Figure 3-4. The coaxial cylinder (CC) transmission line
[Source: Siddiqui and Drnevich (1995)]

temporary detachable template used to locate the probes in the driving stage. After the spikes driving completed, the template is removed and the coaxial head (CH) is placed on top of the spikes heads and a TDR measurement is taken at this stage. Figure 3-5 shows the multiple rod probe (MRP) components.

The most important output from the TDR system is the waveform. With a high resolution waveform output the accurate Interpretation of the waveform then becomes critical in extracting information from the material tested. Lin et al. (2000) stated the following: "For the proposed TDR system, tests have been conducted to verify the first and second reflection points. Discontinuities in impedance occur at the connection of the coaxial cable and the CH, inside the CH, at the top of the soil surface, and at the end of the CC or MRP as shown in Figure 3-6. The goal of the waveform analysis is to find the reflection points that occur at the soil surface (point 1), and at the end of the CC or MRP (point 2). The first reflection point is at the peak of the waveform right before it starts to drop. The second reflection point will be around the portion of the waveform where it starts to rise to the steady state." Waveform interpretation is performed using a notebook connected to the TDR device.

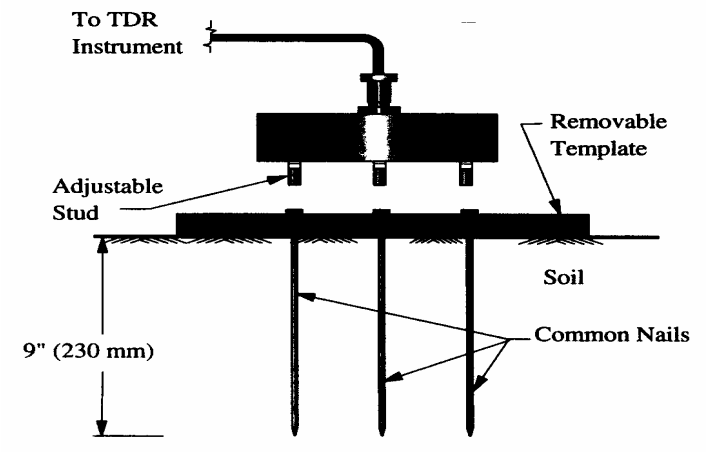

Figure 3-5. The multiple rod probe (MRP)
[Source: Siddiqui and Drnevich (1995)]

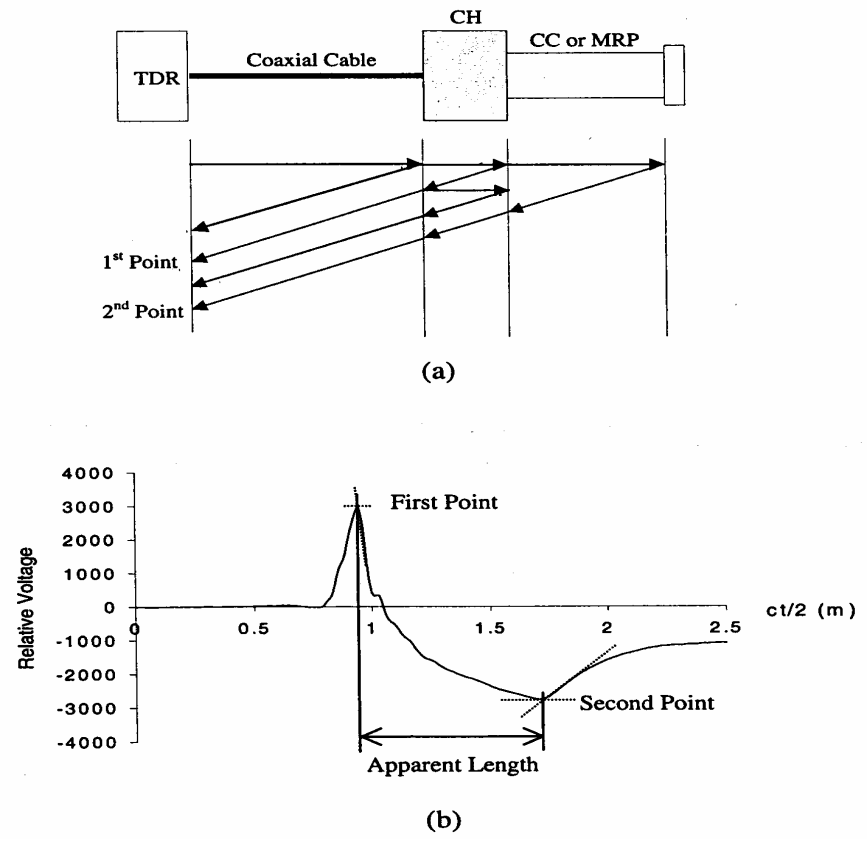

Figure 3-6. Interpretation of waveform measured by the TDR system
[Source: Lin et al. (2000)]

3.3. Procedure

1. Try to level the surface of the tested soil as possible.
2. Place the template on the leveled soil surface and begin to drive the spikes using the attached steel hammer, Figure 3-7. It is preferable to begin driving the perimeter spikes simultaneously. After you are done with the perimeter spikes, drive the central spike.
3. Remove the template exposing the heads of the four spikes (Figure 3-8).
4. Place the coaxial head (CH) on the heads of the four spikes. It is very important to ensure full contact between the four studs of the coaxial head and the four spikes heads. This will be achieved with the help of the adjustable perimeter stud. After placing the coaxial head and ensuring contact, make a measurement of the dielectric constant of the soil in-situ (Figure 3-9).
5. Remove the four spikes and excavate soil from zone within spikes area as quick as possible to maintain the same moisture content (Figure 3-10).
6. Compact the removed soil into a mold with a pre-measured weight and pre-calibrated volume using a hand tamper in six layers (Figure 3-11). In order to obtain a reasonably uniform specimen, the compacting energy has to be increased from the bottom layer to the top layer gradually. This result can be achieved by either increasing the force per drop applied to the tamper as layers are advanced or by increasing the number of tamps per layer as layers are advanced, keeping the same force and drop for each tamp. The second choice was chosen and the number of tamps per layer was increased from 10 to 20 gradually from the first to the sixth layer. The energy for one tamp was maintained constant by ensuring free drop for the tamper from a 2 inch height.
7. Determine the mass of the mold and the soil to get the soil density (Figure 3-12).
8. Use the plastic cylinder guide template and drive the central stainless steel rod into the mold using the acrylic.
9. Place the adaptor ring on the mold.
10. Place the coaxial head (CH) on the adaptor ring. Take a TDR measurement and determine the mold dielectric constant for the soil (Figure 3-13).

Figure 3-7. Driving spikes through template into soil surface.
[Source: TDR Manual]

Figure 3-8. Removal of the template exposing the heads of the four spikes
[Source: TDR Manual]

Figure 3-9. Placement of coaxial head (CH) on spikes heads
[Source: TDR Manual]

Figure 3-10. Removal of soil from zone enclosed by the driven spikes
[Source: TDR Manual]

Figure 3-11. Soil from in-place test compacted in the mold
[Source: TDR Manual]

Figure 3-12. Placement of compaction mold filled with soil on the scale
[Source: TDR Manual]

Figure 3-13. Coaxial head measuring in-mold dielectric constant
[Source: TDR Manual]

3.4. TDR Software

The TDR software was designed with a user-friendly interface. It consists of two main screens. The first screen is the In-Situ MRP Test in which the user has to input project name, contract No., operator, test location, test No., temperature, and type of soil (cohesive or cohesionless). The **Get Waveform** button is then pushed in order to obtain a waveform (Figure 3-14). The soil dielectric constant in field, $K_{a,field}$, is calculated as the **Calculate** button is pushed. After the value of is obtained, the file has to be saved and the **Go To Mold** button has to be pushed.

The second screen is the CC Mold Test in which the user has to input mass of empty mold, mass of mold and wet soil, volume of mold, and soil constants a and b. The **Get Waveform** button is then pushed in order to obtain a waveform (Figure 3-15). The soil dielectric constant in mold, $K_{a,mold}$, is calculated as the **Calculate** button is pushed. In order to get the final results (dry density in field and moisture content), the **Compute** button has to be pushed. After the final values are obtained, the file has to be saved with the same name of the In-Situ file.

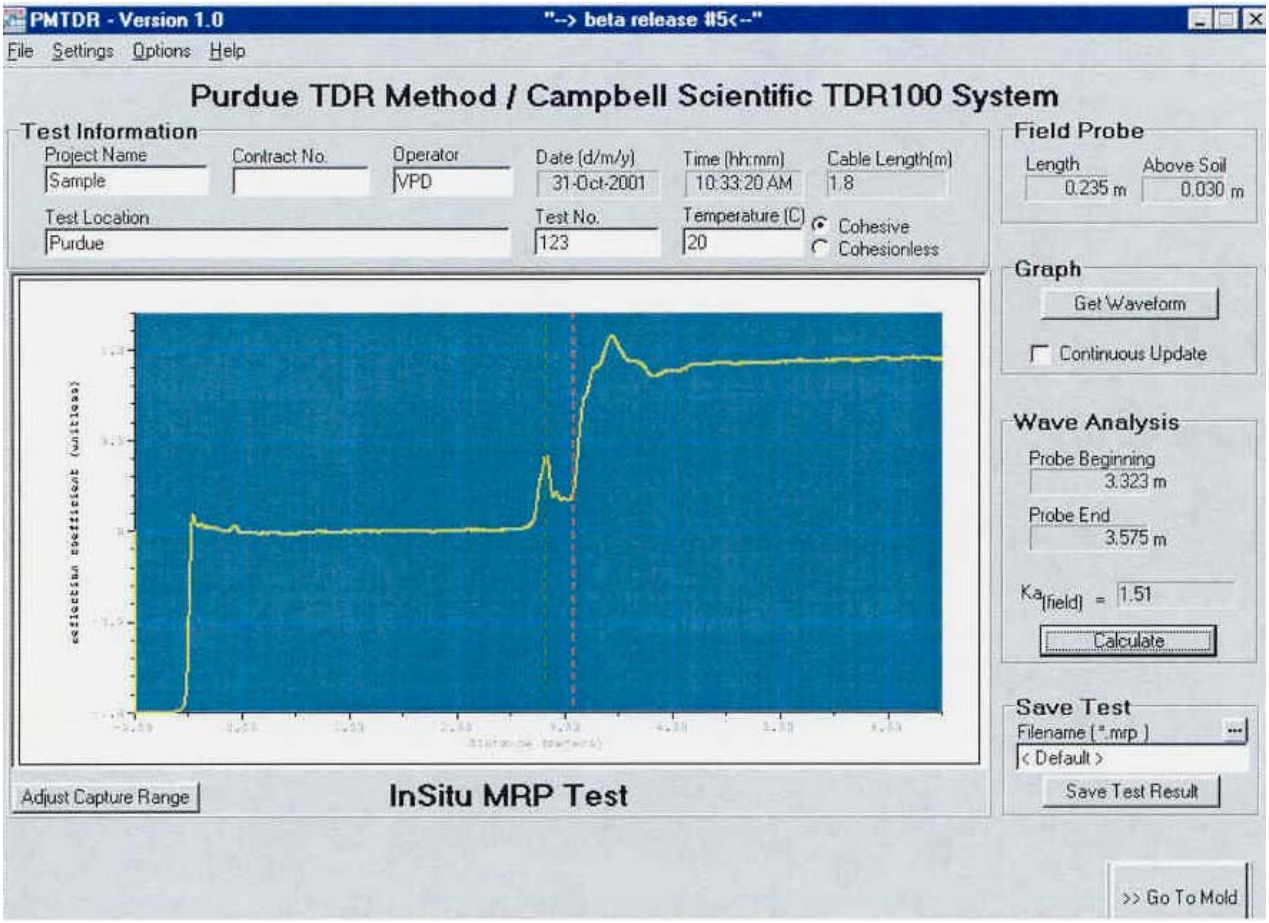

Figure 3-14. In-field Test Screen. [Source: TDR Manual]

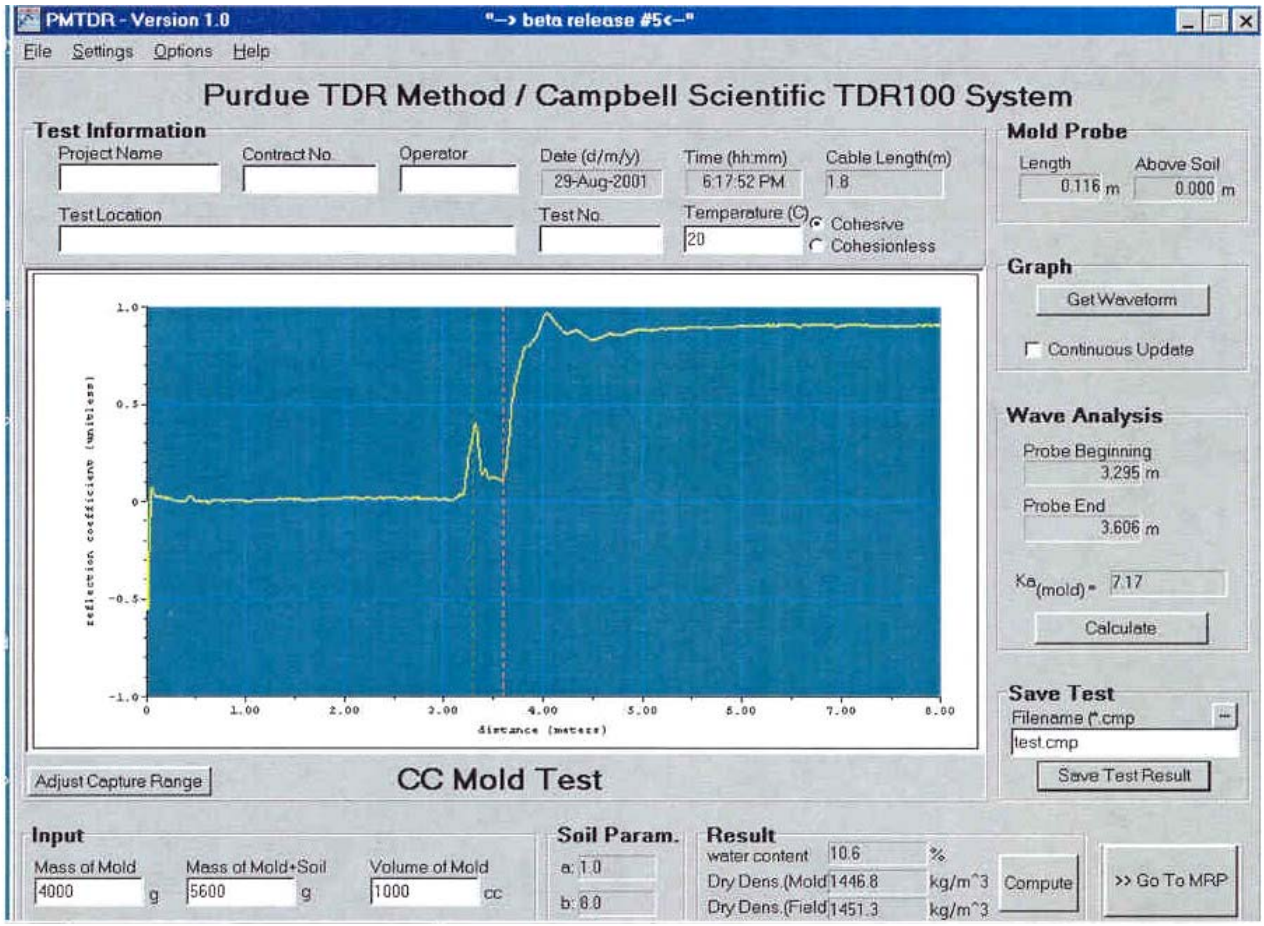

Figure 3-15. In-Mold Test Screen. [Source: TDR Manual]

4. Evaluation of Soil Parameters "a" and "b"

4.1. Introduction

The soil constants "a" and "b" are parameters that relate the gravimetric moisture content to the soil dielectric constant through the equation developed by Siddiqui and Drnevich (1995), which will be introduced later in this chapter. The aim of this chapter is to evaluate these parameters for typical Florida construction soils. The dependency of these constants on soil type, temperature, and dry density will be addressed. In this chapter, results from an experimental study on different soil types will be presented and analyzed. The soils were provided by the FDOT State Materials Office and the District One Materials Office. In order to determine the constants "a" and "b", a series of TDR tests in the mold were performed at different moisture contents for each particular soil. Based on the findings for several soil types, average values for soil parameters are recommended for use in conjunction with the TDR method for typical Florida construction soils.

4.2. Theoretical Background

There are basic empirical equations, which have been developed to correlate the volumetric or gravimetric moisture content to the soil dielectric constant. The volumetric water content (θ) is defined as:

$$\theta = \frac{V_{water}}{V_{solids}} \tag{4-1}$$

Whereas the gravimetric water content (w_c) is defined as:

$$w_c = \frac{W_{water}}{W_{solids}} \tag{4-2}$$

The two are related by the following equation:

$$\theta = w_c \frac{\rho_d}{\rho_w} \tag{4-3}$$

Topp et al. (1980) developed an equation to describe the relationship between volumetric moisture content (θ) and apparent dielectric constant K_a:

$$\theta = -0.053 + 2.92 \times 10^{-2} K_a - 5.5 \times 10^{-4} K_a^{\ 2} + 4.3 \times 10^{-6} K_a^{\ 3} \tag{4-4}$$

As an alternative to Eqn. (4-4), Ledieu et al. (1986), Alharthi and Lange (1987) proposed a linear calibration equation:

$$\sqrt{K_a} = a + b\theta \tag{4-5}$$

Where a and b are calibration constants: a = 1.545 and b = 8.787 according to Ledieu et al. (1986); a = 1.594 and b = 7.83 in Alharthi and Lange (1987). Lin et al. (2000) stated that "Topp's equation is essentially the same as Eqn. (4-5) in the normal range of water content ($0.05<\theta<0.5$), with a = 1.56 and b = 8.47".

Ledieu et al. (1986) demonstrated that an improvement could be added if the bulk dry density is included in the equation as:

$$\sqrt{K_a} = a\rho_d + b\theta + c \tag{4-6}$$

Where a, b, and c are calibration constants: a = 0.297, b = 8.79, and c = 1.344.
By normalizing the effect of density, Siddiqui and Drnevich (1995) developed an equation similar to Eqn. (4-6), with c = 0. In their equation, the relationship between apparent dielectric constant and gravimetric moisture content is expressed as follows:

$$\sqrt{K_a}\frac{\rho_w}{\rho_d} = a + bw_c \tag{4-7}$$

Lin et al. (2000) noted that Equations (4-6) and (4-7) "provide better calibration than equations (4-4) and (4-5) because the density effect is taken into account". The previous empirical equations were obtained under different density conditions and are therefore inconsistent in terms of interpretation of the constants.

On the other hand, theoretical mixing formulas were found to be satisfactory to produce better calibration, according to Dirksen and Dasberg (1993). Birchak et al. (1974) proposed a volumetric mixing model from which a four-phase soil mixing formula could be obtained:

$$K_a^{\alpha} = \left(\frac{\rho_d}{\rho_s}\right)K_s^{\alpha} + (\theta - \theta_{bw})K_{fw}^{\alpha} + \theta_{bw}K_{bw}^{\alpha} + \left(1 - \frac{\rho_d}{\rho_s} - \theta\right)K_{air}^{\alpha} \tag{4-8}$$

Where K_s, K_{fw}, K_{bw}, and K_{air} are dielectric constants of soil solid, free water, bound water, and air respectively; ρ_s is the soil solids density; θ_{bw} is the volumetric bound water content; and α is the fitting parameter that accounts for the geometry of the medium with respect to the applied electric field ($\alpha = 0.5$, for an isotropic homogenous medium). Dobson et al. (1984) approximated the fraction of the tightly bound water covering the mineral surfaces as:

$$\theta_{bw} = l\delta\rho_d S \tag{4-9}$$

Where l is the number of molecular water layers of tightly bound water, $\delta = 3\times10^{-10}$ m is the thickness of one molecular water layer, and S is the specific surface of the soil particle. Substituting $\alpha = 0.5$ and θ_{bu} in Eqn. (4-8):

$$\sqrt{K_a} = \left(\frac{\sqrt{K_s} - \sqrt{K_{air}}}{\rho_s} + \left(\sqrt{K_{bw}} - \sqrt{K_{fw}}\right)l\delta S\right)\rho_d + \left(\sqrt{K_{fw}} - \sqrt{K_{air}}\right)\theta + \sqrt{K_{air}} \tag{4-10}$$

Equation (4-10) is the theoretical basis and the general case for empirical Eqns. (4-4), (4-5), (4-6), and (4-7). Lin et al. (2000) stated that, "if the soil type effect is neglected, Eqn. (4-10) reduces to Eqn. (4-6). If soil type and density effects are both neglected, Eqn. (4-10) becomes Eqn. (4-5)". It is evident that many empirical equations are available. They are different because they are determined under different experimental conditions or address different considerations. Siddiqui and Drnevich (1995) performed a laboratory work and indicated only marginal benefits in using one calibration equation to another. Their experiments were limited to a range in density of 1.40 to 1.95 Mg/m^3 (87 to 122 pcf).

Lin et al. (2000) performed TDR tests on actual compacted soils over the typical range of compacted densities to evaluate the calibration equations. The tests were conducted on soils taken from actual construction sites in Indiana. The results of their work compared favorably with results published by Topp et al. (1980) which are displayed in Fig. 4-1. The standard error was 1.9% where the maximum error was 4.0%.

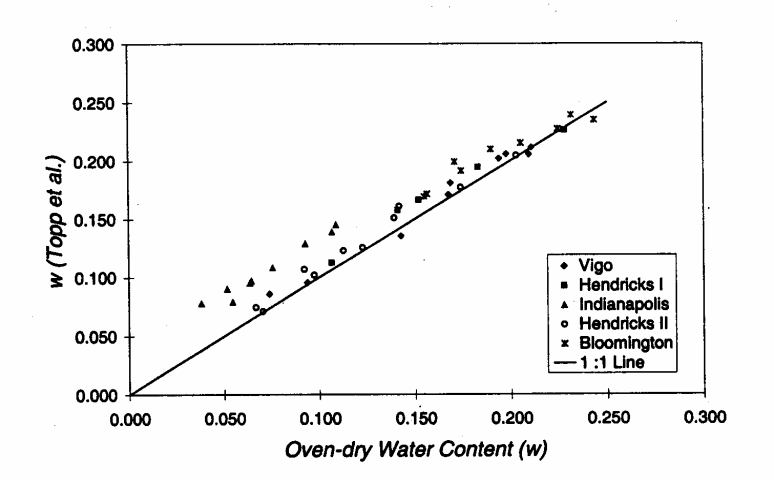

Figure 4-1. Comparison of oven-dry water content and TDR measured water content for different types of soils using Topp's empirical equation. Source: Lin et al. (2000)

In order to get an expression in the form of Eqn. (4-5), values of $\sqrt{K}$ were plotted against the volumetric moisture content as shown in Fig. 4-2. The resulting relation was:

$$\sqrt{K} = 2.13 + 7.00\theta \tag{4-11}$$

The coefficient of determination, R^2-value, was 0.92, the standard error of estimate was 1.5% and the maximum error was 3.2%.

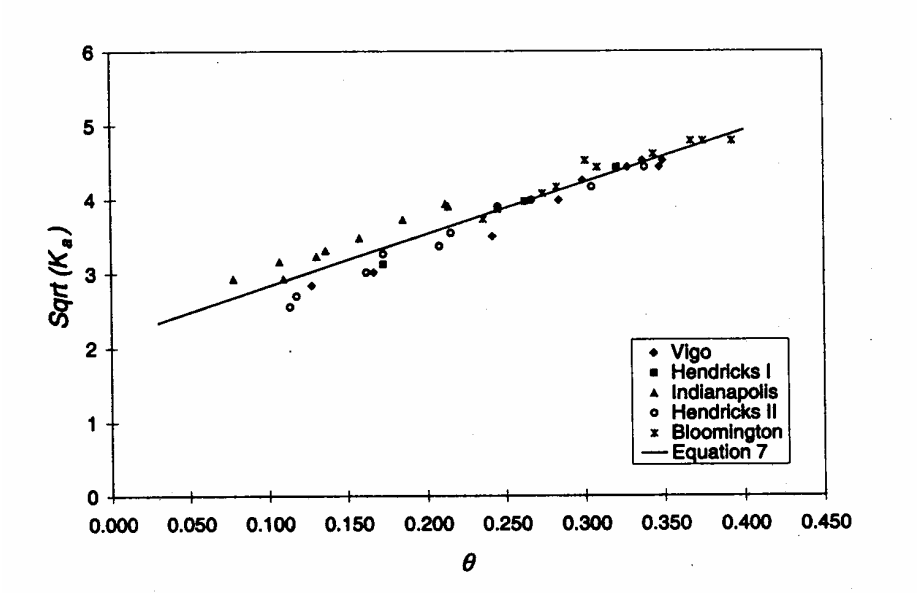

Figure 4-2. $\sqrt{K}$ vs θ relationship for different types of soils. Source: Lin et al. (2000)

The gravimetric moisture content was plotted in Fig. 4-3 and a regression analysis of the data yielded:

$$\sqrt{K_a}\,\frac{\rho_w}{\rho_d} = 1.03 + 8.24 w_c \tag{4-12}$$

The R^2-value was 0.98, the standard error of estimate was 0.9% and the maximum error was 1.9%.

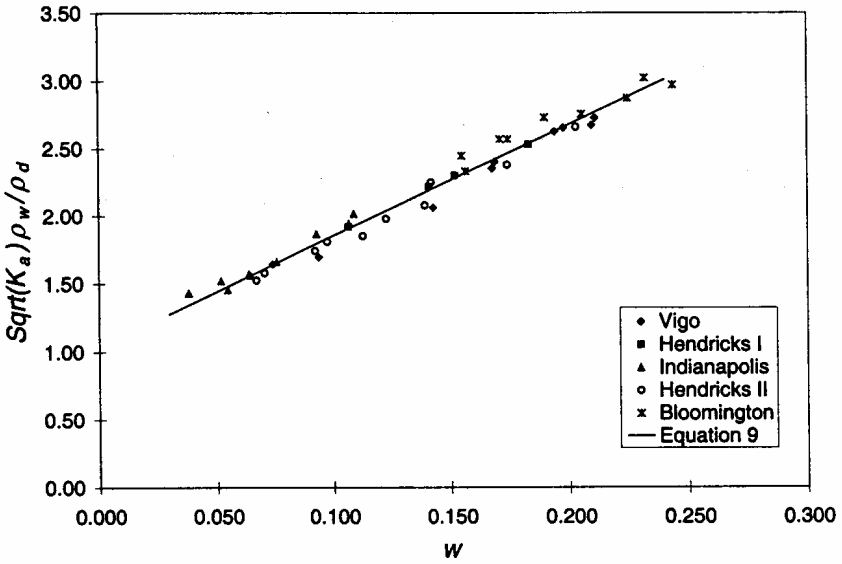

Figure 4-3. Density-compensating water content relationship for different types of soils. Source: Lin et al. (2000)

Lin et al. (2000) concluded that "unless greater accuracy is required or highly plastic soil is encountered, Eqn. (4-12) can be used with approximately 1% standard error for water content measurement if the density of the soil is known".

4.3. Procedure

The Siddiqui and Drnevich (1995) relationship has been used to determine the soil constants "a" and "b". The process relied on performing the TDR method on a particular soil in the mold at different moisture contents. In this case the soil dielectric constant in the mold $K_{a,mold}$ is measured as an output from the TDR software. The wet density is readily measured since the mold's volume and weight are known a priori. The moisture content can be determined by the oven-dry method, ASTM D2216. The two unknowns in this equation are, therefore, the constants "a" and "b". If the left hand side of the equation is plotted against the moisture content, the results could be regressed to a straight line with a slope equal to the constant "b" and an intercept equal to the constant "a". This procedure is performed on 11 soils provided by FDOT and 2 soils from inside and outside the soil laboratory.

4.4. Experimental Results

The results from the tests are summarized in Table 4-1. In order to ensure accuracy, two different operators performed the tests and, in selected cases, the test was performed by both of them to ensure consistent testing procedures. According to Table 4-1, the mathematical average value for constants "a" and "b" were found to be 0.99 and 8.53, respectively.

Table 4-1. Values of constants "a" and "b" for various soil types

Test	Description	Operator	USCS	AASHTO	a	b	Comment
1	Ottawa Sand	Amr	SP	A-1-b	1.22	11.68	Discarded
1-a	Ottawa Sand	Brian	SP	A-1-b	0.95	9.00	Accepted
1-b	Ottawa Sand	Both	SP	A-1-b	0.91	9.41	Accepted
				Average	**0.93**	**9.21**	
2	Outside Lab	Amr	SP	A-3	1.00	8.20	Accepted
2-a	Outside Lab	Brian	SP	A-3	1.03	8.35	Accepted
				Average	**1.02**	**8.28**	
3	MP-1	Amr	SP	A-1-b	0.93	8.78	Accepted
3-a	MP-1	Brian	SP	A-1-b	1.01	7.48	Accepted
3-b	MP-1	Brian	SP	A-1-b	0.98	8.21	Accepted
				Average	**0.97**	**8.16**	
4	Sample # 515	Both	SP	A-3	1.05	8.19	Accepted
4-a	Sample # 515	Brian	SP	A-3	1.01	8.93	Accepted
4-a	Sample # 515	Brian	SP	A-3	1.03	8.73	Accepted
				Average	**1.03**	**8.62**	
5	Sample # 2	Amr	SP	A-1-b	1.10	7.40	Accepted
5-a	Sample # 2	Both	SP	A-1-b	1.04	8.06	Accepted
				Average	**1.07**	**7.73**	
6	Sample # 6944	Amr	SP	A-3	1.08	8.09	Accepted
6-a	Sample # 6944	Brian	SP	A-3	0.99	8.65	Accepted
				Average	**1.04**	**8.37**	
7	Sample with # 6944	Brian	SP	A-1-b	**0.99**	**8.80**	Accepted
8	Sample # 6965	Both	SW	A-1-b	0.99	8.80	Study the effect of compaction
8-a	Sample # 6965	Both	SW	A-1-b	1.04	8.03	Study the effect of compaction
8-b	Sample # 6965	Both	SW	A-1-b	0.99	8.31	Study the effect of compaction
8-c	Sample # 6965	Both	SW	A-1-b	1.00	7.96	Study the effect of compaction
				Average	**1.01**	**8.28**	
9	Sample With # 6965	Brian	SP	A-1-b	**1.02**	**8.20**	Accepted
10	Sample # 6974	Brian	SP	A-1-b	**0.99**	**8.27**	Accepted
11	Sample # 6978	Brian	SP	A-1-b	**1.02**	**7.93**	Accepted
12	Sample # 6926	Brian	SP	A-1-b	0.90	9.24	Accepted
13	Sample # 6927	Brian	SP	A-1-b	0.87	9.83	Accepted

Note – test 1 was discarded due to incorrect procedures used.

The results of all tests are plotted on a single graph, Fig. 4-4. Values of 0.99 and 8.48 were determined for constants "a" and "b" respectively. The correlation factor, or R-value, for the trend line used for all the data was 0.9826, indicative or a strong correlation.

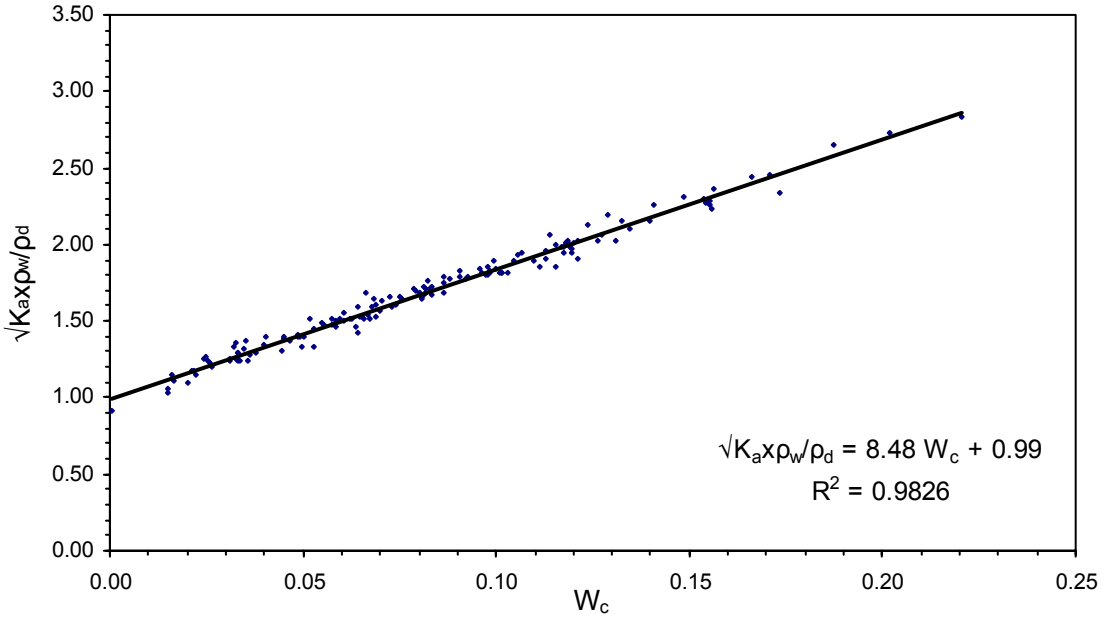

Figure 4-4. Final results of the TDR test in-mold for various soil types

4.5. Effect of Compaction Energy on Soil Constants "a" and "b"

In order to study the effect of compaction energy on the values of constants "a" and "b", TDR tests must be performed at different compaction energies. Sample 6944 was chosen for this study. TDR tests were performed using different compaction efforts by varying the number of rod tamps, as summarized in Table 4–2.

Table 4-2. The different tests performed to study the effect of compaction

Case No.	Number of rod tamps per layer					
	Layer 1	Layer 2	Layer 3	Layer 4	Layer 5	Layer 6
1	5	6	7	8	9	10
2	10	11	12	13	14	15
3	20	21	22	23	24	25
4	30	31	32	33	34	35

For each case, the water content was determined four times to give an accurate value of water content. The results of the four tests are plotted in Fig. 4-5. From the figure, it can be concluded that constant "b" decreases slightly with increasing compaction energy, whereas constant "a" exhibits an increasing trend. However, the difference between cases 2, 3, and 4 is insignificant. Therefore, it can be concluded that the compaction energy affects only slightly the value of constants "a" and "b". It is recommended to use the compaction energy associated with Case 3 to ensure consistent results.

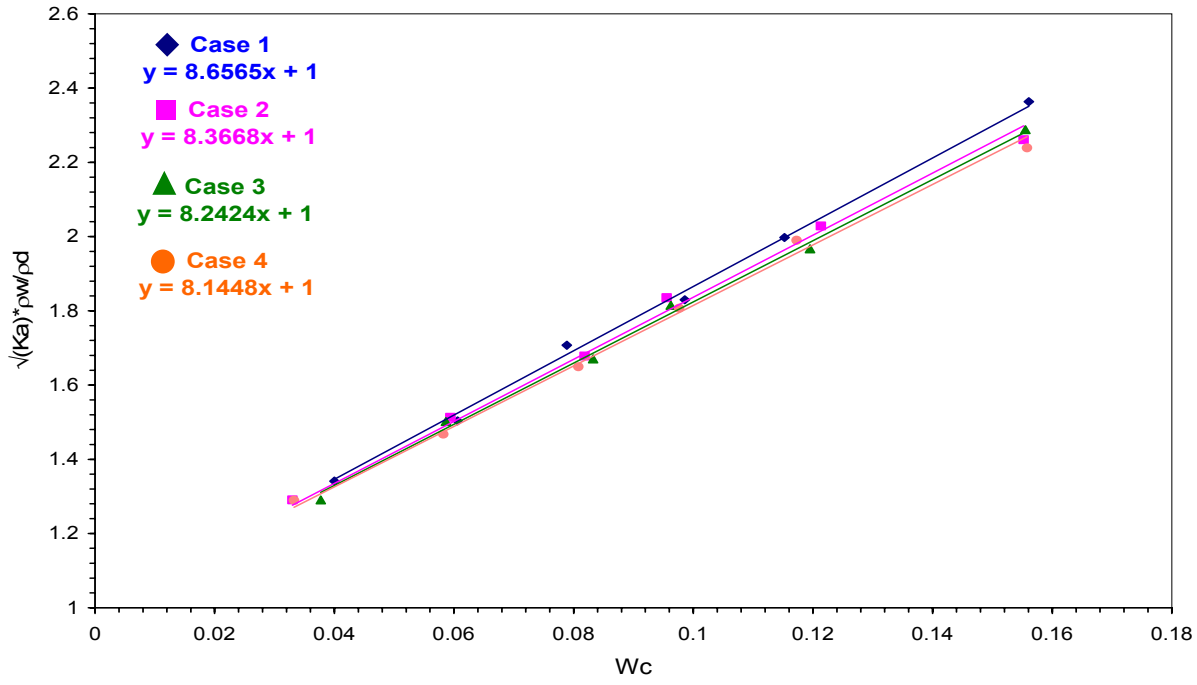

Figure 4-5. Effect of compaction energy on constants "a" and "b".

4.6. Effect of the Accuracy of "a" and "b" on the Calculated Moisture Content

The study was based on Siddiqui and Drnevich (1995) normalized equation, Eqn. (4-7). From the basic definitions and relations of Soil Mechanics, the dry density can be defined as:

$$\rho_d = \frac{\rho}{(1+w_c)} \tag{4-13}$$

Substituting with ρ_d from Eqn. (4-13) into Eqn. (4-7):

$$\sqrt{K_a}\,\frac{\rho_w}{\rho}(1+w_c) = a + bw_c \tag{4-14}$$

Rearranging Eqn. (4-14), we get:

$$w_c = \frac{K^* - a}{b - K^*} \tag{4-15}$$

Where K^* is defined as: $K^* = \sqrt{K_a}\,\frac{\rho_w}{\rho}$

All the quantities defining *K** are presumed to be measured at a high accuracy. Therefore, no error is assumed to result from these quantities. In order to study the effect of changing the constant "a" on the predicted value of moisture content, Eqn. (4-15) was used to calculate the water content from the assumed "a" values at different K^* and "b" values. The "b" values were varied from 7 to 12, whereas the K^* values were varied from 1.2 to 2.4. The results are summarized in Fig. 4-6 and Table 4-3.

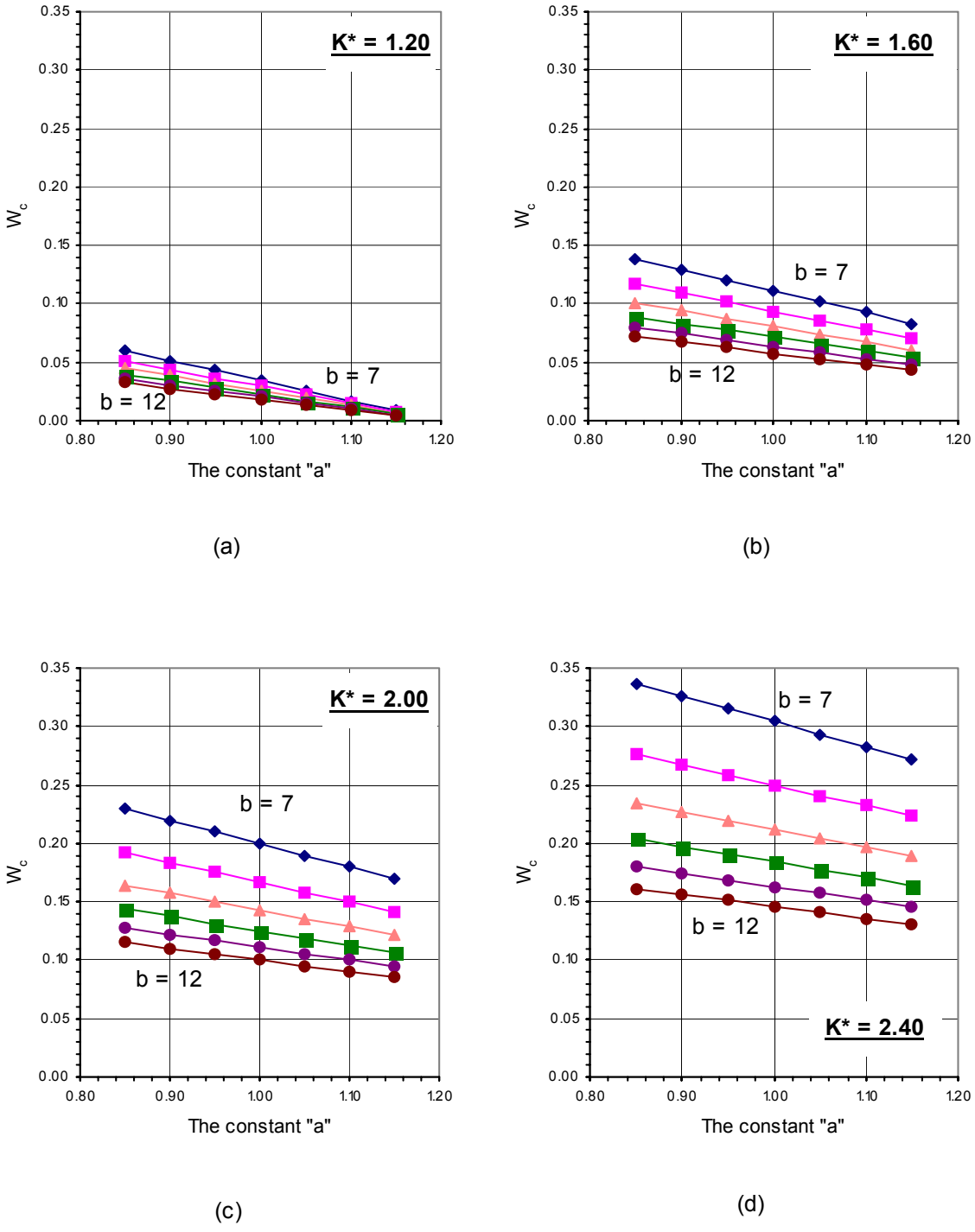

Figure 4-6. Error resulting from changing the constant “a” on the predicted moisture content

Table 4-3. Error resulting from changing the constant "a"

Error range in "a", (b = 9)	Change in the predicting moisture content in percentage			
	$K^* = 1.2$	$K^* = 1.6$	$K^* = 2.0$	$K^* = 2.4$
0.95 – 1.05	1.28	1.35	1.43	1.52
0.90 – 1.10	2.56	2.70	2.86	3.03

It is evident from Fig. 4-6 and Table 4-3 that the predicted value of the moisture content does not change noticeably with changing the constant "a" in a range of 1 ± 0.05. It is also clear that the change in the predicted value of the moisture content varies, depending on the value of K^*. This is logical because the effect of the constant "a", as an intercept, has to be more predominant at lower values of moisture content.

In order to study the effect of changing the constant "b", the water content was calculated from the assumed "b" values at different K^* and "a" values. The "a" values were varied from 0.85 to 1.10, whereas the K^* values were varied from 1.2 to 2.4. The results are summarized in Table 4-4 and Fig. 4-7.

Table 4-4. Error resulting from changing the constant "b"

Error range in "b", (a = 1)	Change in the predicting moisture content in percentage			
	$K^* = 1.2$	$K^* = 1.6$	$K^* = 2.0$	$K^* = 2.4$
8.0 – 10.0	0.67	2.23	4.16	6.82
7.0 – 11.0	1.41	4.73	8.89	14.15

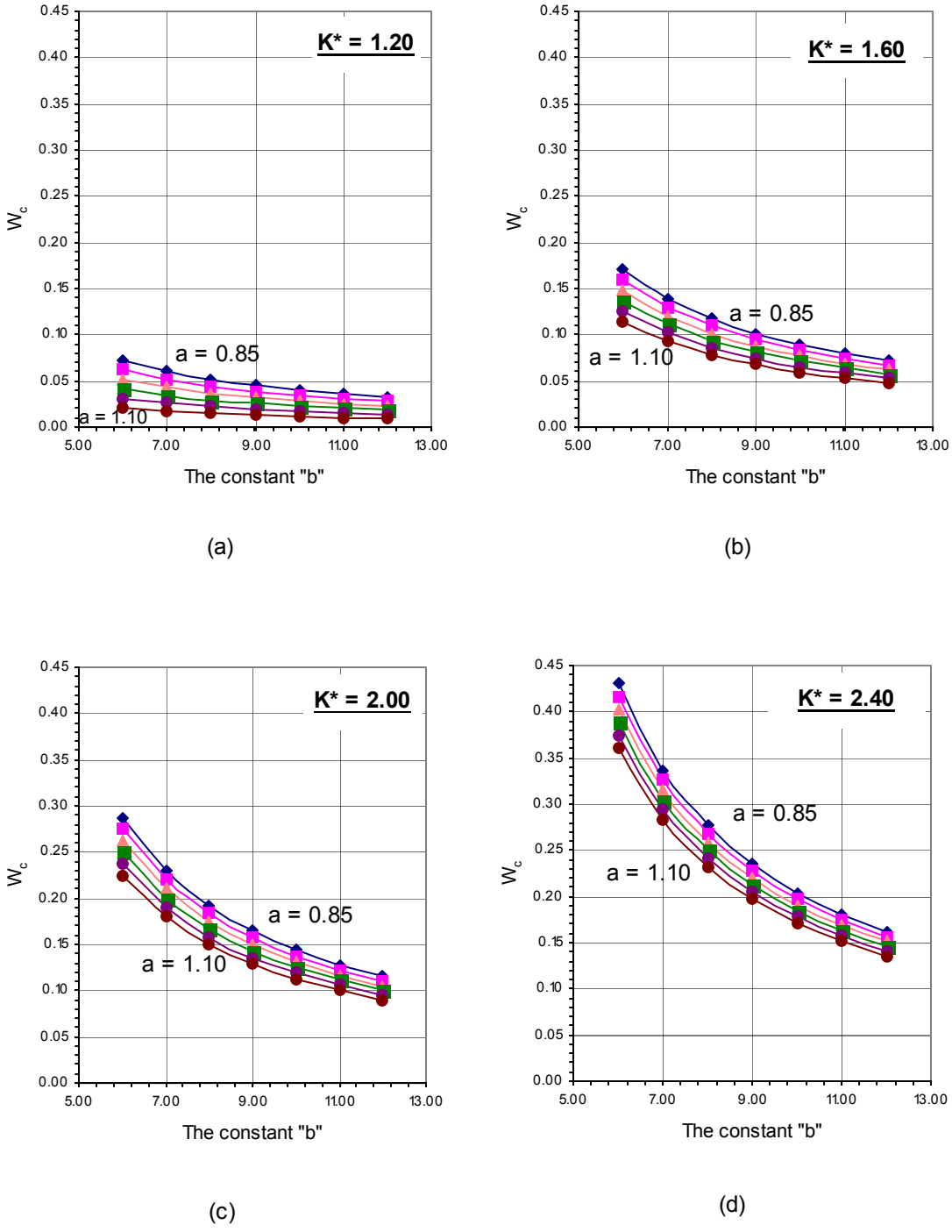

Figure 4-7. Error resulting from changing the constant “b” on the predicted moisture content

The effect of changing the constant "b" was higher than the effect of changing the constant "a." It can be seen from Fig. 4-7 and Table 4-4 that the predicted value of the moisture content changes noticeably with changing the constant "b" especially in a range of 9 ± 2.0.

It is also clear that the change in the predicted value of the moisture content depends on the value of the K^*. The higher the K^* value, the higher the error in the predicted value of the moisture content. This is logical because the change in the predicted moisture content resulting from a change in the constant "b", which is the slope of the straight line, is expected to be dramatic, especially at high water contents.

The study was repeated using a different idea. Based on Eqn. (4-15), the change in the predicted water content, Δw_c, due to a change Δa in the value of the constant "a" can be expressed as:

$$\Delta w_c = \frac{K^* - (a + \Delta a)}{b - K^*} - \frac{K^* - a}{b - K^*} \tag{4-16}$$

This equation can be reduced to:

$$\Delta w_c = \frac{-\Delta a}{b - K^*} \tag{4-17}$$

Using Eqn. (4-17), the change in the predicted water content, Δw_c, due to a change Δa in the value of the constant "a" ranging from –0.2 to 0.2 was determined. The results of the study are shown in Table 4-5 and Fig. 4-8.

Table 4-5. Error resulting from changing the constant "a" on the predicted moisture content, Method 2

Wc	**Δa**								
	-0.2	-0.15	-0.1	-0.05	0	0.05	0.1	0.15	0.2
	ΔW_c, %ge								
0.02	2.72	2.04	1.36	0.68	0.00	-0.68	-1.36	-2.04	-2.72
0.05	2.80	2.10	1.40	0.70	0.00	-0.70	-1.40	-2.10	-2.80
0.1	2.93	2.20	1.47	0.73	0.00	-0.73	-1.47	-2.20	-2.93
0.15	3.07	2.30	1.53	0.77	0.00	-0.77	-1.53	-2.30	-3.07
0.2	3.20	2.40	1.60	0.80	0.00	-0.80	-1.60	-2.40	-3.20
0.25	3.33	2.50	1.67	0.83	0.00	-0.83	-1.67	-2.50	-3.33

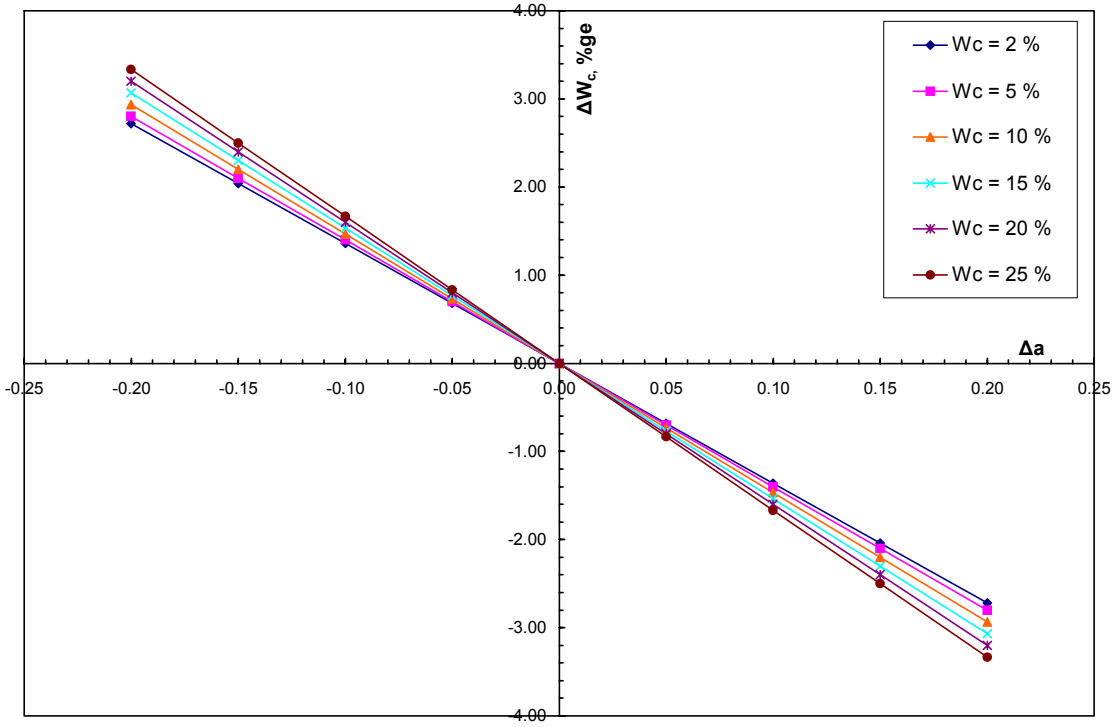

Figure 4-8. Error resulting from changing the constant "a" on the predicted moisture content, Method 2

It is evident from Fig. 4-8 and Table 4-5 that the predicted value of the moisture content changes slightly with changing the constant "a". It is also clear that the change in the predicted value of the moisture content varies slightly with changing the value of w_c for a constant value of Δa. These results confirm the results obtained from the first method used for studying the effect of constant "a" on the predicted value of the moisture content.

The change in the predicted water content, Δw_c, due to a change Δb in the value of the constant "b" can be expressed as:

$$\Delta w_c = \frac{K^* - a}{(b + \Delta b) - K^*} - \frac{K^* - a}{b - K^*} \qquad (4\text{-}18)$$

Using Eqn. (4-18), the change in the predicted water content, Δw_c, due to a change Δb in the value of the constant "b" ranging from –1.0 to 1.0 was determined. The results of the study are shown in Fig. 4-9 and Table 4-6.

Table 4-6. Error resulting from changing the constant "b" on the predicted moisture content, Method 2

Wc	**Δb**								
	-1	-0.75	-0.5	-0.25	0	0.25	0.5	0.75	1
	ΔW_c, %ge								
0.02	0.31	0.23	0.15	0.07	0.00	-0.07	-0.13	-0.19	-0.24
0.05	0.81	0.59	0.38	0.18	0.00	-0.17	-0.33	-0.48	-0.61
0.1	1.72	1.24	0.79	0.38	0.00	-0.35	-0.68	-0.99	-1.28
0.15	2.72	1.95	1.25	0.60	0.00	-0.55	-1.07	-1.55	-1.99
0.2	3.81	2.73	1.74	0.83	0.00	-0.77	-1.48	-2.14	-2.76
0.25	5.00	3.57	2.27	1.09	0.00	-1.00	-1.92	-2.78	-3.57

It is evident from Fig. 4-9 and Table 4-6 that the predicted value of the moisture content changes noticeably with changing the constant "b". It is also clear that the change in the predicted value of the moisture content varies noticeably with changing the value of w_c at a constant value of Δb. These results confirm the results obtained from the first method used for studying the effect of constant "b" on the predicted value of the moisture content.

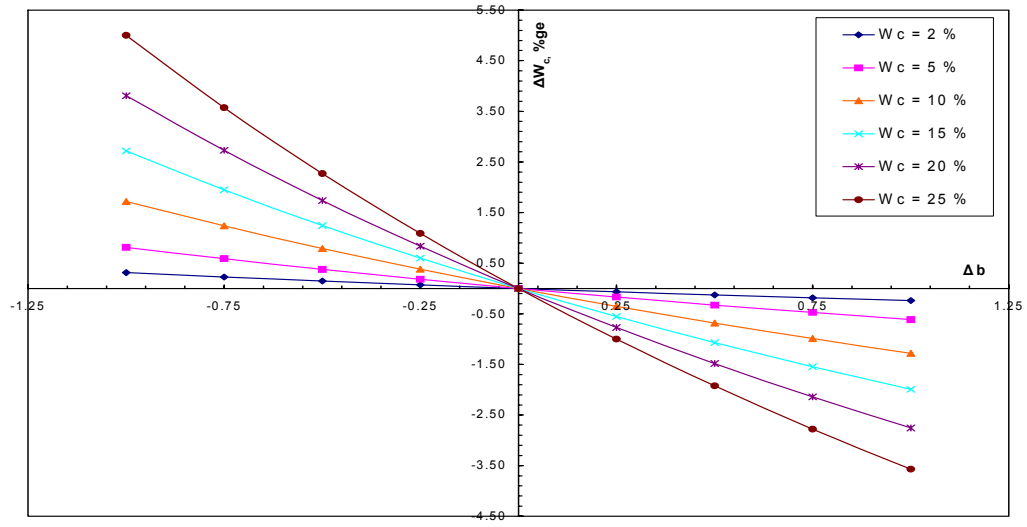

Figure 4-9. Error resulting from changing the constant "b" on the predicted moisture content. Method 2

4.7. Effect of the Accuracy of "a" and "b" on the Calculated Dry Density

The study was based on Siddiqui and Drnevich (1995) normalized equation, Eqn. (4-7). Rearranging this equation:

$$\rho_d = \frac{\sqrt{K_a}\rho_w}{a + bw_c} \tag{4-19}$$

The rate of change in dry density, ρ_d, due to a change of Δa in the value of constant "a" can be expressed as:

$$\frac{\Delta\rho_d}{\rho_{d,true}} = \frac{\rho_d(a^{\backslash} = a + \Delta a, b, w_c = f(a^{\backslash}, b, K^*)) - \rho_{d,true}(a, b, w_{c,true})}{\rho_{d,true}(a, b, w_{c,true})} \tag{4-20}$$

Where:

- $\frac{\Delta\rho_d}{\rho_{d,true}}$ is the rate of change in dry density.

- $\rho_{d,true}$ is the true value of dry density assuming a =1 and b = 8.5 as base values for the soil constants.
- ρ_d is the wrong value of the dry density depending on an error Δa in the value of the constant "a" and a water content which has been determined from the wrong "a" value.

Substituting from Eqns. (4-19) and (4-15) into Eqn. (4-20):

$$\frac{\Delta\rho_d}{\rho_{d,true}} = \frac{\dfrac{1}{(a+\Delta a)+b\left(\dfrac{K^*-(a+\Delta a)}{b-K^*}\right)} - \dfrac{1}{a+bw_{c,true}}}{\dfrac{1}{a+bw_{c,true}}} \tag{4-18}$$

Multiplying both the nominator and the dominator by $\left(a+bw_{c,true}\right)$ and rearranging:

$$\frac{\Delta\rho_d}{\rho_{d,true}} = \frac{a+bw_c}{(a+\Delta a)+b\left(\dfrac{K^*-(a+\Delta a)}{b-K^*}\right)} - 1 \tag{4-22}$$

Substituting from Eqn. (4-15) and simplifying Eqn. (4-22):

$$\frac{\Delta\rho_d}{\rho_{d,true}} = \frac{a+b\dfrac{K^*-a}{b-K^*}}{a+b\dfrac{K^*-a}{b-K^*}+\dfrac{K^*\Delta a}{b-K^*}} - 1 \tag{4-23}$$

Eqn. (4-23) can be reduced to:

$$\frac{\Delta\rho_d}{\rho_{d,true}} = \frac{b-a}{b-a-\Delta a} - 1 \tag{4-24}$$

The previous equation was used to study the effect of an error in the value of constant "a" ranging from –0.2 to 0.2 on the predicted dry density. The results of the study are shown in Figure 4-10 and Table 4-7.

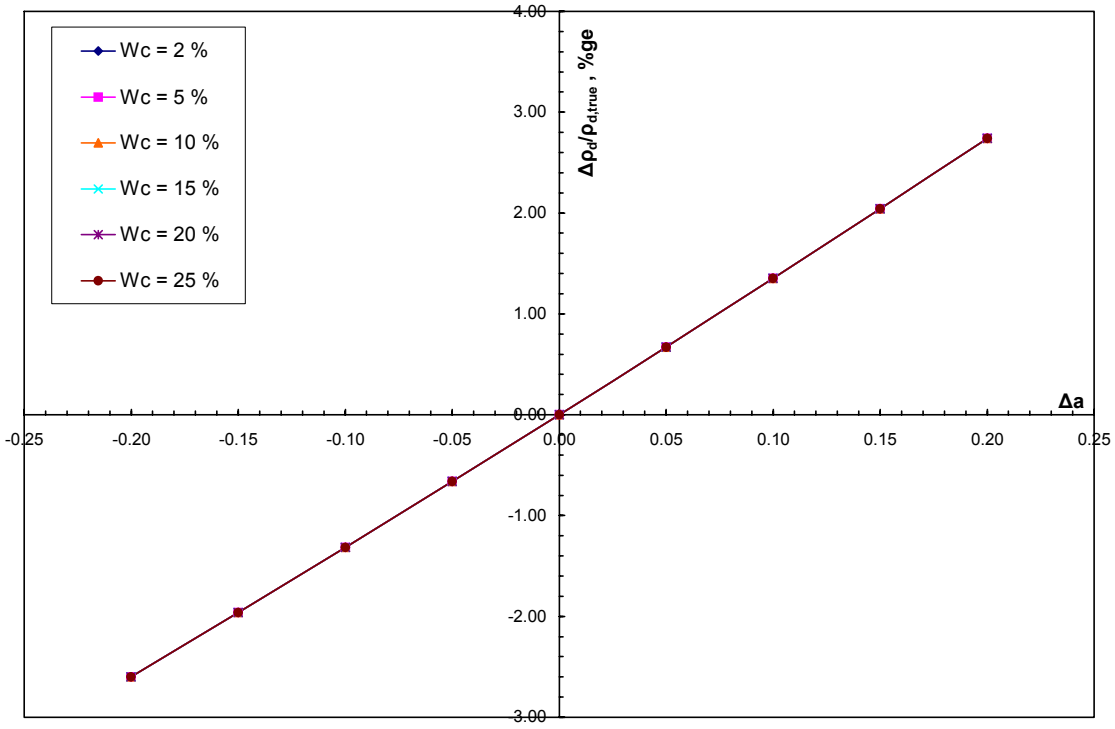

Figure 4-10. Error resulting from changing the constant "a" on the predicted dry density.

Table 4-7. Error resulting from changing the constant "a" on the predicted dry density

Wc	**Δa**								
	-0.2	-0.15	-0.1	-0.05	0	0.05	0.1	0.15	0.2
	$\Delta\rho_d/\rho_{d,true}$, %ge								
0.02	-2.60	-1.96	-1.32	-0.66	0.00	0.67	1.35	2.04	2.74
0.05	-2.60	-1.96	-1.32	-0.66	0.00	0.67	1.35	2.04	2.74
0.1	-2.60	-1.96	-1.32	-0.66	0.00	0.67	1.35	2.04	2.74
0.15	-2.60	-1.96	-1.32	-0.66	0.00	0.67	1.35	2.04	2.74
0.2	-2.60	-1.96	-1.32	-0.66	0.00	0.67	1.35	2.04	2.74
0.25	-2.60	-1.96	-1.32	-0.66	0.00	0.67	1.35	2.04	2.74

It is evident from Fig. 4-10 and Table 4-7 that the predicted value of the dry density changes dramatically while changing constant "a". It is also clear that the change in the predicted value of the dry density is independent of the moisture content value, Eqn. (4-24).

The rate of change in dry density, ρ_d, due to a change of Δb in the value of constant "b" can be expressed as:

$$\frac{\Delta\rho_d}{\rho_{d,true}} = \frac{\rho_d(a, b^{\backslash} = b + \Delta b, w_c = f(a, b^{\backslash}, K^*)) - \rho_{d,true}(a, b, w_{c,true})}{\rho_{d,true}(a, b, w_{c,true})} \tag{4-25}$$

Where: ρ_d is the wrong value of the dry density assuming an error Δb in the value of the constant "b" and water content, which has been determined from the wrong "b" value.

Substituting from Eqns. (4-19) and (4-15) into Eqn. (4-25):

$$\frac{\Delta\rho_d}{\rho_{d,true}} = \frac{\dfrac{1}{a + (b + \Delta b)\left(\dfrac{K^* - (a + \Delta a)}{b - K^*}\right)} - \dfrac{1}{a + bw_{c,true}}}{\dfrac{1}{a + bw_{c,true}}} \tag{4-26}$$

Multiplying both the nominator and the dominator by $\left(a + bw_{c,true}\right)$ and rearranging:

$$\frac{\Delta\rho_d}{\rho_{d,true}} = \frac{a + bw_c}{a + (b + \Delta b)\left(\dfrac{K^* - a}{(b + \Delta b) - K^*}\right)} - 1 \tag{4-27}$$

Substituting from Eqn. (4-15) and simplifying Eqn. (4-27):

$$\frac{\Delta\rho_d}{\rho_{d,true}} = \frac{\dfrac{a(b-K^*)+b(K^*-a)}{b-K^*}}{\dfrac{a(b+\Delta b-K^*)+(b+\Delta b)(K^*-a)}{b+\Delta b-K^*}} - 1 \qquad (4\text{-}28)$$

Eqn. (4-28) can be reduced to:

$$\frac{\Delta\rho_d}{\rho_{d,true}} = \left(\frac{b-a}{b-a+\Delta b}\right)\left(\frac{b+\Delta b-K^*}{b-K^*}\right) - 1 \qquad (4\text{-}29)$$

Equation (4-29) was used to study the effect of an error in the value of constant "b" ranging from –1.0 to 1.0 on the predicted dry density. The results of the study are shown in Fig. 4-11 and Table 4-8.

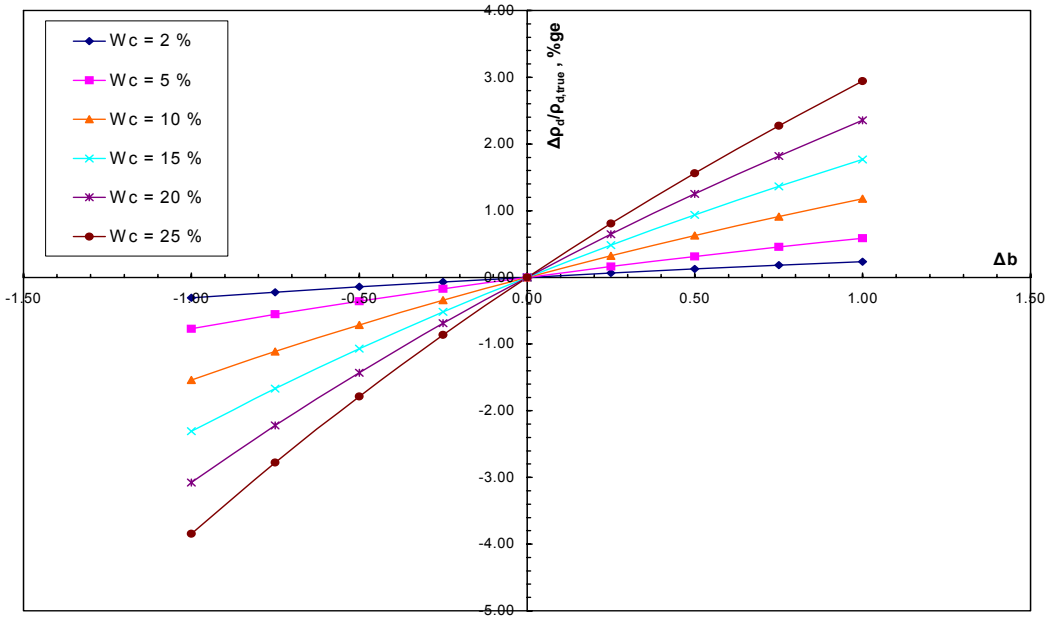

Figure 4-11. Error resulting from changing the constant "b" on the predicted dry

Table 4-8. Error resulting from changing the constant "b" on the predicted dry density

Wc	Δb								
	-1	-0.75	-0.5	-0.25	0	0.25	0.5	0.75	1
	$\Delta\rho_d/\rho_{d,true}$, %ge								
0.02	-0.31	-0.22	-0.14	-0.07	0.00	0.06	0.12	0.18	0.24
0.05	-0.77	-0.56	-0.36	-0.17	0.00	0.16	0.31	0.45	0.59
0.1	-1.54	-1.11	-0.71	-0.34	0.00	0.32	0.63	0.91	1.18
0.15	-2.31	-1.67	-1.07	-0.52	0.00	0.48	0.94	1.36	1.76
0.2	-3.08	-2.22	-1.43	-0.69	0.00	0.65	1.25	1.82	2.35
0.25	-3.85	-2.78	-1.79	-0.86	0.00	0.81	1.56	2.27	2.94

It is evident from Fig. 4-11 and Table 4-8 that the predicted value of the dry density changes dramatically while changing constant "b". It is also clear that the change in the predicted value of the dry density changes noticeably with changing the moisture content value.

4.8. Effect of Scatter in the Predicted Moisture Content on the Calculated Dry Density

The study was based on Siddiqui and Drnevich (1995) normalized equation, Eqn. (4-7) in its rearranged form, Eqn. (4-19). The rate of change in dry density, ρ_d, due to a scatter of Δw_c in the predicted value of moisture content, $w_{c,true}$, can be expressed as:

$$\frac{\Delta\rho_d}{\rho_{d,true}} = \frac{\rho_d(a,b,w_{c,true}+\Delta w_c) - \rho_{d,true}(a,b,w_{c,true})}{\rho_{d,true}(a,b,w_{c,true})} \tag{4-30}$$

Where:

- $\frac{\Delta\rho_d}{\rho_{d,true}}$ is the rate of change in dry density.
- $\rho_{d,true}$ is the true value of dry density taking a =1 and b = 8.5 as base values for the soil constants and the true value of the moisture content.
- ρ_d is the wrong value of the dry density assuming a scatter of Δw_c in the predicted value of moisture content.

Substituting from Eqns. (4-19) and (4-15) into Eqn. (4-30):

$$\frac{\Delta\rho_d}{\rho_{d,true}} = \frac{\dfrac{1}{a + b(w_{c,true} + \Delta w_c)} - \dfrac{1}{a + bw_{c,true}}}{\dfrac{1}{a + bw_{c,true}}} \tag{4-31}$$

Multiplying both the nominator and the dominator by $\left(a + bw_{c,true}\right)$ and rearranging:

$$\frac{\Delta\rho_d}{\rho_{d,true}} = \frac{a + bw_c}{a + b(w_{c,true} + \Delta w_c)} - 1 \tag{4-32}$$

Eqn. (4-32) was used to study the effect of a scatter in the predicted moisture content value ranging from –2.0 to 2.0 on the predicted dry density. The results of the study are shown in Table 4-9 and Fig. 4-12.

Table 4-9. Error resulting from Scatter in the predicted moisture content on the predicted dry density

Wc	**ΔW_c**								
	-2	-1.5	-1	-0.5	0	0.5	1	1.5	2
	-0.02	-0.015	-0.01	-0.005	0	0.005	0.01	0.015	0.02
	$\Delta\rho_d/\rho_{d,true}$, %ge								
0.02	17.00	12.23	7.83	3.77	0.00	-3.51	-6.77	-9.83	-12.69
0.05	13.55	9.83	6.34	3.07	0.00	-2.90	-5.63	-8.21	-10.66
0.1	10.12	7.40	4.82	2.35	0.00	-2.25	-4.39	-6.45	-8.42
0.15	8.08	5.94	3.88	1.90	0.00	-1.83	-3.60	-5.31	-6.95
0.2	6.72	4.96	3.25	1.60	0.00	-1.55	-3.05	-4.51	-5.92
0.25	5.75	4.25	2.80	1.38	0.00	-1.34	-2.65	-3.92	-5.16

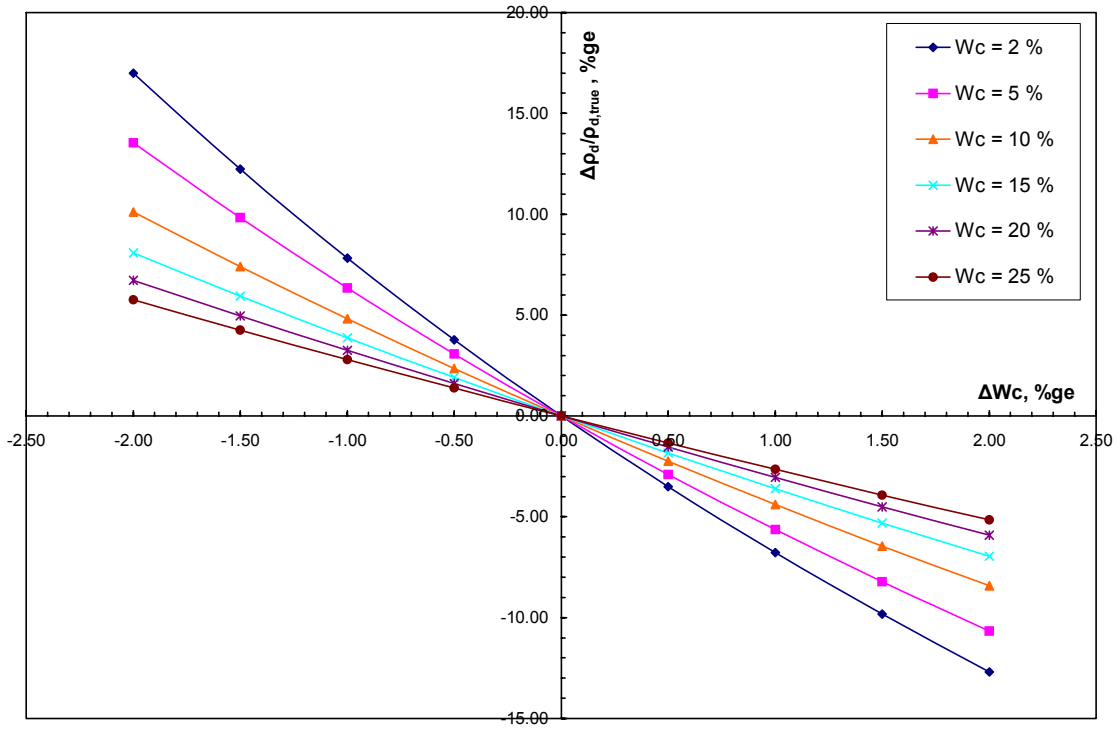

Figure 4-12. Error resulting from scatter in the predicting moisture content on the resulting dry density.

It is clear from Fig. 4-12 and Table 4-9 that there is a huge change in the predicted value of the dry density with small scatter in the predicted moisture content. This effect decreases with the increase of the moisture content value at which the test is performed.

4.9. Conclusions

An experimental testing program was carried out on different Florida construction soils in order to determine the soil constants "a" and "b". In-mold TDR tests, where the soil is prepared at different moisture contents, were conducted on these samples. A measurement was then made for the soil dielectric constant in the mold, the total density, and the water content by oven drying the sample. The "a" and "b" parameters are determined by plotting $\sqrt{K_{a,mold}}\,\frac{\rho_w}{\rho_d}$ versus w_c. A straight line is then fitted to the data. The value of "a" is the intercept of the line, whereas the value of "b" is the slope.

- For the tested soils in this study, the value of the constant "a" ranges from 0.87 to 1.08 with an average value of 0.99. This value is considerably close to 1.00, the value proposed by Lin et al. (2000). The study revealed also that the value of the constant "b" ranges from 7.73 to 9.83 with an average value of 8.53. The value proposed by Lin et al. (2000) for the same parameter is 9.0. In practice, it is recommended based on this study to use a value of **1.00** for constant "**a"** and a value of **8.50** for constant "**b"** for sandy soils used in construction in Florida.

- It is noted that most of the soil types included in this study were sandy soils. The USCS classification for these soil types was SP and SW. The AASHTO classification was A-1-b and A-3. Since no clayey or silty soil was used in this study, no recommendation is made about the values of constants "a" and "b" for these types of soils.

- The effect of compaction energy on the resulting "a" and "b" constants was investigated. The TDR was performed on the same sample using different tamping energies and the resulting "a" and "b" value were calculated accordingly. This study revealed that the compaction energy slightly affects the values of the constant "a" and "b". Based on the results, it is recommended to compact the soil in six layers of 20 through 25 tamps for each layer. This energy level is enough to yield consistent results.

- The effect of the error in the values of constants "a" and "b" on the predicted moisture content has been studied. The study revealed that the predicted value of the moisture content changes slightly with changing the constant "a" and that the change in the predicted value of the moisture content does not depend on the value of K^*. The study also revealed that the predicted value of the moisture content changes more noticeably with changing the constant "b". The level of change or "error" in the predicted value of the moisture content depends on the value of K^*. The higher the value of K^*, the higher the error in the predicted value of the moisture content.

- The study was repeated using different idea and it revealed that the predicted value of the moisture content does not change noticeably with changing the constant "a". It is also clear that the change in the predicted value of the moisture content varies slightly with changing the value of w_c at a constant value of Δa. The study also revealed that the predicted value of the moisture content changes noticeably with changing the constant "b". It is also clear that the change in the predicted value of the moisture content varies noticeably with changing the value of w_c at a constant value of Δb.

- The effect of the error in the values of constants "a" and "b" on the predicted dry density has been investigated. It is concluded that the predicted value of the dry density changes dramatically with changing the constant "a". It is also concluded that the change in the predicted value of the dry density is independent of the moisture content value. The study also revealed that the predicted value of the dry density changes dramatically with changing the constant "b". It is also clear that the change in the predicted value of the dry density changes noticeably with changing the moisture content value.

- The effect of the scatter in the predicted value of the moisture content on the predicted dry density has been investigated. It is concluded that there is a huge change in the predicted value of the dry density with small scatter in the predicted moisture content. This effect decreases with the increase of the moisture content value at which the test is performed.

5. Normalized and Absolute Accuracy of TDR Method

5.1. Introduction

A series of TDR tests were carried out in the laboratory to evaluate soil constants "a" and "b". More than 150 data point have been collected. The goal of this chapter is to evaluate the accuracy of TDR method using the collected data points. There are different sources of error in the TDR method that need to be evaluated. Absolute error, normalized error, error resulting from operator dependency, and inherent error are the sources of error that will be dealt with here. The chapter includes the examination of each one of these error sources through analysis of the collected data. In order to measure the accuracy of the whole TDR method, a comparison to a pre-determined dry density and oven dry water content should be performed. The second part of the chapter contains accuracy measurement for the TDR method through comparison with controlled laboratory boxes, which have been built especially for this purpose.

5.2. Absolute Error in Determining the Moisture Content

The TDR test in the mold has been performed on 13 samples resulting in 152 data points. A straight trend line was used to fit all data points (Fig. 5-1). The absolute error was defined as the difference between the measured and the theoretical moisture content for the same data point:

$$\text{Absolute\_Error} = (w_{c,\text{measured}} - w_{c,\text{theoretical}}) \times 100 \qquad (5\text{-}1)$$

In order to determine the absolute error in the measured moisture content values, the theoretical moisture content values were determined from the equation of the assumed straight trend line. The spreadsheet for the determination of the absolute error is included in the Appendix. The calculated absolute errors for each data point were used to draw the histogram shown in Fig. 5-2. From Figure 5-2, it is clear that 48 points out of 152 points have absolute errors of ±0.2% in moisture content determination whereas 88 points out of 152 points have absolute errors of ±0.4% in moisture content determination. The minimum absolute error in moisture content

determination for the whole data was determined to be -1.59% whereas; the maximum absolute error was determined to be +1.45%. The average absolute error for the whole data set was determined to be 0.01%.

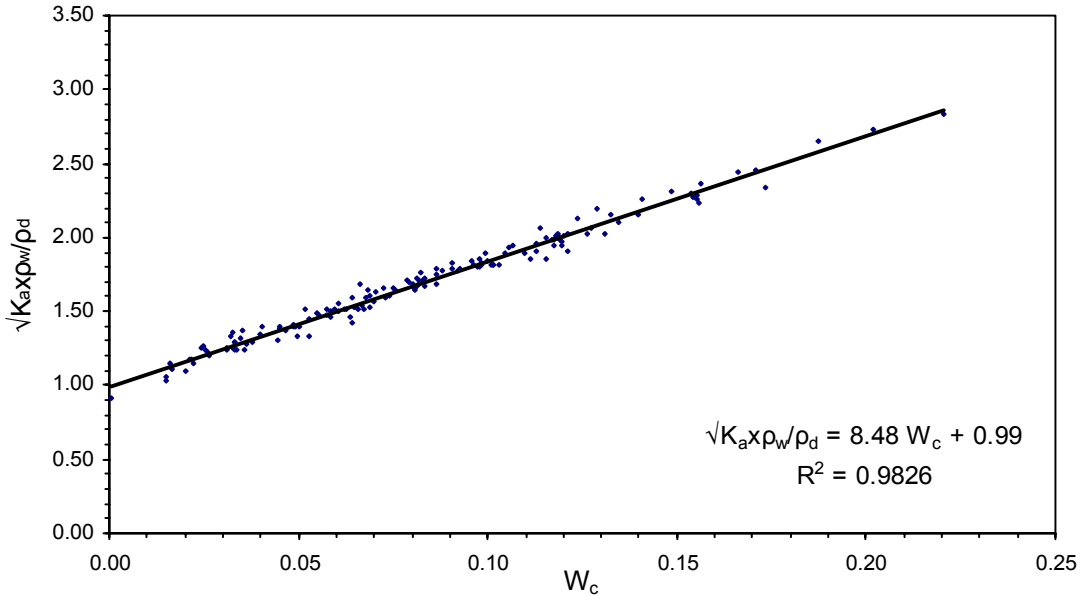

Figure 5-1. Final results of the TDR test in-mold for various soil types

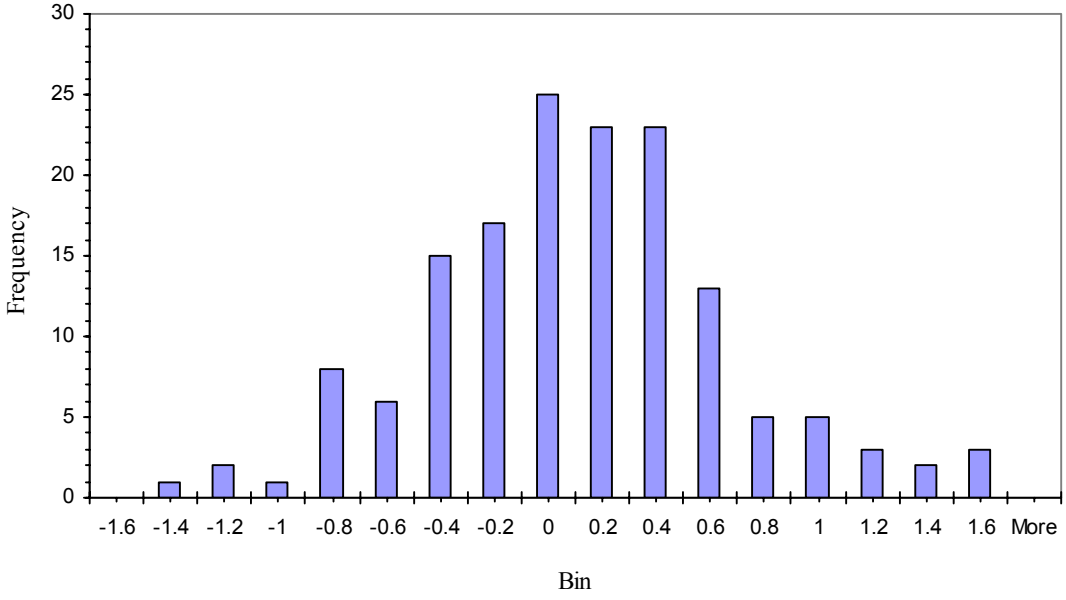

Figure 5-2. Histogram for the absolute error in moisture content determinaton

5.3. Normalized Error in Determining the Moisture Content

The normalized error was defined as the difference between the measured and the theoretical moisture content divided by the measured moisture content:

$$Normalized\_Error = \frac{w_{c,measured} - w_{c,theoritical}}{w_{c,measured}} \times 100 \qquad (5\text{-}2)$$

The same scenario as in the determination of absolute error has been done here. The spreadsheet is included in Appendix ch_5. The calculated normalized errors for each data point were used to draw the histogram shown in Fig. 5-3.

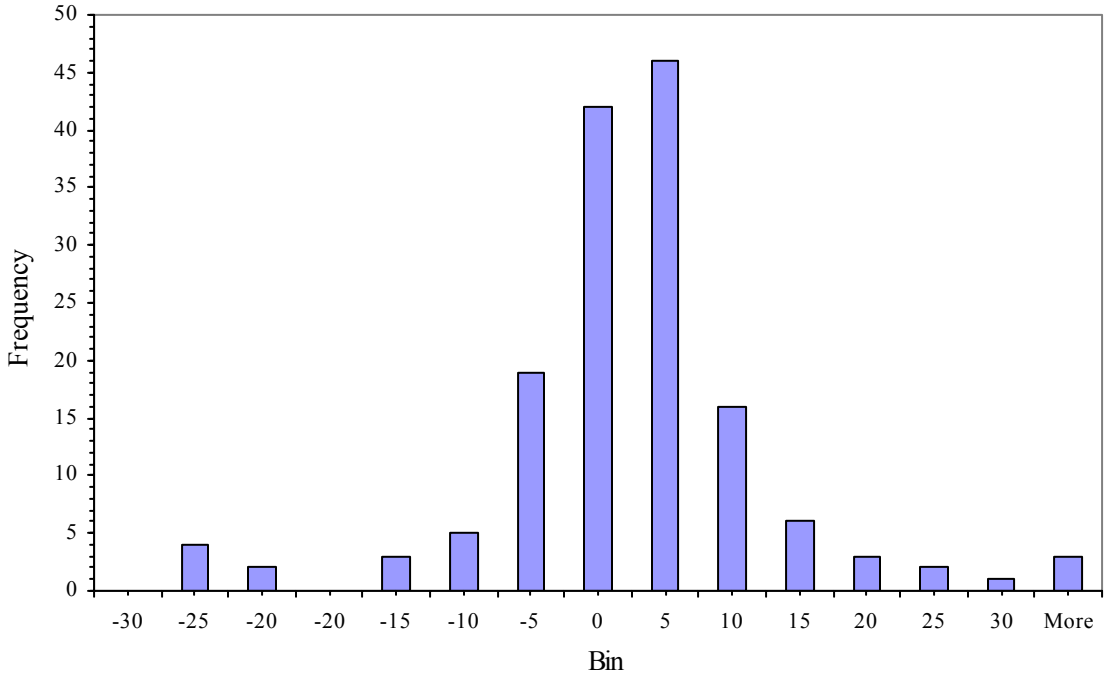

Figure 5-3. Histogram for the normalized error in moisture content determination

From Figure 5-3, it is clear that 88 points out of 152 points have normalized errors of ± 5.0% in moisture content determination whereas 123 points out of 152 points have normalized errors of ± 10.0% in moisture content determination. The minimum normalized error in moisture content

determination for the whole data was determined to be –29.66% whereas; the maximum normalized error was determined to be +67.99%. The average normalized error for the whole data set was determined to be 0.65%.

5.4. Operator Dependency

In order to study the operator dependency on the predicted soil constants "a" and "b", two different operators, Amr and Brian, carried out the TDR test on the same samples. Sometimes the test was carried out by both of them together. The studied samples were Ottawa Sand, soil outside the lab, sample # MP-1, sample # 515, sample # 2, and sample # 6944. The predicted "a" and "b" constants for different soils obtained by Amr, Brian, or both are shown in Figures 5-4 through 5-9.

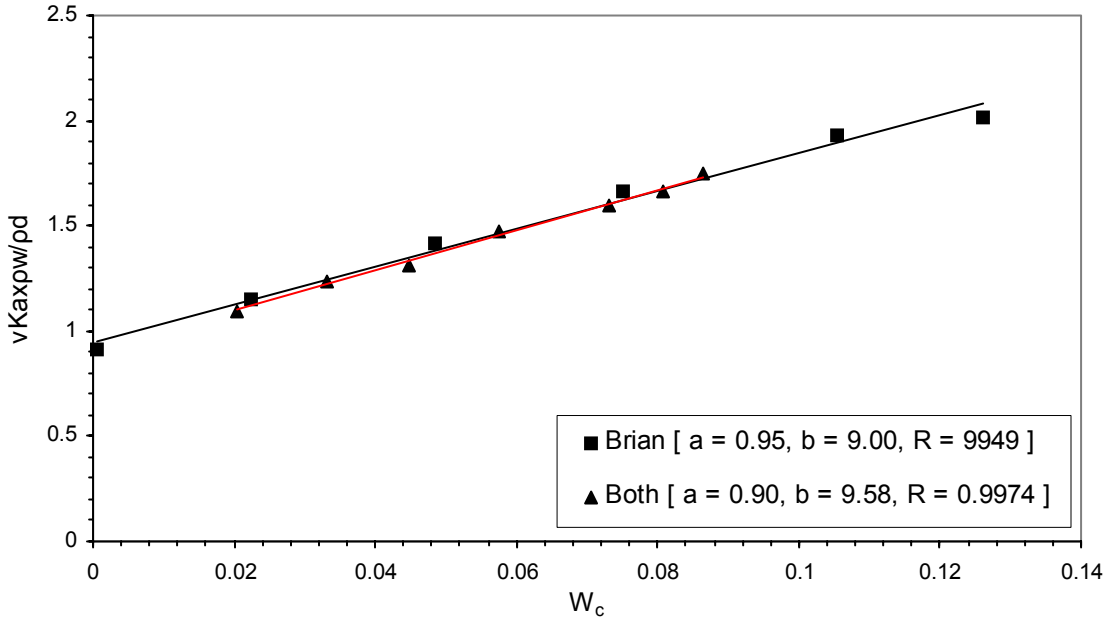

Figure 5-4. Operator dependency for Ottawa Sand

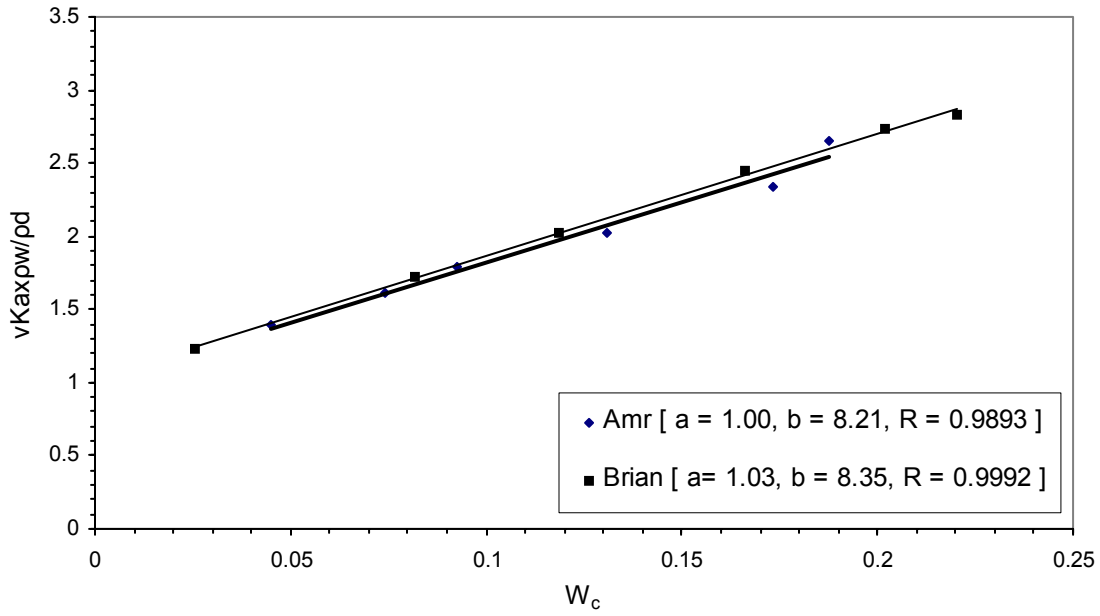

Figure 5-5. Operator dependency for sample Outside Soil-Lab

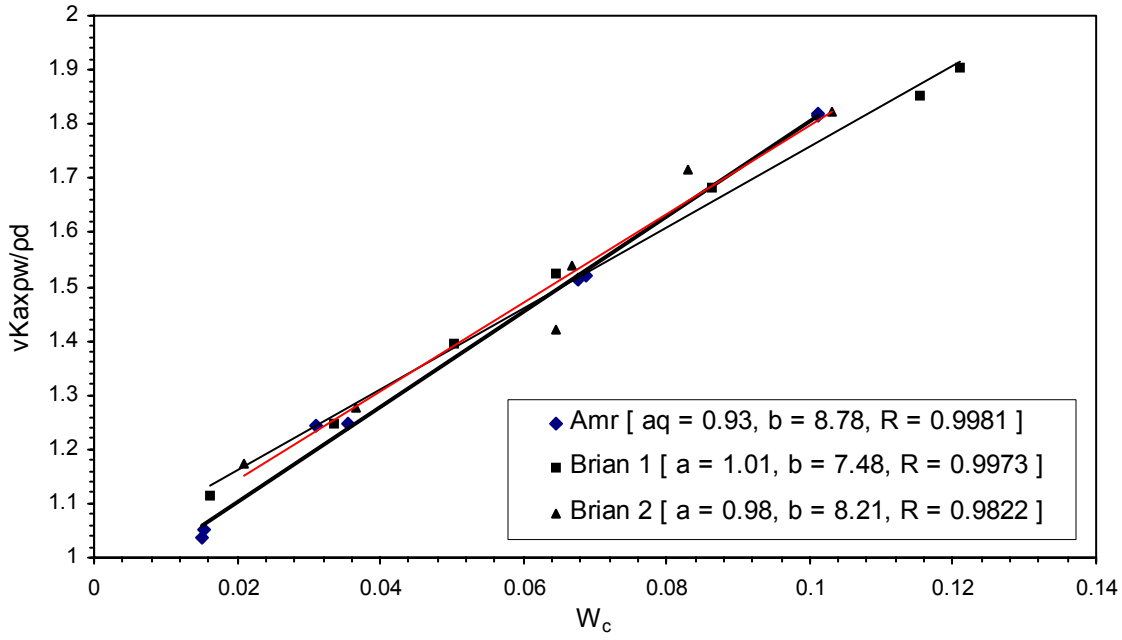

Figure 5-6. Operator dependency for sample # MP-1

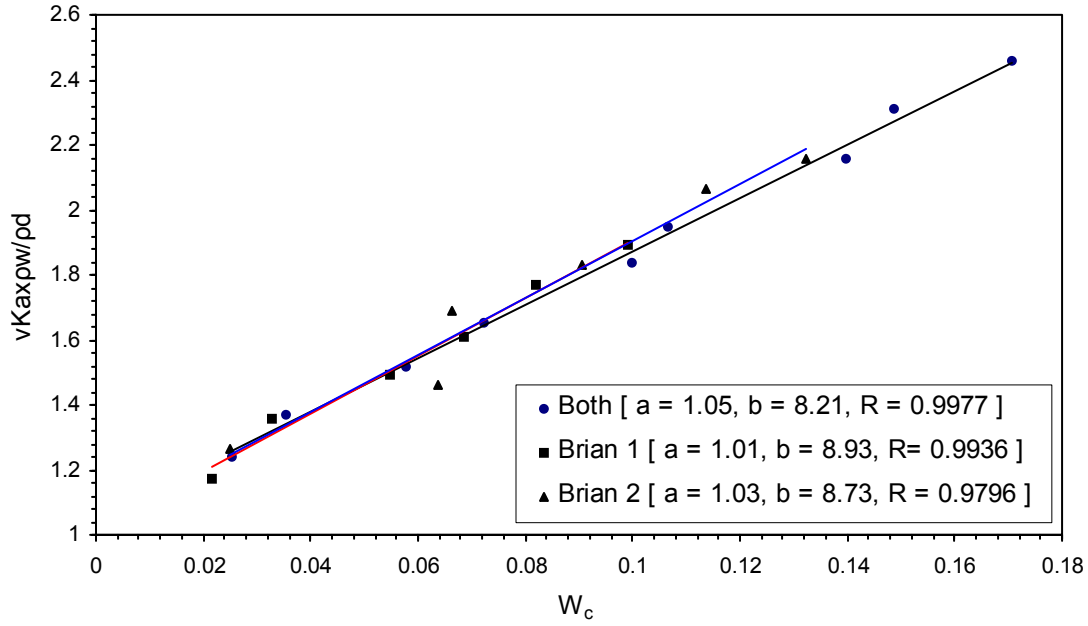

Figure 5-7. Operator dependency for sample # 515

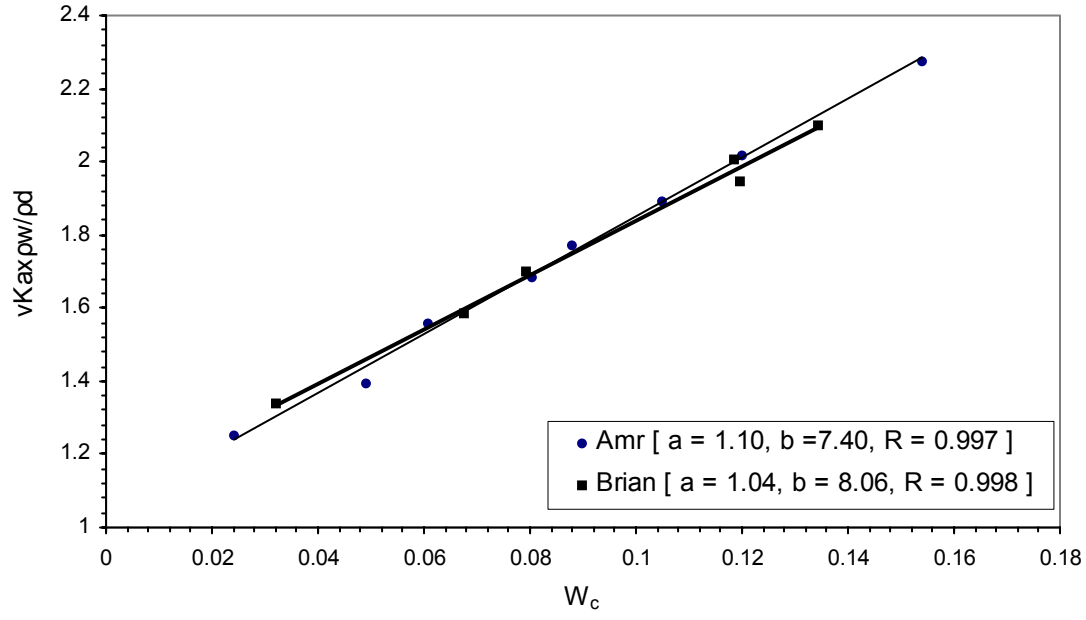

Figure 5-8. Operator dependency for sample # 2

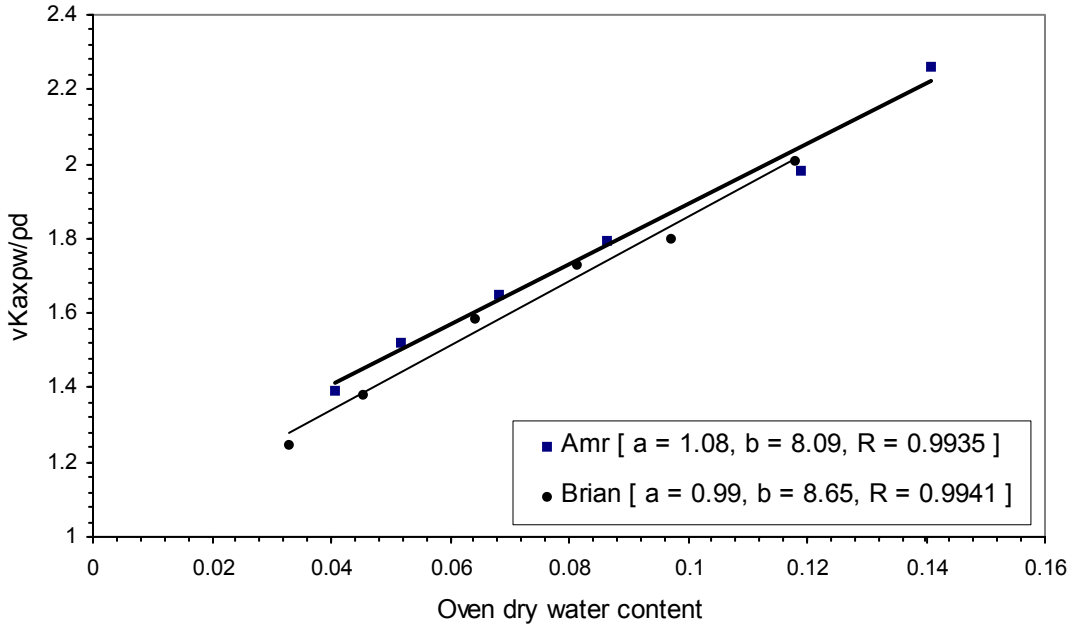

Figure 5-9. Operator dependency for sample # 6944

The absolute errors in determining soil constants "a" and "b" for different soils are summarized in Table 5-1.

Table 5-1. Operator effect on the determination of soil constants "a" and "b"

Sample	Amr / Both		Brian / Both		Amr - Brian	
	a	b	a	b	a	b
Ottawa Sand	0.91	9.41	0.95	9.00	-0.04	0.41
Outside The Lab	1.00	8.20	1.03	8.35	-0.03	-0.15
Sample MP-1	0.93	8.78	0.98	8.21	-0.05	0.57
Sample # 515	1.05	8.19	1.03	8.73	0.02	-0.54
Sample # 2	1.10	7.40	1.04	8.06	0.06	-0.66
Sample # 6944	1.08	8.09	0.99	8.65	0.09	-0.56
				Max.	0.09	0.57
				Min.	-0.05	-0.66
				Avr.	0.01	-0.16

According to Table 5-1, the maximum absolute error resulting from operator dependency in determining the constant "a" is 0.09 whereas the minimum absolute error is –0.05 with an average absolute error of 0.01. The maximum absolute error resulting from operator dependency in determining the constant "b" is 0.57 whereas the minimum absolute error is –0.66 with an average absolute error of –0.16.

5.5. Scatter Resulting from Different Compaction Energies

Four in-mold TDR tests were performed on sample # 6965 in order to study the effect of compaction on the value of soil constants "a" and "b". The only difference between the four tests was in the compaction energies applied during the test. Figure 5-10 summarizes the results obtained from this study.

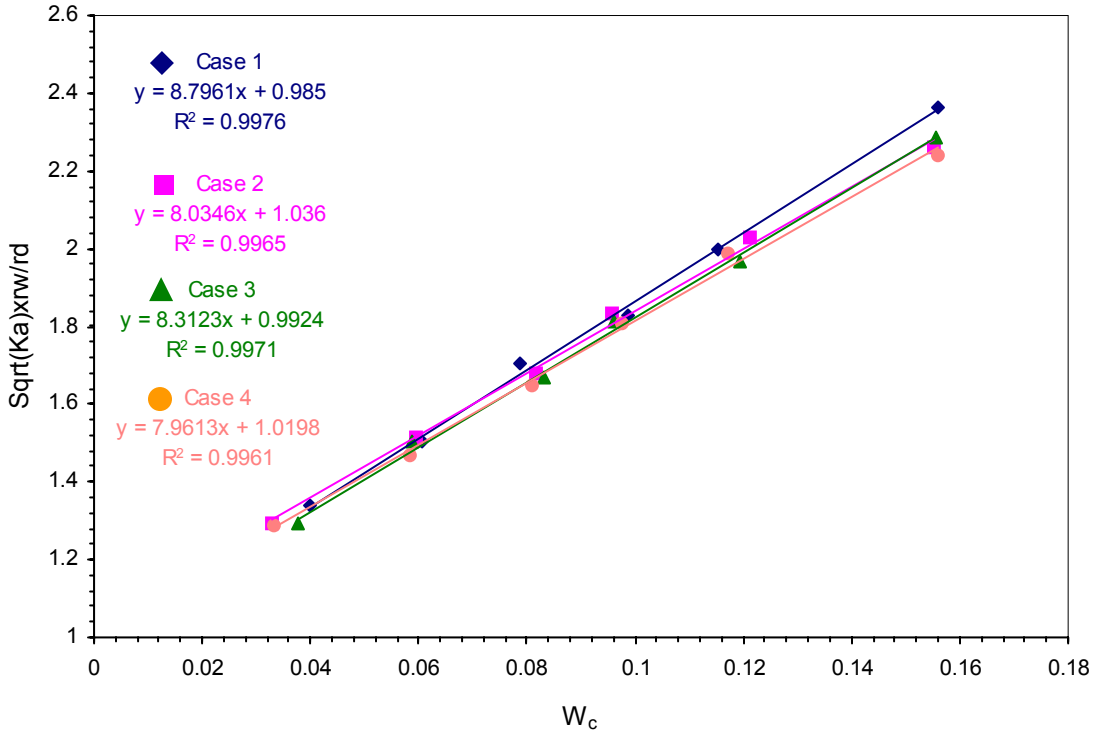

Figure 5-10. Scatter resulting from the difference in compaction energy

The absolute errors in determining soil constants “a” and “b”, assuming base values of a = 1 and b = 8.50, for different compaction energies are summarized in Table 5-2.

Table 5-2. The effect of compaction energy on the determination of soil constants “a” and “b”

Number of blows/layer	Measured Values		Absolute Error	
	a	b	a	b
5-6-7-8-9-10	0.985	8.8	0.015	-0.3
10-11-12-13-14-15	1.04	8.03	-0.04	0.47
20-21-22-23-24-25	0.99	8.31	0.01	0.19
30-31-32-33-34-35	1.02	7.96	-0.02	0.54
		Max.	0.015	0.54
		Min.	-0.04	-0.3
		Avr.	-0.0088	0.225

According to Table 5-2, the maximum absolute error resulting from scatter due to compaction energy in determining the constant “a” is 0.15 whereas the minimum absolute error is –0.04 with an average absolute error of -0.0088. The maximum absolute error from scatter due to compaction energy in determining the constant “b” is 0.54 whereas the minimum absolute error is –0.30 with an average absolute error of 0.225.

5.6. Inherent Error

Some of the tests have been done by the same operator on the same soil in the same laboratory conditions and the determined values for constants “a” and “b” were slightly different. These differences can be attributed to inherent errors, or errors beyond the control of the operator. In order to evaluate the inherent scatter, two TDR tests were performed on samples # MP-1 and 515. These tests were performed by the operator “Brian” under the same laboratory conditions. The results are shown in Fig. 5-6 for sample # MP-1 and Fig. 5-7 for sample # 515. The absolute errors in determining soil constants “a” and “b”, assuming base values of a = 1 and b = 8.50, are summarized in Table 5-3. According to Table 5-3, the absolute inherent error in determining the constant “a” is 0.03 and 0.02 for sample # MP-1 and sample # 515, respectively. The absolute error in determining the constant “b” is 0.73 and 0.2 for sample # MP-1 and sample # 515,

respectively. While the scatter may seem high for each of the individual factors "a" and "b", it is noted that they are highly correlated. In other words, for a given soil, high "a" values correspond to a low "b" values and vice versa. The predicted water content within the range of interest, however, is not sensitive to such variation, provided the correlation between "a" and "b" holds.

Table 5-3. The effect of inherent scatter on the determination of soil constants "a" and "b"

Sample No.	Measured Values		Absolute Error	
	a	b	a	b
Sample # MP-1_(1)	1.01	7.48	0.03	0.73
Sample # MP-1_(2)	0.98	8.21		
Sample # 515_(1)	1.01	8.93	0.02	-0.2
Sample # 515_(2)	1.03	8.73		

5.7. Soil Boxes for Controlled Lab TDR Tests

Two boxes were used in performing the TDR tests in the lab to provide controlled conditions. The larger one is 24×24×20 inches, and is made up of plywood ¾" thick. FDOT provided the box, and a movable extension collar, 4" high, was fabricated at USF (Fig. 5-11).

Figure 5-11. The larger box with the extension collar

The smaller box is 16×16×20 inches, and is also made up of plywood ¾" thick, with a similar collar attachment (Fig. 5-12).

Figure 5-12. The smaller box with the extension collar

The two boxes have been insulated internally to prevent moisture loss or absorption through the box connections or the plywood cracks (Fig. 5-13). Fiberglass mats and hardening resin (Fig. 5-14) were used for the insulation.

(a)

(b)

Figure 5-13. Inner insulation for (a) larger box, (b) smaller box

Figure 5-14. Insulation materials and tools

The insulation technique steps are described in detail as follows:

1. The inner surfaces of the box were dried and cleaned from any dust and residue.
2. The fiberglass mat was cut into pieces consistent with the box inner surfaces, with some corner overlapping to ensure perfect insulation.
3. An amount of hardening liquid was applied to the resin and mixed well following the manufacturer's specifications.
4. A thick layer of the resin was coated on the box surfaces using a soft wide brush.
5. The corresponding fiberglass mat pieces were applied to the resin-coated surface.
6. More resin was coated on the fiberglass mat and distributed gently over the mat, especially at the corners and sides of the box.
7. The resin was allowed to harden for 10-15 minutes before the next surface was applied. The process was continued until all inner sides of the box were covered by the mat.
8. To ensure perfect insulation, fiberglass pieces were added to the box corners and sides.
9. The box was tested by filling it with water and ensuring there were no leaks.

The weight of the larger box when filled with soil was determined to be around 815 lb (370 kg), which is too heavy to be handled by one person. A Bobcat or forklift was used to move the box, so an alteration to the box base was required to accommodate the forks. A 1000 lb scale was used to measure the weight of the compacted soil and calculate the density accordingly.

5.7.1. Calibration of the Boxes

The small box was calibrated by filling it with tap water. Knowing the empty weight of the box and measuring the weight of the box after filling it with water, the water volume, which equals to the box internal volume, can be determined. By repeating this calibration method for 3 times, the volume of the small box was determined to be 2.2917 ft^3 (64893 cm^3). The same procedure was used to determine the volume of the larger box and it was determined to be 5.2644 ft^3 (149071 cm^3).

5.7.2. TDR Calibration Tests

A series of TDR tests have been performed on different soils in order to calibrate the TDR results against a pre-known density and oven dry moisture content. The tests were performed in the smaller box. The first trial was carried out outside the soil laboratory. A pit was dug behind the soil laboratory to get the sample. Generally the testing procedure can be summarized as follows:

1. The soil was mixed with water many times using two shovels in the same time in order to ensure homogeneity (Fig. 5-15).

Figure 5-15. Mixing soil with water

2. The smaller box, with the extension collar, was filled with the soil in 6 layers, with the number of tamps increasing from 20 for the first layer to 25 for the last layer. These tamps were performed using a piece of wood of dimensions 4×4×40 inches (Fig. 5-16).

Figure 5-16. Compacting the soil in the smaller box with the extension collar

3. The extension collar was then removed and a steel straightedge was used to trim the extra soil above the box height (Fig. 5-17). This procedure ensures that the volume of the soil is equal to the volume of the box (Fig. 5-18), as determined from the calibration process.

(a) After taking the extension collar off

(b) While trimming the soil in the box

Figure 5-17. Trimming the soil

Figure 5-18. Soil filled exactly the box volume

4. A mechanical overhead crane was used to lift the box and put it on the scale (Fig. 5-19).

Figure 5-19. Lifting the soil using an overhead crane.

5. The weight of the box filled with soil was determined using a 1000 lbs capacity scale (Fig. 5-20). Knowing the empty weight of the box, the soil weight can be determined and wet density can be calculated.

Figure 5-20. Weighing the box after filling it with soil

6. A TDR test was run inside the box, as the field measurement and the soil dielectric constant in field was determined (Fig. 5-21).
7. The soil within the spikes region was excavated and compacted in the TDR mold in 6 layers, with number of tamps increasing from 20 to 25 per layer.
8. A second TDR measurement was taken into the mold and soil dielectric constant in the mold was determined (Fig. 5-22).
9. The moisture content, the dry density in the mold, and the in-field dry density was determined accordingly
10. The oven dry moisture content was then determined for the soil inside the mold for comparison purposes.

Figure 5-21. Measurement in the box (in-field measurement)

Figure 5-22. Measurement in the mold

The absolute and normalized errors for both moisture content and dry density can be calculated as follows:

$$Absolute\_Error\_W_c = (w_{c,fromTDR} - w_{c,actual}) \times 100 \quad (5\text{-}3)$$

$$Normalized\_Error\_W_c = \frac{w_{c,fromTDR} - w_{c,actual}}{w_{c,fromTDR}} \times 100 \quad (5\text{-}4)$$

$$Absolute\_Error\_\rho_{dry} = (\rho_{dry,fromTDR} - \rho_{dry,actual}) \times 100 \quad (5\text{-}5)$$

$$Normalized\_Error\_\rho_{dry} = \frac{\rho_{dry,fromTDR} - \rho_{dry,actual}}{\rho_{dry,fromTDR}} \times 100 \quad (5\text{-}6)$$

The spreadsheets, which used in calculation for all tested soils are included in the Appendix. The final results are summarized in Table 5-4. The results indicate that the accuracy in measurements in terms of both water content and density are in agreement with the theoretical analysis. Further discussion on this issue is available later in this report.

Table 5-4. Results of TDR calibration tests

Sample	Date	USCS	AASHTO	Moisture content, %ge				Dry Density			
				Actual Value	TDR Value	Absolute Error	Normalized Error	Actual Value, lb/ft3	TDR Value, lb/ft3	Absolute Error, lb/ft3	Normalized Error, %ge
1	8/6/2002	SP	A-3	5.75	5.50	-0.25	-4.60	96.14	94.77	-1.37	-1.45
1-a	8/6/2002	SP	A-3	10.63	9.70	-0.93	-9.56	93.28	95.22	1.93	2.03
1-b	8/6/2002	SP	A-3	12.52	11.40	-1.12	-9.82	95.79	98.70	2.91	2.95
2	8/6/2002	SP	A-1-b	8.84	8.00	-0.84	-10.54	102.63	101.67	-0.96	-0.94
2-a	8/6/2002	SP	A-1-b	11.93	10.40	-1.53	-14.72	106.23	112.31	6.08	5.42
3	8/9/2002	SP	A-1-b	5.47	5.20	-0.27	-5.26	94.74	98.08	3.34	3.40
3-a	8/9/2002	SP	A-1-b	9.62	9.40	-0.22	-2.31	98.72	100.79	2.07	2.05
3-b	8/9/2002	SP	A-1-b	12.21	11.10	-1.11	-9.99	100.72	107.56	6.84	6.36

5.8. Conclusion

The research carried out in this chapter primarily dealt with the evaluation of the TDR method's accuracy. Results from calibration testing indicate that nearly all the measurements recorded for water content (with the exception of a few outliers) fall within the acceptable range for geotechnical applications. The results for density are less accurate (within 5% to 10%), but further validation and comparison with other methods is needed before a definite recommendation is made. Results obtained here and from the Beta testing program at Purdue University indicate the viability of the TDR method as a measurement tool for geotechnical applications. Again, it should be noted that research carried out for the purpose of this report primarily dealt with sandy materials common to Florida. Therefore, no conclusion can be made with respect to the accuracy of the TDR method in fine grained or cohesive material.

6. LBR Test Correlation to the TDR Spike Driving Energy

6.1. Introduction

The TDR method requires that three spikes be driven around a central spike to obtain a TDR waveform. A brass hammer is used to drive the spikes into the ground. The energy required to drive the spikes into the soil varies depending on the soil resistance to penetration, which is directly related to the soil strength. Similar tests that rely on the measurement of resistance to penetration have been used to estimate the soil strength.

Instead of using the brass hammer to drive the spikes, a modified standard proctor hammer is used to measure the amount of effort required to drive the spikes. A steel cap with a groove having the same dimensions as the spike head is attached to the standard hammer. This allows for uniformity in the measurement of the driving energy required to drive the TDR spike to the template. Further modification can be introduced to the standard hammer to allow changes in drop height depending on the anticipated soil strength. A correlation between the energy required to drive the spikes and the soil resilient modulus or LBR (CBR) values is developed in this phase of the research.

6.2. Background

The in-place California Bearing Ratio (CBR) test and Limestone Bearing Ratio (LBR) test involve comparing the penetration load of a soil to that of a standard material. They are commonly used for evaluation and design of flexible pavement components.

6.2.1. Equipment

The ASTM standard Method D4429-93 (in-place CBR test), AASHTO T 193 and FM 5-515 (Florida Method of Test for Limerock Bearing Ratio) were used as guidelines in the acquisition of the equipment required to carry out the necessary tests.

The components of the in-place LBR test according to ASTM standard D 4429-93 are:

1. Mechanical screw jack capable of applying 5950 lbf.
2. Two proving rings of 1984 lbf and 5070 lbf in capacity.
3. Penetration piston 3 in^2 in cross section.
4. Piston adaptors.
5. Pipe extensions.
6. Dial gages.
7. Surcharge plate.
8. Surcharge weights.
9. Reaction truck capable of transmitting a 6970 lbf reaction force.
10. Loading frame and wood supports.
11. Beam used for dial gage support.

The truck, proving rings, jack, and standard piston are already available at University of South Florida. The reaction beam had to be designed and machined in the university workshop. The materials required for the beam, surcharge plates, surcharge loads, and the extension rods were purchased. Figure 6-1 shows typical in place CBR/LBR test equipment. Figure 6-2 displays the actual truck and set up used for testing.

Additional equipment required for the test includes the following items:

1. TDR driving template
2. Four standard TDR spikes.
3. Modified standard Proctor hammer.

The TDR equipment was previously acquired in the purchase of the standard equipment provided by Purdue University. The standard Proctor hammer was modified and machined at the University of South Florida (See Fig. 6-3).

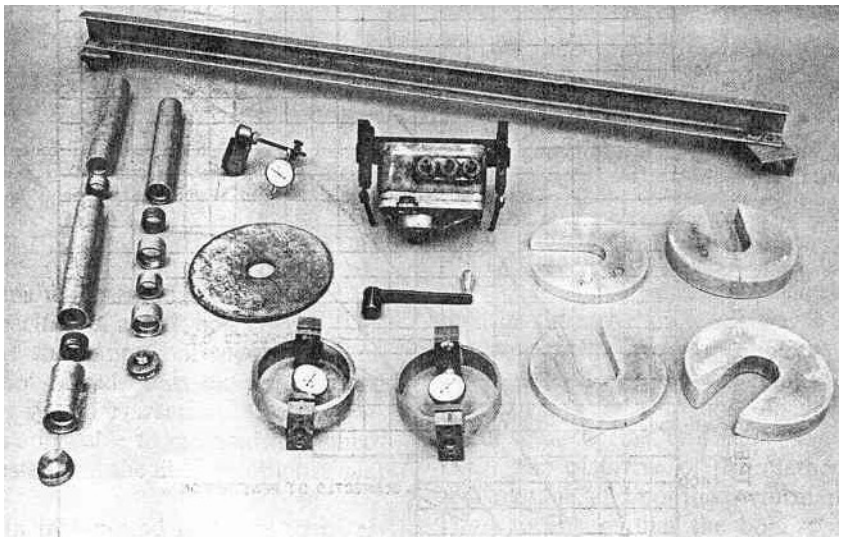

Figure 6-1. Apparatus for Field In-Place test

Source: ASTM D4429

Figure 6-2. LBR in place equipment setup.

Figure 6-3. The standard Proctor hammer with the attached head.

6.2.2. Procedure

1. Select a test location that is relatively flat and that is readily accessible to the truck required for the CBR test.
2. Prepare the testing area by removing any loose material or organics that may lie on the surface that is to be tested. Typically it is necessary to remove the top one to two inches of soil to expose soil that does not show inconsistency from rain or organic growth.
3. Attach the loading frame to the hydraulic jacks located at the front of the truck and position the truck over the desired testing site and lift the truck so no weight rests on the front springs.
4. Attach the jack to the loading frame and connect the proving ring along with the loading piston in series. Extension can be used to come within 4.9 inches of the surface that is to be tested.

Figure 6-4. TDR spike driving technique.

5. Position the circular surcharge plate directly over the material that is to be tested. Align the plate so that the penetration piston passes through the central hole. Place an additional twenty pound surcharge plate over the circular plate to achieve the minimum total surcharge of thirty pounds.
6. Place the dial support as to not interfere with the penetration piston and sufficiently removed as to not disturb the material being tested. Attach the dial gage to the beam and place it over the penetration piston were it can readily be viewed.
7. Zero the dial gages for the proving ring and displacement gage.
8. Apply the load to the penetration piston. The rate of penetration should be approximately 0.05 inch/min. This is accomplished by varying the amount of load being applied with the jacking arm while monitoring the displacement gage. Record the deflection of the proving ring at increments of 0.025 inches to a final depth of 0.500 inches.
9. Prepare a location for the TDR driving template as close to the penetration piston as possible, but no closer than the ASTM recommended distance of 15 inches. The area should be cleared of any organic material and leveled.

10. Place the first spike into the template. The spike may need to be held in place manually. Place the modified standard Proctor hammer over the spike fitting the grove over the head of the spike. The Proctor hammer is then dropped in the traditional manner as the number of drops is recorded. To ensure the hammer drops are being applied perpendicularly to the ground and in alignment with the spike someone can view the process at ground level while holding the spikes in position for proper stake driving technique. Figure 6-4 displays the TDR spike driving technique.
11. Repeat the process outlined in the previous step until all four spikes are driven. The number of blows required to drive each stake to the template should be recorded. The average value of blows required to drive the stakes is then calculated.
12. After testing is completed take a soil sample to be used to classify the soil.

6.2.3. Calculation

1. Compute the average number of blows required to drive the TDR spikes from the four recorded values.
2. Calculate the applied stress at each displacement recorded from the CBR test. Generate a plot of the stress penetration curve by graphing the stress versus displacement.
3. If necessary, correct the penetration graph for surface irregularities or upward concavity (See ASTM D 4429 for complete explanation). Figure 6-5 shows an example of a corrected penetration curve.
4. Record the stress at 0.1 in. and 0.2 in. penetration from the corrected penetration curve. Divide the recorded stress at 0.1 in. by a value of 800 psi and then multiply by 100. Divide the stress at 0.2 in penetration by a value of 1200 psi and then multiply by 100. Record the values obtained for both the 0.1 in. and 0.2 in. penetrations. If the 0.1 in. value is greater this number is recorded as the LBR number. If the 0.2 in. value is greater, the test should be repeated and if the results are consistent with the first test, the 0.2 in. number should be reported as the LBR number.

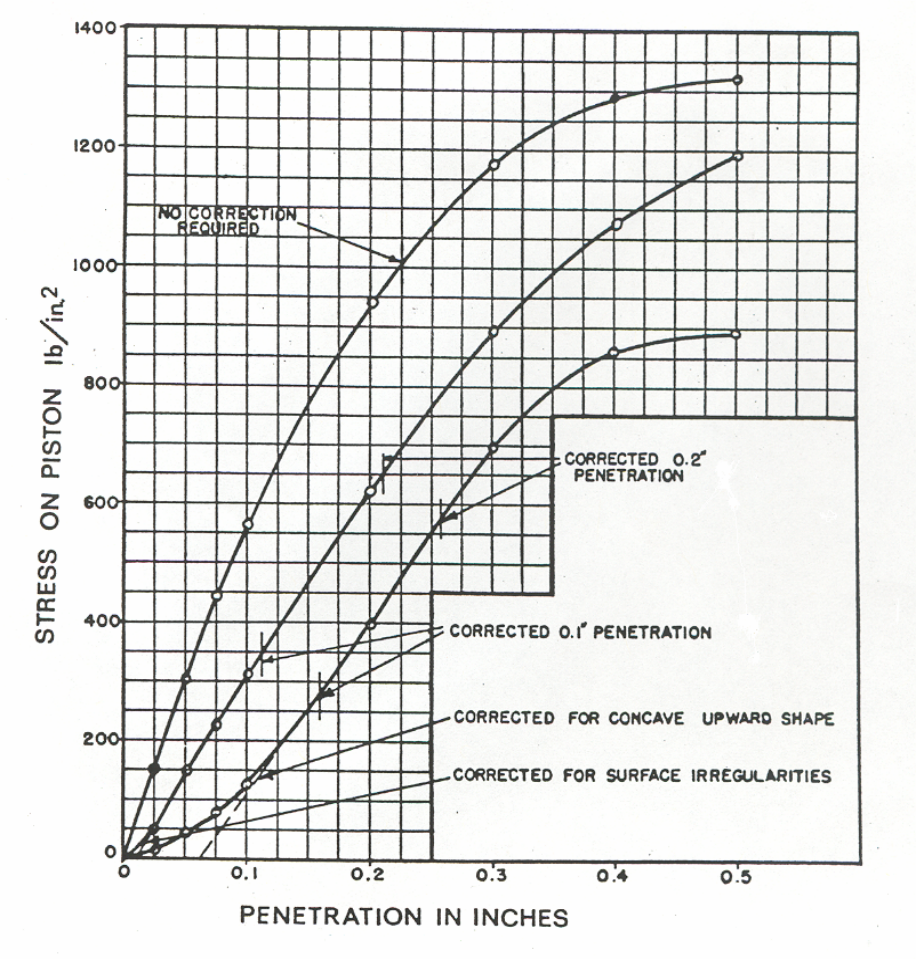

Figure 6-5. Correction of penetration curve.

Source: ASTM D 4429

6.3. Theoretical Background

6.3.1. CBR/LBR Comparison

The testing procedure described above is largely based on ASTM standard D 4429-93, which is the standard test method for California Bearing Ratio of soils in place. The CBR test compares the strength of the tested material to that of crushed rock. Due to the wide spread use of limestone in the state of Florida as a base material, the CBR value of crushed limestone is used as the standard value to compare all other soils. Thus, the test in Florida is referred to as the Limerock Bearing Ratio. The testing procedure is essentially the same with the only critical

difference coming in the calculation portion of the data analysis. The CBR test calls for a division of the 0.1 inch penetration of 1,000 psi and a division of 1,500 psi at the 0.2 inch penetration. The LBR values are calculated using 800 psi at 0.1 in. penetration. This reduction in the denominator is accredited to the reduction in the CBR value when limerock is used as the standard as opposed to the standard crushed rock. It follows that the LBR value is simply the CBR number multiplied by a factor of 1.25.

6.3.2. TDR/LBR Correlation

The TDR procedure requires that four 12 inch stakes be driven into the soil to obtain a TDR waveform (That is used for the measurement of soil properties as previously explained in chapter 3). The driving of the stakes into the soil requires a driving energy that is variable. The amount of blows needed to drive the stakes into the template is related to the strength of the soil. The stronger the material is the more hammer blows are required to drive the stakes. The amount of energy required to drive the spikes to the needed displacement varies with the strength of the given material.

The LBR test operates on the same principle. The piston is pushed into the ground as both force and displacement are measured. A measurement of strength is then derived from the relationship of stress to penetration. The measurement varies according to the strength of the material. The LBR strength parameter is then used to estimate the bearing capacity of the soil for design and analysis purposes.

Both the LBR test and the driving of the TDR spikes can be used to measure the amount of energy required to displace a soil a given amount. As a result, it is proposed that a correlation exists between the energy required to drive the TDR spikes into the template and the LBR number for the same soil. A modified proctor hammer is used to introduce consistency in the TDR stake driving process. The number of blows required to drive the 12 inch stakes into the TDR template can then be recorded. The average of the four stakes can then be taken and compared to the in-situ LBR values obtained for the same soil specimen.

6.3.3. Existing Empirical Correlations to the LBR Test

Correlative research to the LBR test has been carried out using the dynamic cone penetration test (DCP), the standard penetration test (SPT), the vane shear test and unconfined compression tests. The vane shear strength and the unconfined compression tests are primarily concerned with silty and clayey subgrades and for that reason will not be dealt with here. The DCP test is used to approximate soil strength to depths of one meter. This is accomplished by driving a rod with a penetration cone at the end into the soil. The penetration associated with each drop is recorded and a relationship is derived between the number of drops and the penetration of each drop. The SPT test is widely used in site-investigation works. The SPT test is also a measure of penetration as a result of an applied force. The measurement of penetration to blows has been used to formulate a correlative relationship between the SPT test and the LBR test. Using the penetration to resistance relationship the strength and relative density of the material can be estimated.

Research done by Kleyn (1975) formulated a DCP/LBR relationship. Investigation by Harison (1989) and data obtained both from field experiments and laboratory studies proposed the following equation used for determining LBR values from DCP test results for granular soils:

$$\log\left(\frac{LBR}{1.25}\right) = 2.698 - 1.12 * \log(DCP) \tag{6-1}$$

where,

DCP is the DCP penetration resistance of the soil in blows per 12 inches.

LBR is the material LBR in percent at the depth of the DCP penetration.

Research based again on the work of Kleyn (1975) done by Livneh and Ishai (1987) yielded the following modified DCP/LBR correlation:

$$\log\left(\frac{LBR}{1.25}\right) = 2.20 - 0.71 * (\log DCP)^{1.5} \tag{6-2}$$

Several other correlations have been made, and all equations have similar values, with the constant ranging from 2.555 to 2.81 and the log multiplier ranging from 1.12 to 1.32. The only exception is Liveneh's (1987) equation (Eq. 6-2). The Liveneh and Ishai (1987) approach creates the additional exponential increase in the DCP value. The differences between proposed correlations can be attributed to the differences in cone head angle and other slight variations in data collection and procedure. A final recommendation based on previous research was formulated by Harison (1989), he proposes the following equation:

$$\log\left(\frac{LBR}{1.25}\right) = 2.55 - 1.14 * \log(DCP) \tag{6-3}$$

Equation 6-3 varies only slightly when compared to the correlation proposed by Smith and Pratt (1983). Figure 6-6 is a graphical representation of the several proposed correlations between the DCP and LBR tests (Harison 1989). Research done on granular materials by Harison (1989) suggests that a slightly steeper relationship exists for granular materials.

Due to the wide spread use of the SPT test in site-investigation, Livneh and Ishai (1987) developed an equation for transforming SPT values to LBR numbers. Further improvements were made yielding the following equation (Livneh and Ishai, 1988):

$$\log\left(\frac{LBR}{1.25}\right) = -5.13 + 6.55 * (\log SPT)^{-0.26} \tag{6-4}$$

where,

SPT is the SPT blowcount at the depth of penetration.

Figure 6-7 shows the relationship between the SPT values and LBR values derived by Livneh (1989). Note that the data is displayed in SPT blow count per 12 inches for comparative purposes.

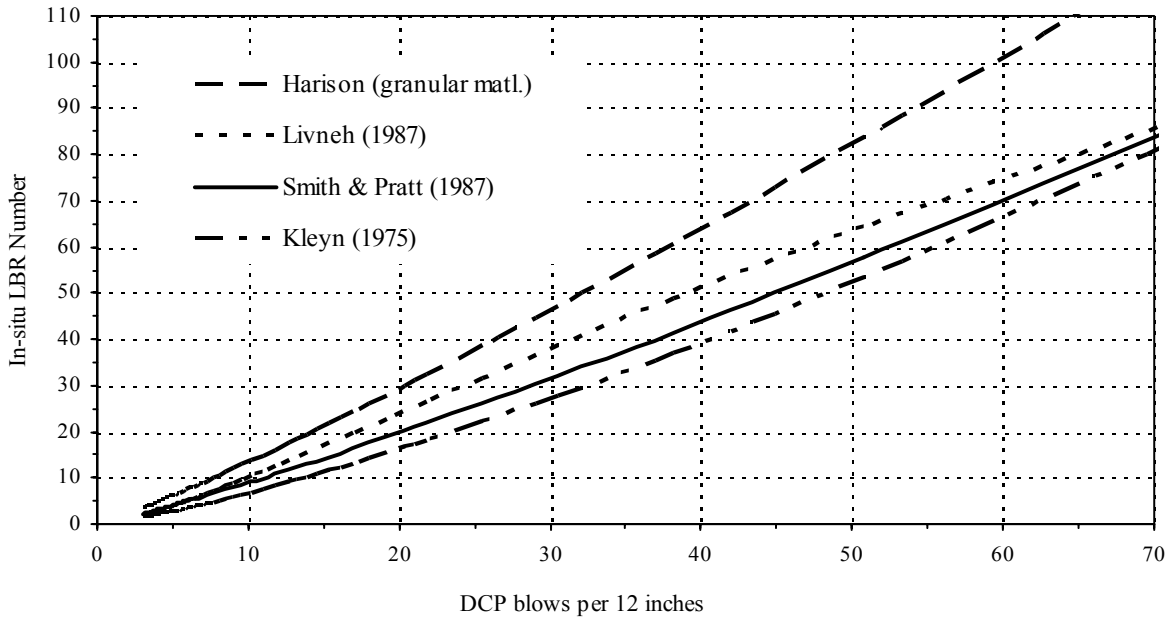

Figure 6-6. DCP and LBR relationship

Source: Harison 1989

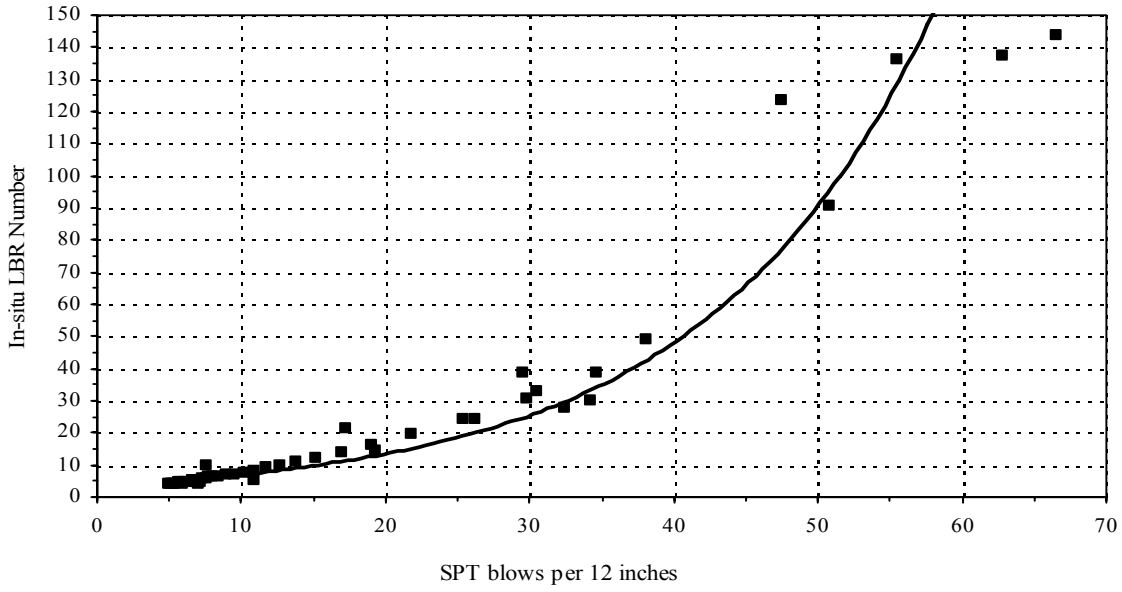

Figure 6-7. SPT and LBR relationship

Source: Livneh (1989)

The DCP and SPT tests all rely on the penetration to resistance relationship to evaluate the strength of a material. The LBR test relies on the same principle. The correlations developed for the DCP and SPT to the LBR test all indicate that an exponential relationship exists between them. The same type of relationship between the energy required to drive the TDR spikes and the LBR test is expected.

6.4. Test Results

6.4.1. Data Collection

Several LBR field tests were run along with TDR spike driving tests in attempt to establish a correlative transformation equation. Tests were mainly carried out at various locations on the University of South Florida campus. A smaller number of tests were performed on roadway projects in the greater Tampa area (SR 54 tests). Test locations were selected to give a wide range of LBR values that would cover the typical values encountered in Florida. All materials that were tested were A-3 or A-1-b type soil. Each test was performed in accordance with the procedure outlined previously. A summary of test locations, soil types and results is displayed in Table 6-1. Table 6-1 also displays the variation between the TDR spikes driven in the form of a standard deviation. Significant variability was encountered in driving the TDR stakes; however most standard deviation values were under 3. Table 6-1 also indicates that at higher LBR values the support system used was prone to slipping. This was evident in the wooden support blocks sliding against each other at higher loading conditions. Slippage between the wooden blocks was caused by higher loading conditions (above 2400 pounds) and also by frictional force induced by a slight inclination experienced by the truck as it was raised by the hydraulic jack system. This limited data collection to LBR values approximately 80. However, based on previously discussed DCP correlative research, the TDR/LBR relationship developed is expected to yield acceptable results at higher range LBR values.

Table 6-1. Summary of field testing

Test Location	Operator	Soil Type	Avg. # Blows	Stnd Dev	CBR #	LBR #	Comment
Water Chase	Newel & Rory	SP / A-3	11.75	0.5	3	4	OK
Shriners 1	Newel	SP / A-1-b	35.75	3.95	25	31	OK
Shriners 2	Newel	SP / A-1-b	29.25	2.5	20	25	OK
Shriners 3	Newel	SP / A-1-b	29.5	1.73	19	24	OK
Shriners 4	Newel	SP / A-1-b	36.75	2.5	35	44	OK
Shriners 5	Newel	SP / A-1-b	33	2.58	23	29	OK
Shriners 6	Newel	SP / A-1-b	29.5	2.08	18	23	OK
Moffit 1	Newel	SP / A-1-b	42.5	5.32	37	46	OK
Moffit 2	Newel	SP / A-1-b	63.75	2.22	54	68	OK
Moffit 3	Newel	SP / A-1-b	59	7.39	60	75	OK
Moffit 4	Newel	SP / A-1-b	59	7.39	68	85	OK
Botanical 2	Newel & Rory	SP / A-3	17.75	1.5	9	11	OK
Botanical 3	Newel & Rory	SP / A-3	25.25	2.22	24	30	OK
Botanical 4	Newel	SP / A-3	23.5	1.29	15	19	OK
Botanical 5	Newel	SP / A-3	27.25	1.71	20	25	OK
Botanical 7	Newel	SP / A-3	22.5	1.29	24	30	OK
Botanical 8	Newel	SP / A-3	17	2.31	16	20	OK
Botanical 9	Newel	SP / A-3	19.5	2.87	18	23	OK
Botanical 10	Newel	SP / A-3	11.5	0.5	9	11	OK
SR 54-2	Newel & Rory	SP / A-3	67	1.15	65	81	OK
Botanical 6	Newel	SP / A-3	17.25	2.97	19	24	OK
Botanical 1	Newel & Rory	SP / A-3	15.25	0.957	17	21	OK
Moffit 5	Newel	SP / A-1-b	54.5	13.72	71	89	Support slipped
SR 54-1	Newel & Rory	SP / A-3	70.25	6.8	57	71	Support slipped
Moffit 6	Newel	SP / A-1-b	41.5	3.7	68	85	Support slipped

6.4.2. Discussion/Analysis

As the results indicate, the correlation obtained for the TDR spikes to the LBR number compare favorably with the DCP transformation equations previously discussed (Figures 6-8 and 6-6). This was expected, as the driving of the TDR spikes is similar to the DCP test. Both tests operate on the same principle of using the penetration to resistance relationship to estimate soil strength by driving a cone shaped rod into the ground. It follows that the correlative transformation equations developed are similar in shape to the DCP correlations previously developed.

6.5. Proposed Model

The data from Table 6-1 was plotted and a relationship was derived between the TDR spike driving and the LBR test (Figure 6-8).

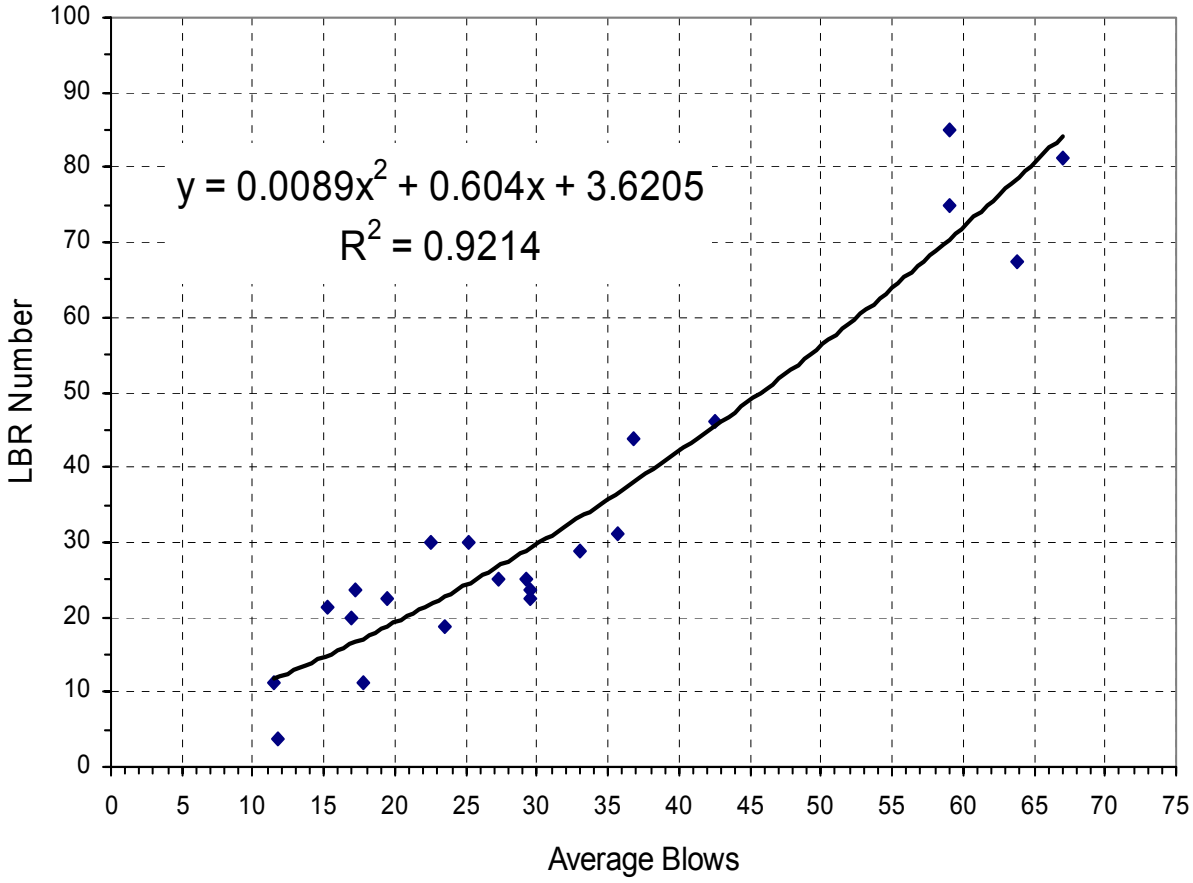

Figure 6-8. Proposed TDR spike and LBR relationship

Figure 6-8 clearly shows a range of LBR values may exist for a given average stake blow count. These results are consistent with efforts to correlate DCP values to LBR values (Figure 6-6). After careful examination and analysis of the data collected it is proposed that the following transformation equation is used to estimate the in-situ LBR number from the average number of blows required to drive the TDR stakes:

$$LBR = 0.0089 * TDR^2 + 0.604 * TDR + 3.62 \qquad (6\text{-}5)$$

where,

TDR is the average number of blows required to drive the 12 inch TDR spikes to the TDR template.

It is also proposed that a range be developed for the final LBR value obtained from equation 6-5. A range of +/- 10% of the obtained LBR value can be considered as an acceptable range for the in-situ LBR number.

6.6. Conclusion

The collection of data from a variety of field tests can greatly aid in the design of earthwork structures. Moisture content and density are two parameters that can be obtained with the Purdue TDR method. An additional approximation of the LBR number can be obtained through the correlation to the spikes driven when TDR measurements are taken. This additional measurement can readily provide an estimate of the in place LBR number that otherwise would require the mobilization of special equipment that in most cases is costly to operate and maintain. This additional feature allows the TDR operator to obtain three important soil parameters that are important in design and construction: in place moisture content, in place density and an in place LBR number.

7. Comparison of TDR with Other Methods

7.1. Introduction

Previous discussion has been centered on the evaluation of the TDR methods accuracy. This chapter is primarily concerned with the comparison between the accuracy of the TDR method with the nuclear, sand cone and drive sleeve methods. The nuclear method has become increasingly popular in recent years, due to its ability to measure both density and water content. Previous studies have indicated the method to be sufficiently accurate for geotechnical measurement. Particularly, FDOT has adopted the method for widespread use across the state. Due to its common usage, the nuclear method was selected for purposes of this study to assess the TDR methods accuracy relative to current methods. The drive sleeve method and the sand cone method results were also compared to TDR field measurements.

It is worth noting that the nuclear method is only used by FDOT for rock base materials, not for embankment or subgrade soils. Because the nuclear moisture measurement uses the back scatter method and has a limited depth of measurement, the speedy moisture method is typically used for embankments and subgrades. In the context of the comparative study outlined in this chapter, the oven dry moisture content was taken in order to get the most accurate baseline.

7.2. Testing Program

The widespread use of the nuclear method by the Florida DOT allows for ready access to a large amount of data. The nuclear method is commonly used to take several measurements at a variety of locations at a variety of job sites across the state of Florida. These same measurements can easily be tested using the TDR method to evaluate the accuracy of TDR measurements relative to the nuclear method. For purposes of this study an effort was made to collect comparative data for both the sand cone and drive sleeve methods. Samples can then be taken to the lab to obtain a baseline oven dry water content. Due to the lack of a baseline method for measuring in-situ soil dry density, the nuclear moist density was used as a baseline, with the dry density back-calculated from the oven dry moisture content. This, of course, is not entirely accurate, however

it was the method most readily available. A brief review of the nuclear, sand cone and drive sleeve methods are contained in Chapter 2 and will not be dealt with here.

7.3. Results

A series of side-by-side tests were carried out at several locations throughout the state using the nuclear, sand cone and drive sleeve methods and the TDR method. Blanket values of "a" = 1 and "b" = 9 were used for field TDR measurements. Samples were then brought to the lab and oven dry moisture contents were obtained. A summary of test locations and soil types for the nuclear to TDR comparison is displayed in Table 7-1. Table 7-2 displays the water content measurements recorded at each test site along with percent error and absolute error, while Table 7-3 summarizes the corresponding dry densities along with error. Figure 7-1 displays graphic results obtained from Table 7-2 and Figure 7-2 displays graphic results obtained from Table 7-3. Table 7-4 and Table 7-5 display test information for the sand cone tests and drive sleeve tests respectively. Figure 7-3 and Figure 7-4 display sand cone and drive sleeve results respectively.

Table 7-1. Nuclear testing locations and information

Location	County/City	No. of Samples	Soil Type(s)
I-295 / I-95	Duval Co.	2	A-3
SR44	Sumter Co.	5	A-3
SR54 E 41	Pasco	6	A-2-4
SR 207	St Johns	8	A-3/A-2-4
Santa Fe	Union	7	A-3/A-2-4
SR 54 E 19	Pasco	6	A-3
SR 98	Walton	4	A-3
SR 291	Pensacola	6	A-2-4
I-4	Volusia	6	A-3/A-2-4

Table 7-2. Nuclear water content comparison results.

Location	Test	Oven w_c	TDR w_c	Nuclear w_c	% error TDR	% error Nuclear	Absolute TDR	Absolute Nuclear
Duval Co.	1	9.0%	13.0%	10.2%	44.4%	13.3%	4.00%	1.20%
Duval Co.	2	9.7%	12.5%	9.2%	28.9%	-5.2%	2.80%	-0.50%
Sumter Co.	3	7.6%	7.2%	7.9%	-5.3%	3.9%	-0.40%	0.30%
Sumter Co.	4	8.0%	7.6%	7.9%	-5.0%	-1.3%	-0.40%	-0.10%
Sumter Co.	5	7.9%	7.1%	7.6%	-10.1%	-3.8%	-0.80%	-0.30%
Sumter Co.	6	12.9%	12.2%	13.4%	-5.4%	3.9%	-0.70%	0.50%
Sumter Co.	7	14.0%	13.6%	16.4%	-2.9%	17.1%	-0.40%	2.40%
Sumter Co.	8	13.2%	12.3%	14.8%	-6.8%	12.1%	-0.90%	1.60%
Pasco	1	6.3%	5.9%	6.2%	-6.3%	-1.6%	-0.40%	-0.10%
Pasco	2	6.2%	5.7%	5.3%	-8.1%	-14.5%	-0.50%	-0.90%
Pasco	3	7.2%	6.0%	7.2%	-16.7%	0.0%	-1.20%	0.00%
Pasco	4	5.5%	4.7%	5.0%	-14.5%	-9.1%	-0.80%	-0.50%
Pasco	5	6.6%	5.7%	6.9%	-13.6%	4.5%	-0.90%	0.30%
Pasco	6	8.6%	8.4%	8.7%	-2.3%	1.2%	-0.20%	0.10%
St Johns	1	13.8%	13.4%	14.1%	-2.9%	2.2%	-0.40%	0.30%
St Johns	2	9.7%	9.3%	9.0%	-4.1%	-7.2%	-0.40%	-0.70%
St Johns	3a	11.4%	10.8%	12.2%	-5.3%	7.0%	-0.60%	0.80%
St Johns	3b	11.0%	10.8%	12.4%	-1.8%	12.7%	-0.20%	1.40%
St Johns	4	12.2%	11.4%	13.4%	-6.6%	9.8%	-0.80%	1.20%
St Johns	5	8.2%	11.9%	13.8%	45.1%	68.3%	3.70%	5.60%
St Johns	6	8.7%	6.9%	8.7%	-20.7%	0.0%	-1.80%	0.00%
St Johns	7	12.8%	8.8%	8.6%	-31.3%	-32.8%	-4.00%	-4.20%
Union	1	10.2%	9.4%	12.3%	-7.8%	20.6%	-0.80%	2.10%
Union	2	10.3%	9.2%	11.4%	-10.7%	10.7%	-1.10%	1.10%
Union	3	9.4%	8.4%	10.1%	-10.6%	7.4%	-1.00%	0.70%
Union	4	7.5%	6.6%	11.6%	-12.0%	54.7%	-0.90%	4.10%
Union	5	10.5%	8.9%	9.8%	-15.2%	-6.7%	-1.60%	-0.70%
Union	7	9.1%	8.0%	13.4%	-12.1%	47.3%	-1.10%	4.30%
Pasco	1	4.0%	3.5%	4.5%	-12.5%	12.5%	-0.50%	0.50%
Pasco	2	6.9%	6.3%	9.1%	-8.7%	31.9%	-0.60%	2.20%
Pasco	3	6.6%	6.1%	9.6%	-7.6%	45.5%	-0.50%	3.00%
Pasco	4	5.8%	5.3%	7.2%	-8.6%	24.1%	-0.50%	1.40%
Pasco	5	6.6%	6.0%	7.7%	-9.1%	16.7%	-0.60%	1.10%
Pasco	6	5.2%	4.5%	6.3%	-13.5%	21.2%	-0.70%	1.10%
Walton	1	14.0%	9.6%	15.1%	-31.4%	7.9%	-4.40%	1.10%
Walton	2	13.2%	10.2%	13.1%	-22.7%	-0.8%	-3.00%	-0.10%
Walton	3	12.8%	9.9%	12.9%	-22.7%	0.8%	-2.90%	0.10%
Walton	4	13.5%	10.5%	13.6%	-22.2%	0.7%	-3.00%	0.10%
Pensacola	1	9.2%	6.6%	7.2%	-28.3%	-21.7%	-2.60%	-2.00%
Pensacola	2	8.7%	5.5%	6.5%	-36.8%	-25.3%	-3.20%	-2.20%
Pensacola	3	8.4%	5.5%	6.7%	-34.5%	-20.2%	-2.90%	-1.70%
Pensacola	4	9.7%	6.6%	7.7%	-32.0%	-20.6%	-3.10%	-2.00%
Pensacola	5	9.7%	6.6%	8.4%	-32.0%	-13.4%	-3.10%	-1.30%
Pensacola	6	9.2%	6.3%	7.4%	-31.5%	-19.6%	-2.90%	-1.80%
Volusia	1	10.0%	9.2%	12.3%	-8.0%	23.0%	-0.80%	2.30%
Volusia	2	11.3%	9.8%	13.1%	-13.3%	15.9%	-1.50%	1.80%
Volusia	3	12.0%	10.2%	12.3%	-15.0%	2.5%	-1.80%	0.30%
Volusia	4	8.9%	7.5%	8.7%	-15.7%	-2.2%	-1.40%	-0.20%
Volusia	5	10.3%	8.8%	10.0%	-14.6%	-2.9%	-1.50%	-0.30%
Volusia	6	7.5%	6.6%	8.9%	-12.0%	18.7%	-0.90%	1.40%

Table 7-3. Nuclear dry density comparison

Location	Test	Oven ρ_d	TDR ρ_d	Nuclear ρ_d	% error TDR	% error Nuclear	Absolute TDR	Absolute Nuclear
Duval Co.	1	102.8	94.1	101.6	-8.5%	-1.2%	-8.70	-1.20
Duval Co.	2	102.6	88.0	103.1	-14.2%	0.5%	-14.60	0.50
Sumter Co.	3	112.0	105.5	111.7	-5.8%	-0.3%	-6.50	-0.30
Sumter Co.	4	112.5	108.3	112.6	-3.7%	0.1%	-4.20	0.10
Sumter Co.	5	112.9	108.3	113.2	-4.1%	0.3%	-4.60	0.30
Sumter Co.	6	108.8	107.1	108.3	-1.6%	-0.5%	-1.70	-0.50
Sumter Co.	7	107.3	102.2	105.1	-4.8%	-2.1%	-5.10	-2.20
Sumter Co.	8	111.2	127.7	109.7	14.8%	-1.3%	16.50	-1.50
Pasco	1	108.9	103.8	109.0	-4.7%	0.1%	-5.10	0.10
Pasco	2	107.8	100.1	108.7	-7.1%	0.8%	-7.70	0.90
Pasco	3	107.3	106.7	107.3	-0.6%	0.0%	-0.60	0.00
Pasco	4	107.2	101.4	107.7	-5.4%	0.5%	-5.80	0.50
Pasco	5	112.2	110.4	111.9	-1.6%	-0.3%	-1.80	-0.30
Pasco	6	107.4	96.1	107.3	-10.5%	-0.1%	-11.30	-0.10
St Johns	1	101.3	98.0	101.1	-3.3%	-0.2%	-3.30	-0.20
St Johns	2	101.5	94.6	102.2	-6.8%	0.7%	-6.90	0.70
St Johns	3a	103.3	99.1	102.6	-4.1%	-0.7%	-4.20	-0.70
St Johns	3b	107.0	100.0	105.7	-6.5%	-1.2%	-7.00	-1.30
St Johns	4	103.0	106.0	101.9	2.9%	-1.1%	3.00	-1.10
St Johns	5	108.7	100.8	103.3	-7.3%	-5.0%	-7.90	-5.40
St Johns	6	100.8	100.1	100.8	-0.7%	0.0%	-0.70	0.00
St Johns	7	99.0	98.1	102.9	-0.9%	3.9%	-0.90	3.90
Union	1	98.1	87.8	96.2	-10.5%	-2.0%	-10.28	-1.92
Union	2	100.1	102.4	99.1	2.3%	-1.0%	2.30	-0.99
Union	3	105.7	99.7	105.0	-5.6%	-0.6%	-5.92	-0.67
Union	4	107.2	108.1	103.2	0.9%	-3.7%	0.93	-3.94
Union	5	102.9	107.7	103.6	4.7%	0.6%	4.81	0.66
Union	7	109.6	103.8	105.5	-5.3%	-3.7%	-5.80	-4.10
Pasco	1	102.6	98.0	102.1	-4.5%	-0.5%	-4.63	-0.49
Pasco	2	106.0	100.9	103.8	-4.8%	-2.0%	-5.04	-2.14
Pasco	3	107.6	98.6	104.7	-8.4%	-2.7%	-9.00	-2.95
Pasco	4	102.8	96.1	101.5	-6.5%	-1.3%	-6.69	-1.34
Pasco	5	105.1	96.8	104.0	-7.8%	-1.0%	-8.24	-1.07
Pasco	6	105.1	97.4	104.0	-7.4%	-1.0%	-7.75	-1.09
Walton	1	109.4	111.9	108.3	2.3%	-1.0%	2.50	-1.10
Walton	2	110.1	108.9	110.2	-1.1%	0.1%	-1.20	0.10
Walton	3	111.0	107.3	110.9	-3.3%	-0.1%	-3.70	-0.10
Walton	4	108.9	105.9	108.8	-2.8%	-0.1%	-3.00	-0.10
Pensacola	1	115.9	112.9	118.1	-2.6%	1.9%	-3.05	2.16
Pensacola	2	116.4	118.1	118.8	1.5%	2.1%	1.75	2.40
Pensacola	3	114.7	116.6	116.5	1.7%	1.6%	1.91	1.83
Pensacola	4	114.7	117.9	116.8	2.8%	1.9%	3.24	2.13
Pensacola	5	116.1	117.7	117.5	1.3%	1.2%	1.55	1.39
Pensacola	6	116.1	112.7	118.1	-3.0%	1.7%	-3.46	1.95
Volusia	1	115.5	109.7	113.2	-5.0%	-2.0%	-5.82	-2.37
Volusia	2	114.1	113.0	112.3	-1.0%	-1.6%	-1.13	-1.82
Volusia	3	108.2	106.3	107.9	-1.7%	-0.3%	-1.88	-0.29
Volusia	4	112.1	106.6	112.3	-4.9%	0.2%	-5.48	0.21
Volusia	5	112.5	107.8	112.8	-4.2%	0.3%	-4.76	0.31
Volusia	6	109.9	113.4	108.4	3.2%	-1.3%	3.49	-1.41

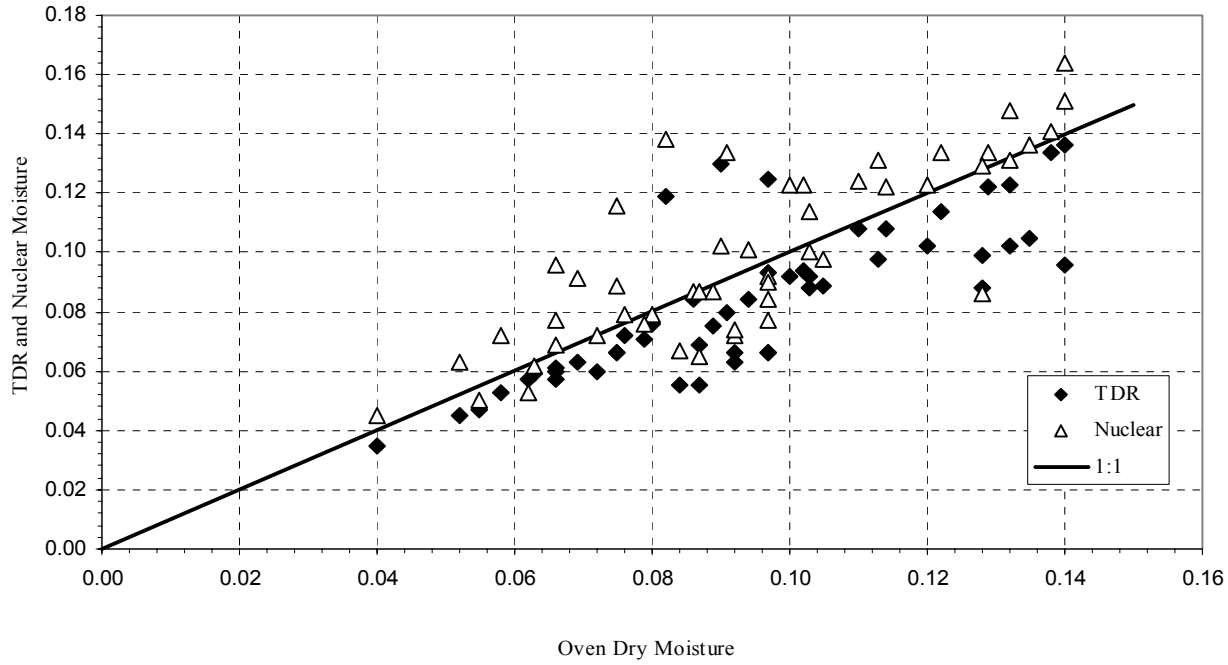

Figure 7-1. Nuclear versus TDR water content.

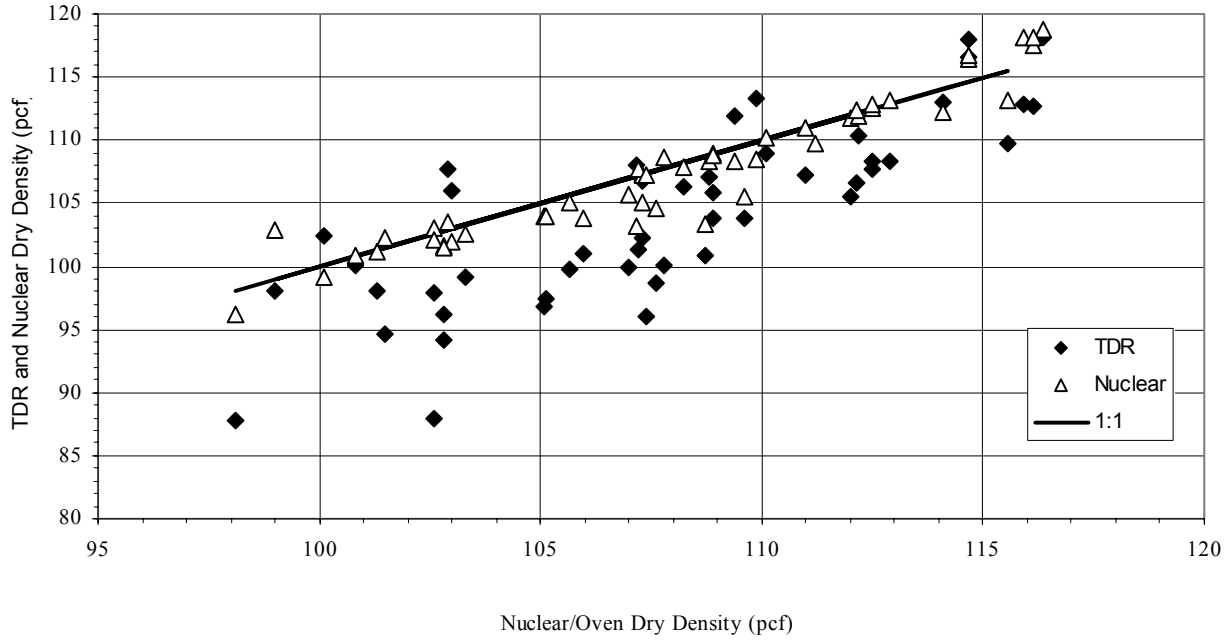

Figure 7-2. Nuclear versus TDR dry density.

Table 7-4. Sand cone dry density comparison results.

Location	Test	Oven ρ_d	TDR ρ_d	Sand Cone ρ_d	% error TDR	% Error Sand Cone
I-295 / I-95	1	102.8	94.1	95	-8.46%	-7.59%
I-295 / I-95	2	102.6	88	97.4	-14.23%	-5.07%
Sumter Co.	3	112	105.5	112.4	-5.80%	0.36%
Sumter Co.	4	112.5	108.3	111.9	-3.73%	-0.53%
Sumter Co.	5	112.9	108.3	114.3	-4.07%	1.24%
Sumter Co.	6	108.8	107.1	106.8	-1.56%	-1.84%
Sumter Co.	7	107.3	102.2	114.3	-4.75%	6.52%
Sumter Co.	8	111.2	127.7	110.5	14.84%	-0.63%

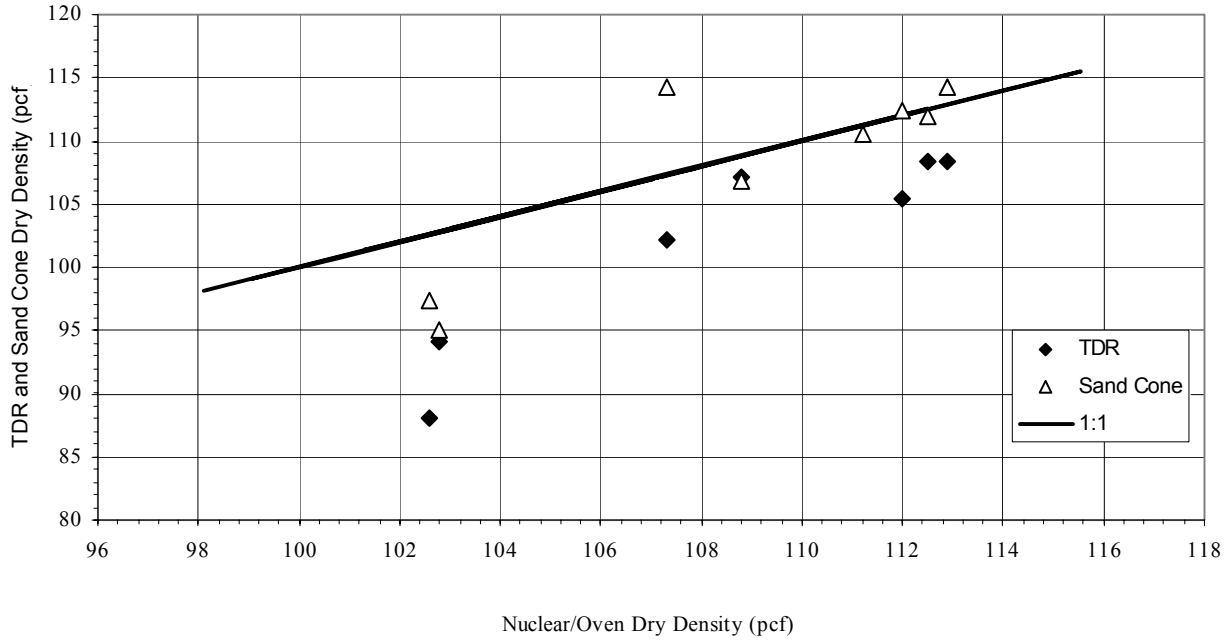

Figure 7-3. Sand cone versus TDR dry density.

Table 7-5. Drive sleeve dry density comparison results.

Location	Test	Oven ρ_d	TDR ρ_d	Drive Sleeve ρ_d	% error TDR	% Error Drive Sleeve
I-295 / I-95	1	102.8	94.1	102.8	-8.46%	0.00%
I-295 / I-95	2	102.6	88	101.3	-14.23%	-1.27%
Sumter Co.	3	112	105.5	112.9	-5.80%	0.80%
Sumter Co.	4	112.5	108.3	115.5	-3.73%	2.67%
Sumter Co.	5	112.9	108.3	114.8	-4.07%	1.68%
Sumter Co.	6	108.8	107.1	109.6	-1.56%	0.74%
Sumter Co.	7	107.3	102.2	121.8	-4.75%	13.51%
Sumter Co.	8	111.2	127.7	112.9	14.84%	1.53%

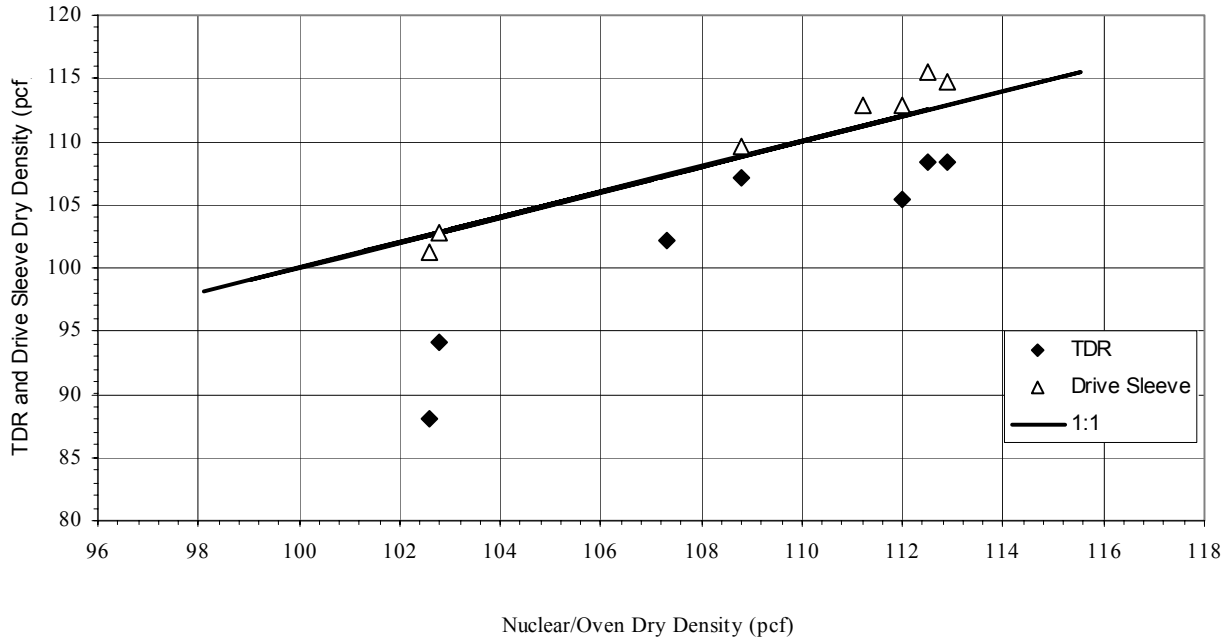

Figure 7-4. Drive sleeve versus TDR dry density.

7.4. Discussion

The majority of soils tested were sandy materials (A-3 and A-2-4 soils). This is consistent with testing throughout this project, one of the main objectives being to evaluate the applicability of the TDR method to soils common to Florida construction. The water content measurement comparison displayed in Table 7-2 shows the absolute error for TDR varied between -4.4 and 4.0 and the percent error varied accordingly. Typical TDR measured water content values under predicted the oven dry water content. This is consistent with observed results from the evaluation of the accuracy of the TDR method. As indicated in this report, a more appropriate "b" value of 8.5 should be used for Florida sands. The reduction in the "b" value will predict slightly higher water content values in the field and TDR measurements displayed in Figure 7-1 would be shifted upwards towards the 1:1 line. Measured water contents for the nuclear method had a range of -4.2 to 5.6 for absolute error and the percent errors varied accordingly. A graphic representation of scatter for both the nuclear and TDR methods compared to the oven dry method is displayed in Figure 7-1, which indicates that the nuclear method consistently over predicted the water content while the TDR method under predicted the water content. Figure 7-1 also indicates that there is more scatter inherent to the nuclear method. If the suggested correction for constant "b" it is reasonable to suggest that the TDR water content measurement is more accurate than the nuclear method for water content measurement.

Table 7-3 can only be used for reference purposes, since the baseline dry density was calculated from a combination of the nuclear moist density and the oven dry moisture content. It is to be expected that the nuclear measurements be more accurate than the TDR measurements, as evident from the table. The bias towards the accuracy of the nuclear method is also apparent in Figure 7-2. In order to evaluate the true accuracy of both the nuclear and TDR methods, the use of an objective and independent point of reference for density is needed. The development of such independent measurements was, however, beyond the scope of the current project.

Table 7-4 and Figure 7-3 should only be used for comparative purposes. Again, the dry density baseline is taken as the nuclear moist density back calculated to the dry density using the oven

dry water content. As displayed in Figure 7-3 the scatter between the two methods appears to be comparable. However, more data needs to be collected to make a realistic determination of the relative accuracy of the TDR method to the sand cone method.

Again in Table 7-5 and Figure 7-4 the TDR and drive sleeve dry density results are compared to the measured nuclear density and oven dry water content. The drive sleeve method appears to compare favorably with the nuclear dry density baseline. More testing would be needed to make a reasonable statement of the relative accuracy of TDR compared to the drive sleeve method.

7.5. Conclusions

The nuclear method has been accepted as a reliable method for both water content and density for base course materials, due to its ability to measure both water content and dry density, and its perceived reliability and accuracy. The sand cone method and the drive sleeve method are other methods that have been commonly used to estimate dry density in the field. Side-by side measurements comparing the TDR to the nuclear method for water content measurement on Florida construction soils indicate that the TDR displays less scatter than the nuclear gauge and as a result is likely more accurate than the nuclear gauge with the proper selection of constants "a" and "b." It thus appears that the TDR method is more reliable than the nuclear method, at least in terms of water content measurement. Density results were inconclusive, due to the lack of a comparison baseline. However, a comparison of the data scatter between methods is similar. Further research is required to fully evaluate the absolute accuracy of the methods for field density measurement.

8. Database Management System Design

8.1. Introduction

In order to evaluate the TDR data nationwide, a Beta testing program has been conducted by Purdue University researchers. A number of agencies have collaborated in the evaluation of the TDR method. Among the collaborating agencies are Florida Department of Transportation (FDOT), and the University of South Florida (USF). Due to the large amounts of data that was and will be collected, a need for a database managing system has arisen. The database management system has to be simple and user-friendly, and the interface easy for users to understand. Microsoft Access 2000 was selected to design an easy-to-use and manageable database. The database consists of one form that includes agency information. The rest of the data is entered in a logical sequence as sub-forms.

There are many advantages of a database approach rather than the traditional system management method by a file processing system. Some of the benefits are program-data independence, minimal data redundancy, improved data consistency, increased productivity of application development, improved data quality, and improved data accessibility and responsiveness.

8.2. Data, Database, and Metadata

In general, data types can be divided into textual, numeric, documents, images, sound, and video segments. When the data is processed to increase the reader's knowledge, it is then called information. The database is defined as the organized collection of logically related data. Metadata is defined as the data that describes the properties of other data (Kafle and Ashmawy, 2001).

8.3. Database Development Process

The database development process passes through various development phases **(**Kafle and Ashmawy, 2001):

1- *Conceptual Data Modeling*: There are two phases in this stage; planning and analysis phases. During planning, the relationships among the entities, high-level categories of data, are established. During the analysis, the detailed data model is presented.

2- *Logical Database Design*: The conceptual data model is transferred into relations, the nature and specifications of the data are determined, the normalization of the design is performed, and a complete picture of the database is obtained.

3- *Physical Database Design and Creation*: The database is organized and stored in the computer, the database management system is selected, and the data transactions processing programs are outlined.

4- *Database Implementation*: The programs for processing the database are coded, tested, and installed, and the data are loaded from the existing sources and tested.

5- *Database Maintenance*: The structure of the database is added, deleted, or changed in order to be consistent with the business needs.

8.4. Data Model

The *Relational Data Model* has been used in the database design. It consists of the following three components:

1- Data Structure: Data is organized into tables, which consist of known number of named columns and arbitrary number of unnamed rows. Table 8-1 shows an example of a table containing compaction data. Comp ID, Lab Test ID, Sample Number, Date, Time, Technician, Dry Density, Labcomp filename, and moisture content are the attributes. The table contains 19 rows of data corresponding to 19 different compaction tests. Every

table has to have a primary key that uniquely identifies each row. In Table 8-1, the primary key is Comp ID. A foreign key is an attribute/combination of attributes in a table, which serves as the primary key for another table. In Table 8-1, the foreign key is Lab Test ID. Table 8-2 shows a part of the agency table, Table 8-3 shows GSD table, Table 8-4 shows the Lab table, and Table 8-5 shows a part of the PMTDR table.

2- Data Manipulation: Structured Query Language (SQL) is used to manipulate data in the relational database. SQL has the ability to process the data in a single table as well as in the multiple tables using joints.
3- Data Integrity: The relational data model includes some integrity constraints to ensure accuracy of data when they are inserted or manipulated such as: domain constraints, entity integrity, referential integrity, and operational constraints.

8.5. Database Design

The data needed to be stored in this project can be divided into 5 parts: Agency, PMTDR, Lab, Compaction, and GSD. The relationships between the different tables are established as follows:

1. Each agency could have zero, one, or more PMTDR record, while each PMTDR record has to be related to exactly one Agency.
2. Each PMTDR record could have zero, one, or more Lab records, whereas each lab record has to be related to exactly one PMTDR record.
3. Each Lab record could have zero, one, or more GSD records, but each GSD record has to be related to exactly one Lab record.
4. Each Lab record could have zero, one, or more Compaction records, and each Compaction record has to be related to exactly one Lab record.
5. Each Lab record could have zero, one, or more GSD records, where each GSD record has to be related to exactly one Lab record.

Table 8-1. Compaction table with sample data

CompID	LabTestID	Sample_Number	Date	Time	Technician	Dry_Density	LabCMP_filename	Moisture
3	8		26-May-1998	10:54:54 AM	Feng, Lin, Vogel	1687	Geotechnical\TDR Data\Lin\Rev_Lin\tdrtest\REV_M1\rev_M1_1_1	3.84
4	12	M1_1_2	26-May-1998	11:06:47 AM	Feng, Lin, Vogel	1864	Geotechnical\TDR Data\Lin\Rev_Lin\tdrtest\REV_M1\rev_M1_1_2	3.76
5	13	M1_1_3	26-May-1998	11:48:10 AM	Feng, Lin, Vogel	1960	Geotechnical\TDR Data\Lin\Rev_Lin\tdrtest\REV_M1\rev_M1_1_3	3.82
6	14	M1_1_4	26-May-1998	11:48:10 AM	Feng, Lin, Vogel	2121	Geotechnical\TDR Data\Lin\Rev_Lin\tdrtest\REV_M1\rev_M1_1_3	3.65
7	15		26-May-1998	10:54:54 AM	Feng, Lin, Vogel	1687	Geotechnical\TDR Data\Lin\Rev_Lin\tdrtest\REV_M1\rev_M1_2_1	3.84
8	16		26-May-1998	10:54:54 AM	Feng, Lin, Vogel	1687	Geotechnical\TDR Data\Lin\Rev_Lin\tdrtest\REV_M1\rev_M1_2_2	3.84
9	17		26-May-1998	10:54:54 AM	Feng, Lin, Vogel	1687	Geotechnical\TDR Data\Lin\Rev_Lin\tdrtest\REV_M1\rev_M1_2_3	3.84
10	18		26-May-1998	10:54:54 AM	Feng, Lin, Vogel	1687	Geotechnical\TDR Data\Lin\Rev_Lin\tdrtest\REV_M1\rev_M1_2_4	3.84
11	19		26-May-1998	10:54:54 AM	Feng, Lin, Vogel	1687	Geotechnical\TDR Data\Lin\Rev_Lin\tdrtest\REV_M1\rev_M1_3_1	3.84
12	20		26-May-1998	10:54:54 AM	Feng, Lin, Vogel	1687	Geotechnical\TDR Data\Lin\Rev_Lin\tdrtest\REV_M1\rev_M1_3_2	3.84
13	21		26-May-1998	10:54:54 AM	Feng, Lin, Vogel	1687	Geotechnical\TDR Data\Lin\Rev_Lin\tdrtest\REV_M1\rev_M1_3_3	3.84
14	22		26-May-1998	10:54:54 AM	Feng, Lin, Vogel	1687	Geotechnical\TDR Data\Lin\Rev_Lin\tdrtest\REV_M1\rev_M1_3_4	3.84
15	23		26-May-1998	10:54:54 AM	Feng, Lin, Vogel	1687	Geotechnical\TDR Data\Lin\Rev_Lin\tdrtest\REV_M1\rev_M1_4_1	3.84
16	24		26-May-1998	10:54:54 AM	Feng, Lin, Vogel	1687	Geotechnical\TDR Data\Lin\Rev_Lin\tdrtest\REV_M1\rev_M1_4_2	3.84
17	25		26-May-1998	10:54:54 AM	Feng, Lin, Vogel	1687	Geotechnical\TDR Data\Lin\Rev_Lin\tdrtest\REV_M1\rev_M1_4_3	3.84
18	26		26-May-1998	10:54:54 AM	Feng, Lin, Vogel	1687	Geotechnical\TDR Data\Lin\Rev_Lin\tdrtest\REV_M1\rev_M1_4_4	3.84
19	27		26-May-1998	10:54:54 AM	Feng, Lin, Vogel	1687	Geotechnical\TDR Data\Lin\Rev_Lin\tdrtest\REV_M1\rev_M1_5_1	3.84

Table 8-2. Sample view of Agency table with sample data

Agency ID	Agency_Name	Contract_Number	Street_Address_1	Street_Address_2	City	Zip	State	Country	Phone_Number	Extension	Fax_Number	Email_Address
11	Geotech. Engr. (Dmevich)		Geotechnical Engineering,	Purdue University	West Lafayette	47906	IN	U.S.A.	(765) 494-5029	0000	(765) 496-1364	dmevich@purdue.edu

Table 8-3. GSD table with sample data

LabTestID	Grain_Size	Sieve_Number	Percent_finer
12	0.075	200	0.413
13	0.075	200	0.413

Table 8-4. Lab table with sample data

LabTestID	PMTDRID	Lab_Name	Supervisor	Sample_ID	Visual_Manual	Visual_Manual_Date	Visual_Manual_Tech	LL	PL	G_s	Atterberg_Date	Atterberg_Tech	GSD_date	GSD_Tech	USCS	Comment	AASHTO
8	13	Geotech. Lab	VPD	M1_1_1						2.76	26-May-1998		26-May-1998	Feng, Lin, Vogel	SM-SC		
12	15	Geotech. Lab	VPD	M1_1_2						2.76	26-May-1998		26-May-1998	Feng, Lin, Vogel	SM-SC		
13	16	Geotech. Lab	VPD	M1_1_3						2.76	26-May-1998		26-May-1998	Feng, Lin, Vogel	SM-SC		
14	17	Geotech. Lab	VPD	M1_1_4						2.76	26-May-1998		26-May-1998	Feng, Lin, Vogel	SM-SC		
15	22	Geotech. Lab	VPD	M1_2_1						2.76	26-May-1998		26-May-1998	Feng, Lin, Vogel	SM-SC		
16	23	Geotech. Lab	VPD	M1_2_2						2.76	26-May-1998		26-May-1998	Feng, Lin, Vogel	SM-SC		
17	24	Geotech. Lab	VPD	M1_2_3						2.76	26-May-1998		26-May-1998	Feng, Lin, Vogel	SM-SC		
18	25	Geotech. Lab	VPD	M1_2_4						2.76	26-May-1998		26-May-1998	Feng, Lin, Vogel	SM-SC		
19	26	Geotech. Lab	VPD	M1_3_1						2.76	26-May-1998		26-May-1998	Feng, Lin, Vogel	SM-SC		
20	27	Geotech. Lab	VPD	M1_3_2						2.76	26-May-1998		26-May-1998	Feng, Lin, Vogel	SM-SC		
21	28	Geotech. Lab	VPD	M1_3_3						2.76	26-May-1998		26-May-1998	Feng, Lin, Vogel	SM-SC		
22	29	Geotech. Lab	VPD	M1_3_4						2.76	26-May-1998		26-May-1998	Feng, Lin, Vogel	SM-SC		
23	30	Geotech. Lab	VPD	M1_4_1						2.76	26-May-1998		26-May-1998	Feng, Lin, Vogel	SM-SC		
24	31	Geotech. Lab	VPD	M1_4_2						2.76	26-May-1998		26-May-1998	Feng, Lin, Vogel	SM-SC		
25	32	Geotech. Lab	VPD	M1_4_3						2.76	26-May-1998		26-May-1998	Feng, Lin, Vogel	SM-SC		
26	33	Geotech. Lab	VPD	M1_4_4						2.76	26-May-1998		26-May-1998	Feng, Lin, Vogel	SM-SC		
27	34	Geotech. Lab	VPD	M1_5_1						2.76	26-May-1998		26-May-1998	Feng, Lin, Vogel	SM-SC		

Table 8-5. Sample view of PMTDR table

PMTDRID	AgencyID	Project_Name	Project_Number	Test_Number	Location_Description	State	County	Longitude	Latitude	Operator
13	11	Compaction of Mixture Soil 1~5		M1-1-1	Laboratory	IN	U.S.A.			Feng, Lin, Vogel
15	11	Compaction of Mixture Soil 1~5		M1-1-2	Laboratory	IN	U.S.A.			Feng, Lin, Vogel
16	11	Compaction of Mixture Soil 1~5		M1-1-3	Laboratory	IN	U.S.A.			Feng, Lin, Vogel
17	11	Compaction of Mixture Soil 1~5		M1-1-4	Laboratory	IN	U.S.A.			Feng, Lin, Vogel
22	11	Compaction of Mixture Soil 1~5		M1-2-1	Laboratory	IN	U.S.A.			Feng, Lin, Vogel
23	11	Compaction of Mixture Soil 1~5		M1-2-2	Laboratory	IN	U.S.A.			Feng, Lin, Vogel
24	11	Compaction of Mixture Soil 1~5		M1-2-3	Laboratory	IN	U.S.A.			Feng, Lin, Vogel
25	11	Compaction of Mixture Soil 1~5		M1-2-4	Laboratory	IN	U.S.A.			Feng, Lin, Vogel
26	11	Compaction of Mixture Soil 1~5		M1-3-1	Laboratory	IN	U.S.A.			Feng, Lin, Vogel
27	11	Compaction of Mixture Soil 1~5		M1-3-2	Laboratory	IN	U.S.A.			Feng, Lin, Vogel
28	11	Compaction of Mixture Soil 1~5		M1-3-3	Laboratory	IN	U.S.A.			Feng, Lin, Vogel
29	11	Compaction of Mixture Soil 1~5		M1-3-4	Laboratory	IN	U.S.A.			Feng, Lin, Vogel
30	11	Compaction of Mixture Soil 1~5		M1-4-1	Laboratory	IN	U.S.A.			Feng, Lin, Vogel
31	11	Compaction of Mixture Soil 1~5		M1-4-2	Laboratory	IN	U.S.A.			Feng, Lin, Vogel
32	11	Compaction of Mixture Soil 1~5		M1-4-3	Laboratory	IN	U.S.A.			Feng, Lin, Vogel
33	11	Compaction of Mixture Soil 1~5		M1-4-4	Laboratory	IN	U.S.A.			Feng, Lin, Vogel
34	11	Compaction of Mixture Soil 1~5		M1-5-1	Laboratory	IN	U.S.A.			Feng, Lin, Vogel

Since the data sets are highly related to each other, a relational database model was used to design the database. Figure 8-1 shows the database design elements, while Fig. 8-2 shows the developed database schema.

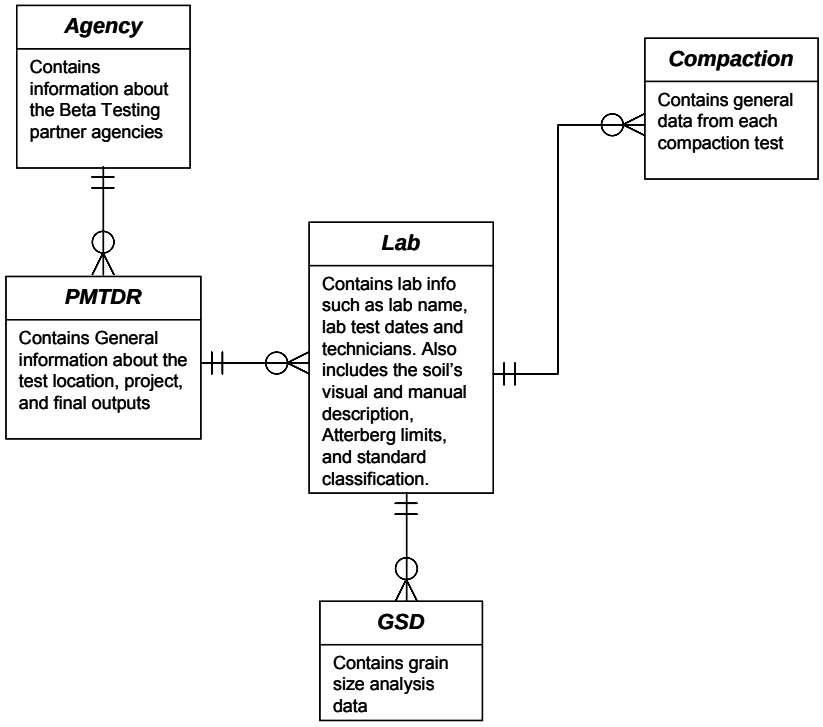

Figure 8-1. Database Design Elements

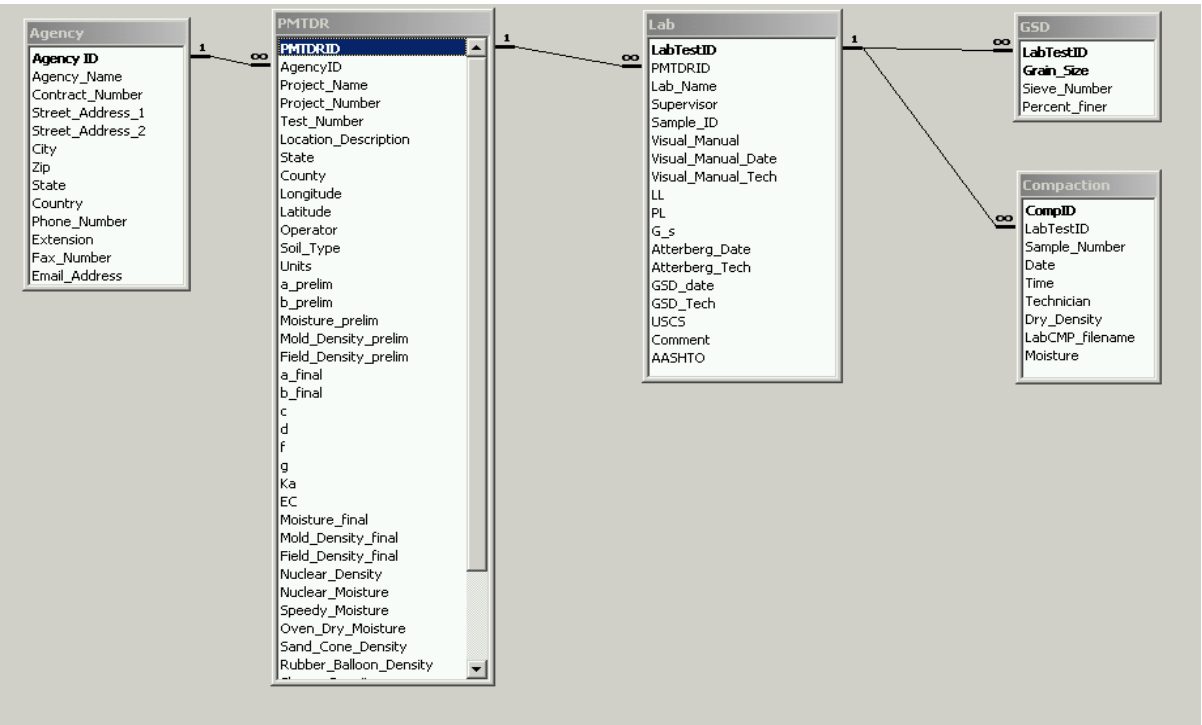

Figure 8-2. Database Schema

8.6. Data Access and Display

Microsoft Access 2000 was used to access and display the database. Five tables were created to display information pertinent to the Agency, PMTDR test, Lab data, Compaction data and Grain Size Distribution (GSD). A separate form was created for each table, with the main form being the Agency form. The PMTDR form was included as a sub-form of the Agency form, and the Lab form as a sub-form of the PMTDR form. Both Compaction and GSD forms are accessible through tabs from the Lab form (Fig. 8-3). Function buttons were used to facilitate routine functions such as navigating between the records, adding and deleting records, and performing basic functions such as undo, save, print, and find. The interface was designed to be user friendly and in logical consequence.

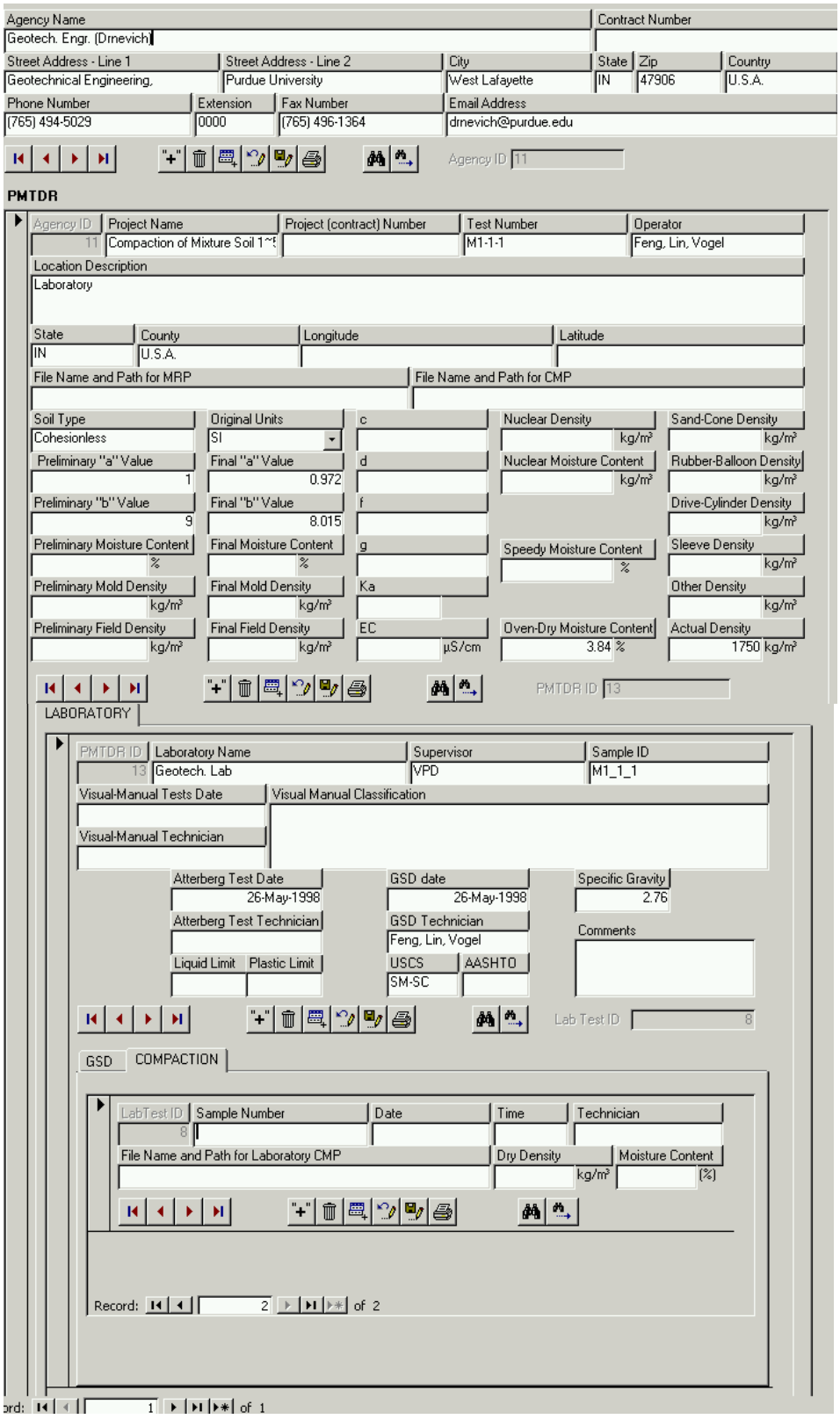

Figure 8-3. Database interface

8.7. Conclusion

With the anticipation of large amounts of data to be collected in the Beta testing phase of the project, the need to design a functional database arose. The data obtained from calibration tests for multiple soil types can be stored and made readily accessible from the Microsoft Access 2000 designed here. The database serves as a valuable resource for storing and retrieving information that can readily be used when future TDR tests are carried out.

9. Conclusions and Recommendations

9.1. Conclusions

The purpose of this report was to assess the viability of the Purdue TDR method for measuring soil water content and density (ASTM D6780). The main focus of this research was to evaluate the TDR method for possible widespread implementation of the TDR method statewide in Florida. As a result, research carried out for this report helped in evaluating the utility and practicality of the TDR method in soils often encountered in FDOT projects. Several key questions were addressed and answered with respect to the method's accuracy and reliability.

Results indicate that the Purdue TDR method was sufficiently accurate for use in geotechnical applications in terms of water content measurement only. An independent evaluation of the accuracy of the nuclear, TDR, sand cone and drive sleeve methods for density measurements, however, could not be carried out due to the lack of a standard or baseline to which the density results could be compared. The TDR method relies on the use of relatively new technology to the field of geotechnical engineering, namely time domain reflectometry.

Upon review of current methods, TDR appears to have several advantages: 1) TDR measures both water content and density virtually simultaneously on the same soil sample. 2) TDR appears to be as accurate as other current methods for determining field water content. 3) TDR does not required special licensing to operate. 4) TDR method does not require extensive calibration compared to the nuclear method. 5) TDR measurements are available upon test completion. 6) Operator dependency does not contribute to significant variability in measurement. The limitations associated with TDR include the following: 1) The TDR method requires the excavation of soil and is therefore destructive in nature. This results in significant delay, especially to inexperienced operators. Moreover, the destructive aspect of the test makes it necessary to repair the hole resulting from the excavation step. 2) TDR test duration exceed that

of comparable methods. 3) The TDR equipment needed to perform a test is more cumbersome to operate than other methods (i.e. laptop, mold, scale etc.)

In order to expedite and improve TDR field testing, a new method has been developed and is currently being evaluated to enable the measurement of both the water content and the density in a single step. Preliminary results indicate that TDR is capable of more accurate estimates of the water content and dry density. The new method eliminates the need of excavating soil samples. Also the one-step equipment is being streamlined with the use of a PDA based data collection and storage system. The method and the corresponding software will be relayed to FDOT upon becoming available.

Research indicates the Purdue TDR method (ASTM D6780) to be a viable method for use in field measurement of soil water content. With ongoing research and improvements the use of TDR measurement for dry density may also become a viable method for field measurement. Results show that the TDR method may be suitable for use in a variety of earthwork applications. It is important to note that no effort was taken to evaluate the method's effectiveness in fine grained material and therefore no recommendations are made to that effect.

9.2. Recommendations

1) In the absence of soil-specific calibration information, a value of 1.00 should be used for soil constant "a" and a value of 8.50 for soil constant "b" for sandy construction soils (A-3, A-1-b and A-2-4 soils) in the state of Florida. For A-2-4 soils, the percent fines must be below 15%.
2) The accuracy of the Purdue TDR method has been proven to be acceptable in terms of water content.
3) The following correlation was developed for the in place LBR test:

$$LBR = 0.0089 * TDR^2 + 0.604 * TDR + 3.62$$

where,
TDR is the average number of blows required to drive the 12 inch TDR spikes to the TDR template and LBR is the in place LBR number.

4) With the imminent development of a one-step method, the time limitations and the destructive aspect of the TDR method should be eliminated.

References

Alharthi, A., and Lange, J., (1987), "Soil Water Saturation: Dielectric Determination," *Water Resources Research*, Vol. 23, pp. 591-595.

Birchak, J.R., Gardner, C.G., Hipp, J.E., and Victor, J.M., (1974), "High Dielectric Constant Microwave Probes for Sensing Soil Moisture," *Proceedings IEEE*, Vol. 62, pp. 93-98.

Clarkson, T. S., Glasser, L., Tuxworth, R. W., and Williams, G. (1977), "An appreciation of experimental factors in Time-Domain Spectroscopy," Adv. Mol. Relax. Processes, Vol. 10, pp. 173-202.

Dasberg, S. and Dalton, F. N. (1985), "Time Domain Reflectometry Field Measurement of Soil Water Content and Electrical Conductivity," *Soil Science Society of America Journal,* Vol. 49, pp. 293-297.

Dirksen, C, and Dasberg, S., (1993), "Improved Calibration of Time Domain Reflectometry Soil Water Content Measurements," *Soil Science Society of America Journal*, Vol. 57, pp. 660-667.

Drnevich, V., Lin, C., Quanghee, Y., Yu, X., Lovell, J., (2000), "Real-Time determination of soil type water content, and density using electromagnetic," *Final report, FHWA/IN/JTRP-2000/20.*

Fellner-Feldegg, J., (1969), "The Measurement of Dielectrics in Time Domain". *Journal of Physical Chemistry*, Vol. 73, pp. 616-623.

Feng, W., Lin, C. P., Deschamps, R. J. and Drnevich, V. P. (1999), "Theoretical Model of a Multisection Time Domain Reflectometry Measurement System," *Water Resources Research,* Vol. 35, No. 8, pp. 2321-2331.

Giese, K. and Tiemann, R. (1975), "Determination of the complex permittivity from thin-sample Time Domain Reflectometry: Improved analysis of the syep response Wave form," Adv. Mol. Relax. Processes, Vol. 7, pp. 45-59.

Harison, J. A. (1989), "In -situ CBR Determination by DCP Testing Using a Laboratory-based Correlation," *Australian Road Research*, Vol. 19, pp. 313-317.

Heimovaara, T. J. (1993), "Design of Triple-Wire Time Domain Reflectometry Probes in Practice and Theory," *Soil Science Society of America Journal,* Vol. 57, pp. 1410-1417.

Heimovaara, T. J. and Bouten, W. (1990), "A Computer-Controlled 36-Channel Time Domain Reflectometry System for Monitoring Soil Water Contents," *Water Resources Research,* Vol. 26, No.10, pp. 2311-2316.

Herkelrath, W. N., Hamburg, S. P. and Murphy, Fred (1991), " Automatic, Real Time Monitoring of Soil Moisture in a remote Field Area with Time Domain Reflectometry," *Water Resources Research,* Vol. 27, No. 5, pp. 857-864.

Kafle, S., and Ashmawy, A., (2001), "ISIS, An Integrated Subsurface Information System". A Master Thesis Submitted To Department Of Civil And Environmental Engineering, College Of Engineering, University Of South Florida, May 2001.

Kleyn, E. G. (1975), "The Use of the Dynamic Cone Penetrometer (DCP)," *Transvaal Roads Department Report,* No. L2/74.

Krauss, J. D., (1984), "Electromagnetics ," *McGraw-Hill, New York*.

Ledieu, J.P., Ridder, De., and Dautrebande, A., (1986), "A Method for Measuring Soil Moisture Content by Time Domain Reflectometry ," *Journal of Hydrology*, Vol. 88, pp. 319-328.

Lin, C., Siddiqui, S.I., Feng, W., Drnevich, V., and Deschamp, R., (2000), "Quality Control of Earth Fills Using Time Domain Reflectometry (TDR)", *Constructing and Controlling Compaction of Earth Fills, ASTM STP 1384*, D. W. Shankin, K. R. Rademacher, and J. R. Talbot. Eds., American Society for Testing and Materials, West Conshohocken, PA,2000.

Livneh, M. (1989) "In-situ CBR testing by indirect methods," *Proceedings of the 12th International Conference on Soil Mechanics and Foundation Engineering*, Rio de Janero, Vol. 1, pp. 267-270.

Livneh, M. and Ishai, I. (1987), "The Use of Between Dynamic Cone Penetrometer in Determining the Strength of Existing Pacements and Subgrades," *Proceedings of the 9th Southeast Asian Geotechnical Conference,* Bangkok, Thailand.

Livneh, M. and Ishai, I. (1988), "The Relationship Between In-Situ CBR Test and Various Penetration Tests," *Proceedings of the First International Synapse on Penetration Testing,* Orlando, Florida, ISOPT-1.

Mojid, M. A., Wyseure, G. C. L. and Rose, D. A. (2003), "Electrical Conductivity Problems Associated With Time-Domaon Reflectometry (TDR) Measurement in Geotechnical Engineering," *Geotechnical and Geological Engineering,* Vol. 21, Is. 3, pp. 243-258.

Nadler, A., Dasberg S. and Lapid, I. (1991), "Time Domain Reflectometry Measurements of Water Content and Electrical Conductivity of Layered Soil Columns," *Soil Science Society of America Journal,* Vol.55, pp. 938-943.

O'Connor, K., and Dowding, C., (1999), "GeoMeasurements *by* Pulsing TDR Cables *and* Probes" A book published by CRC Press LLC.

Siddiqui, S.I. and Drnevich, V.P., (1995), "Use of Time Domain Reflectometry for the Determination of Water Content and Density of Soil," FHWA/IN/JHRP-95/9, Purdue University.

Smith, R.B. and Pratt, D. N. (1983), "A field Study of In-Situ California Bearing Ratio and Dynamic Penetrometer Testing for Road Subgrade Investigation," *Australian Road Research*, Vol.13, No.4, pp. 285-294.

Topp, G.C., Davis, J.L., and Annan, A.P., (1980), "Electromagnetic Determination of Soil Water Content and Electrical Conductivity Measurement Using Time Domain Reflectometry," *Water Resources Research*, Vol. 16, pp. 574-582.

Yanuka, M., Topp, G. C., Zegelin, S. and Zebchuk, W. D. (1988), "Multiple Reflection and Attenuation of Time Domain Reflectometry Pulses: Theoretical Considerations for Applications to Soil and Water," *Water Resources Research,* Vol. 24, No.7, pp. 939-944.

Zegelin, S. J., White, I. and Jenkins, D. R. (1989), "Improved Field Probes for Soil Water and Electrical Conductivity Measurement Using Time Domain Reflectometry," *Water Resources Research,* Vol. 25, No. 11, pp. 2367-2376.

APPENDIX

Meaured W_c	Meaured W_c, %ge	Measured $[K^* (1+W_c)]$	Theoritical W_c	Theoritical W_c, %ge	Absolute Error in W_c, %ge	Normalized Error, %ge
0.00059	0.06	0.91	-0.01016	-1.02	1.07	1823.50
0.02227	2.23	1.15	0.01874	1.87	0.35	15.86
0.04855	4.86	1.41	0.04921	4.92	-0.07	-1.34
0.07519	7.52	1.66	0.07888	7.89	-0.37	-4.90
0.10545	10.55	1.93	0.11083	11.08	-0.54	-5.10
0.12621	12.62	2.02	0.12082	12.08	0.54	4.27
0.02030	2.03	1.09	0.01133	1.13	0.90	44.19
0.03313	3.31	1.24	0.02886	2.89	0.43	12.91
0.04470	4.47	1.31	0.03726	3.73	0.74	16.63
0.05752	5.75	1.48	0.05691	5.69	0.06	1.06
0.07319	7.32	1.60	0.07087	7.09	0.23	3.16
0.08065	8.06	1.66	0.07893	7.89	0.17	2.13
0.08644	8.64	1.75	0.08867	8.87	-0.22	-2.58
0.04509	4.51	1.39	0.04699	4.70	-0.19	-4.21
0.07416	7.42	1.61	0.07225	7.23	0.19	2.57
0.09249	9.25	1.78	0.09323	9.32	-0.07	-0.80
0.13095	13.10	2.02	0.12104	12.10	0.99	7.57
0.17348	17.35	2.34	0.15895	15.90	1.45	8.37
0.18757	18.76	2.65	0.19562	19.56	-0.80	-4.29
0.02564	2.56	1.23	0.02724	2.72	-0.16	-6.25
0.08196	8.20	1.72	0.08524	8.52	-0.33	-4.01
0.11836	11.84	2.03	0.12223	12.22	-0.39	-3.27
0.16640	16.64	2.45	0.17168	17.17	-0.53	-3.18
0.20208	20.21	2.73	0.20501	20.50	-0.29	-1.45
0.22034	22.03	2.83	0.21701	21.70	0.33	1.51
0.01523	1.52	1.05	0.00656	0.66	0.87	56.95
0.01507	1.51	1.04	0.00482	0.48	1.02	67.99
0.03558	3.56	1.25	0.02948	2.95	0.61	17.13
0.03109	3.11	1.24	0.02903	2.90	0.21	6.60
0.06871	6.87	1.52	0.06212	6.21	0.66	9.59
0.06750	6.75	1.51	0.06103	6.10	0.65	9.58
0.10129	10.13	1.82	0.09706	9.71	0.42	4.18
0.10125	10.12	1.82	0.09712	9.71	0.41	4.08
0.01633	1.63	1.11	0.01397	1.40	0.24	14.40
0.03360	3.36	1.25	0.02966	2.97	0.39	11.73
0.05036	5.04	1.40	0.04730	4.73	0.31	6.08
0.06459	6.46	1.52	0.06249	6.25	0.21	3.26
0.08633	8.63	1.68	0.08114	8.11	0.52	6.01
0.11544	11.54	1.85	0.10132	10.13	1.41	12.24
0.12113	12.11	1.90	0.10728	10.73	1.38	11.43
0.02102	2.10	1.17	0.02090	2.09	0.01	0.56

Meaured W_c	Meaured W_c, %ge	Measured $[K^* (1+W_c)]$	Theoritical W_c	Theoritical W_c, %ge	Absolute Error in W_c, %ge	Normalized Error, %ge
0.03647	3.65	1.28	0.03328	3.33	0.32	8.75
0.06443	6.44	1.42	0.05036	5.04	1.41	21.84
0.06691	6.69	1.54	0.06410	6.41	0.28	4.20
0.08304	8.30	1.72	0.08520	8.52	-0.22	-2.59
0.10302	10.30	1.82	0.09760	9.76	0.54	5.26
0.04062	4.06	1.39	0.04673	4.67	-0.61	-15.04
0.05188	5.19	1.52	0.06168	6.17	-0.98	-18.89
0.06816	6.82	1.65	0.07741	7.74	-0.93	-13.57
0.08651	8.65	1.79	0.09437	9.44	-0.79	-9.09
0.11900	11.90	1.98	0.11651	11.65	0.25	2.10
0.14088	14.09	2.26	0.14939	14.94	-0.85	-6.04
0.03280	3.28	1.25	0.02977	2.98	0.30	9.24
0.04527	4.53	1.38	0.04557	4.56	-0.03	-0.67
0.06414	6.41	1.59	0.06988	6.99	-0.57	-8.94
0.08131	8.13	1.73	0.08651	8.65	-0.52	-6.40
0.09731	9.73	1.80	0.09507	9.51	0.22	2.30
0.11808	11.81	2.01	0.11964	11.96	-0.16	-1.33
0.02525	2.52	1.24	0.02876	2.88	-0.35	-13.90
0.03528	3.53	1.37	0.04441	4.44	-0.91	-25.88
0.05763	5.76	1.52	0.06163	6.16	-0.40	-6.94
0.07244	7.24	1.65	0.07766	7.77	-0.52	-7.19
0.09990	9.99	1.84	0.09926	9.93	0.06	0.64
0.10672	10.67	1.94	0.11221	11.22	-0.55	-5.15
0.13983	13.98	2.15	0.13698	13.70	0.28	2.04
0.14859	14.86	2.31	0.15555	15.55	-0.70	-4.68
0.17075	17.07	2.46	0.17272	17.27	-0.20	-1.15
0.02178	2.18	1.17	0.02099	2.10	0.08	3.62
0.03282	3.28	1.36	0.04255	4.25	-0.97	-29.66
0.05477	5.48	1.49	0.05893	5.89	-0.42	-7.60
0.06873	6.87	1.61	0.07277	7.28	-0.40	-5.88
0.08204	8.20	1.77	0.09117	9.12	-0.91	-11.12
0.09925	9.93	1.89	0.10585	10.58	-0.66	-6.65
0.02492	2.49	1.26	0.03154	3.15	-0.66	-26.57
0.06354	6.35	1.46	0.05534	5.53	0.82	12.91
0.06625	6.63	1.69	0.08215	8.22	-1.59	-24.00
0.09042	9.04	1.83	0.09840	9.84	-0.80	-8.83
0.11382	11.38	2.06	0.12622	12.62	-1.24	-10.89
0.13247	13.25	2.16	0.13753	13.75	-0.51	-3.82
0.02421	2.42	1.25	0.02990	2.99	-0.57	-23.55
0.04902	4.90	1.39	0.04712	4.71	0.19	3.88
0.06081	6.08	1.56	0.06640	6.64	-0.56	-9.19
0.08029	8.03	1.69	0.08151	8.15	-0.12	-1.51
0.08777	8.78	1.77	0.09163	9.16	-0.39	-4.40
0.10480	10.48	1.89	0.10569	10.57	-0.09	-0.85

Meaured W_c	Meaured W_c, %ge	Measured $[K^* (1+W_c)]$	Theoritical W_c	Theoritical W_c, %ge	Absolute Error in W_c, %ge	Normalized Error, %ge
0.11989	11.99	2.01	0.12046	12.05	-0.06	-0.48
0.15401	15.40	2.28	0.15138	15.14	0.26	1.70
0.03197	3.20	1.34	0.04048	4.05	-0.85	-26.62
0.06771	6.77	1.59	0.06991	6.99	-0.22	-3.25
0.07938	7.94	1.70	0.08291	8.29	-0.35	-4.45
0.11838	11.84	2.01	0.11941	11.94	-0.10	-0.87
0.11965	11.97	1.95	0.11266	11.27	0.70	5.85
0.13433	13.43	2.10	0.13017	13.02	0.42	3.09
0.04864	4.86	1.39	0.04677	4.68	0.19	3.85
0.07015	7.01	1.64	0.07558	7.56	-0.54	-7.74
0.09236	9.24	1.78	0.09219	9.22	0.02	0.18
0.11279	11.28	1.96	0.11404	11.40	-0.13	-1.11
0.12905	12.91	2.19	0.14165	14.16	-1.26	-9.76
0.15378	15.38	2.30	0.15397	15.40	-0.02	-0.13
0.04000	4.00	1.34	0.04083	4.08	-0.08	-2.06
0.06061	6.06	1.50	0.06001	6.00	0.06	0.99
0.07884	7.88	1.71	0.08408	8.41	-0.52	-6.64
0.09858	9.86	1.83	0.09857	9.86	0.00	0.01
0.11526	11.53	2.00	0.11842	11.84	-0.32	-2.74
0.15610	15.61	2.36	0.16170	16.17	-0.56	-3.59
0.03300	3.30	1.29	0.03484	3.48	-0.18	-5.58
0.05941	5.94	1.51	0.06107	6.11	-0.17	-2.81
0.08185	8.18	1.68	0.08066	8.07	0.12	1.45
0.09557	9.56	1.84	0.09921	9.92	-0.36	-3.81
0.12134	12.13	2.03	0.12211	12.21	-0.08	-0.64
0.15522	15.52	2.26	0.14955	14.96	0.57	3.65
0.03772	3.77	1.29	0.03484	3.48	0.29	7.64
0.05867	5.87	1.50	0.05981	5.98	-0.11	-1.95
0.08325	8.33	1.67	0.07976	7.98	0.35	4.20
0.09623	9.62	1.82	0.09684	9.68	-0.06	-0.64
0.11950	11.95	1.97	0.11480	11.48	0.47	3.93
0.15550	15.55	2.29	0.15282	15.28	0.27	1.72
0.03325	3.33	1.29	0.03470	3.47	-0.14	-4.35
0.05823	5.82	1.47	0.05574	5.57	0.25	4.27
0.08080	8.08	1.65	0.07722	7.72	0.36	4.43
0.09766	9.77	1.81	0.09586	9.59	0.18	1.84
0.11726	11.73	1.99	0.11754	11.75	-0.03	-0.24
0.15581	15.58	2.24	0.14697	14.70	0.88	5.68
0.01584	1.58	1.15	0.01851	1.85	-0.27	-16.86
0.03486	3.49	1.32	0.03887	3.89	-0.40	-11.53
0.05541	5.54	1.47	0.05628	5.63	-0.09	-1.57
0.07006	7.01	1.57	0.06772	6.77	0.23	3.35
0.08111	8.11	1.67	0.07964	7.96	0.15	1.82

Meaured W_c	Meaured W_c, %ge	Measured $[K^* (1+W_c)]$	Theoritical W_c	Theoritical W_c, %ge	Absolute Error in W_c, %ge	Normalized Error, %ge
0.09770	9.77	1.85	0.10127	10.13	-0.36	-3.65
0.02660	2.66	1.20	0.02402	2.40	0.26	9.68
0.04636	4.64	1.38	0.04496	4.50	0.14	3.01
0.06582	6.58	1.52	0.06209	6.21	0.37	5.66
0.08048	8.05	1.67	0.07993	7.99	0.06	0.68
0.11135	11.13	1.85	0.10135	10.13	1.00	8.98
0.11682	11.68	1.99	0.11762	11.76	-0.08	-0.68
0.03130	3.13	1.25	0.03017	3.02	0.11	3.60
0.05267	5.27	1.44	0.05293	5.29	-0.03	-0.48
0.06213	6.21	1.51	0.06081	6.08	0.13	2.14
0.08186	8.19	1.68	0.08098	8.10	0.09	1.08
0.10076	10.08	1.81	0.09628	9.63	0.45	4.44
0.11775	11.77	1.94	0.11192	11.19	0.58	4.95
0.05283	5.28	1.33	0.03913	3.91	1.37	25.93
0.06499	6.50	1.53	0.06358	6.36	0.14	2.17
0.08353	8.35	1.73	0.08636	8.64	-0.28	-3.38
0.09848	9.85	1.82	0.09733	9.73	0.12	1.17
0.10961	10.96	1.89	0.10543	10.54	0.42	3.82
0.12744	12.74	2.06	0.12575	12.58	0.17	1.33
0.04959	4.96	1.33	0.03946	3.95	1.01	20.43
0.06274	6.27	1.51	0.06120	6.12	0.15	2.45
0.07549	7.55	1.65	0.07673	7.67	-0.12	-1.64
0.09050	9.05	1.79	0.09394	9.39	-0.34	-3.79
0.11277	11.28	1.91	0.10810	10.81	0.47	4.14
0.12366	12.37	2.13	0.13406	13.41	-1.04	-8.41
				Average	**0.01**	**0.65**
				Maximum	**1.45**	**67.99**
				Minimum	**-1.59**	**-29.66**

Spreadsheets for TDR calibration tests

Evaluation of TDR Accuracy

Soil Information

Location: Out of soil lab, Trial # 1. Date: 8/6/2002

Visual-Manual Classification: Yellow med. To coarse sand

USCS: AASHTO:

Determination of Wet Density

Weight Of Empty Box =	40.5	lb
Weight Of Empty Box + Soil =	273.5	lb
Volume Of Box =	2.2917	ft^3
Wet density =	101.67	lb/ft^3

Determination Of Moisture Content

Cup No.	W_1	W_2	W_3	W_c, %ge
1	16.68	101.81	97.33	5.55
2	16.83	103.22	98.39	5.92
3	16.89	111.85	106.66	5.78
Average Moisture Content, %ge =				5.75

Determination Of Actual Dry Density

ρ_{dry} = 96.14 lb/ft^3

TDR Results:

$\rho_{dry,\ mold}$ =	1537.2	Kg/m^3	==	95.77	lb/ft^3
$\rho_{dry,\ field}$ =	1521.2	Kg/m^3	==	94.77	lb/ft^3
Wc =	5.5	%			

Calibration Results

Absoulute Error in Moisture Content, %ge =	**-0.25**
Normalized Error in Moisture Content, %ge =	**-4.60**
Absoulute Error in Dry Density, lb/ft^3 =	**-1.37**
NormalizedError in Dry Density,%ge =	**-1.45**